Aus dem Institut für Virologie

Direktor: Prof. Dr. Stephan Becker

des Fachbereichs Medizin der Philipps-Universität Marburg

The species-specific effects of guinea pig-adaptive mutations in Marburg virus VP40 and L on the protein's functions and viral fitness

Inaugural-Dissertation zur Erlangung des Doktorgrades

der Naturwissenschaften (Dr. rer. nat.)

dem Fachbereich Medizin der Philipps-Universität Marburg
vorgelegt von

Alexander Köhler
aus Paderborn

Marburg, 2017

Die Untersuchungen zur vorliegenden Arbeit wurden von Oktober 2013 bis März 2017 am Institut für Virologie der Philipps Universität Marburg unter der Leitung von Prof. Dr. Stephan Becker durchgeführt.

Angenommen vom Fachbereich 20 Humanmedizin
Der Philipps-Universität Marburg am 02.03.2017

gedruckt mit Genehmigung des Fachbereichs

Dekan: Prof. Dr. Helmut Schäfer
Referent: Prof. Dr. Stephan Becker
Korreferent: Prof. Dr. Ulrich Steinhoff

Im Zusammenhang mit der vorliegenden Arbeit wurden folgende Publikationen erstellt:

Koehler A., Kolesnikova L., Welzel U., Schudt G., Herwig A., Becker S. (2015).

A single amino acid change in the Marburg virus matrix protein VP40 provides a replicative advantage in a species-specific manner. J Virol 90 1444–1454.

Koehler A., Kolesnikova L., Becker S. (2016).

An active site mutation increases the polymerase activity of the guinea pig-lethal Marburg virus. J. Gen. Virol., 97: 2494-2500

Die Arbeit wurde auf folgenden Kongressen und Tagungen präsentiert:

24. Frühjahrstagung der Gesellschaft für Virologie

März 2014, Alpbach, Österreich

Koehler A., Welzel U., Schudt G., Becker S. and Kolesnikova L.

Role of a single amino acid mutation in VP40 for the enhanced virulence of guinea pig-adapted Marburg Virus. (Poster).

25. Frühjahrstagung der Gesellschaft für Virologie

März 2015, Bochum, Deutschland

Koehler A., Welzel U., Schudt G., Herwig A., Becker S. and Kolesnikova L.

A single amino acid change in the matrix protein VP40 of Marburg virus improves viral fitness (Vortrag).

Negative strand virus Meeting

Juni 2015, Siena, Italien

Koehler A., Welzel U., Schudt G., Becker S. and Kolesnikova L.

A single amino acid change in the Marburg virus matrix protein VP40 improves viral fitness in a species-specific manner (Poster).

26. Frühjahrstagung der Gesellschaft für Virologie

April 2016, Münster, Deutschland

Koehler A., Welzel U., Schudt G., Kolesnikova L. and Becker S.

A Single Amino Acid Change in the Marburg Virus Matrix Protein VP40 Provides a Replicative Advantage in a Species-Specific Manner (Poster).

List of contents

1 Introduction

1.1 Taxonomy and epidemiology of filoviruses

Marburg virus (MARV) belongs together with the Ebolaviruses (EBOV) and the recently described Lloviuvirus (LLOV) to the family of *Filoviridae* in the order of *Mononegavirales* (Bukreyev et al., 2014; Kuhn et al., 2010; Negredo et al., 2011). Viruses from the order of *Mononegavirales* including *Paramyxoviruses*, *Rhabdoviruses* and *Bornaviruses* share a non-segmented negative sense RNA genome. The name *Filoviridae* derives from the filamentous (lat. *filum* = thread) appearance of the virions (Geisbert & Jahrling, 1995; Murphy *et al.*, 1978). The complete taxonomy of the *Filoviridae* is shown in table 1. Filoviruses induce severe diseases in humans, associated with high fatality rates (Bausch *et al.*, 2006; Siegert *et al.*, 1967; Towner *et al.*, 2006). The severity of the filoviral disease and the lack of effective treatments and vaccines leads to the classification of filoviruses as BSL-4 agents.

Family	Genus	Species	Virus name (abbreviation)
Filoviridae	Marburgvirus	Marburg marburgvirus	Marburg virus (MARV) Ravn virus (RAVV)
	Ebolavirus	Bundibugyo ebolavirus	Bundibugyo virus (BDBV)
		Reston ebolavirus	Reston virus (REBOV)
		Sudan ebolavirus	Sudan virus (SUDV)
		Taï Forest ebolavirus	Tai Forest virus (TAFV)
		Zaire ebolavirus	Ebola virus (ZEBOV)
	Cuevavirus	Lloviu cuevavirus	Lloviu cuevavirus (LLOV)

Table 1: Taxonomy of filoviruses, (ICTV 2015)

The Marburg virus is named after the city Marburg (Hesse, Germany), which happened to be the first place of a known filoviral disease and virus isolation (Siegert *et al.*, 1967). The initial Marburg virus outbreak occurred in parallel in Marburg, Frankfurt and Belgrade in 1967. Laboratory workers and zookeepers were infected by direct contact with specimens from infected African green monkeys (Fig. 1-2). Thirty-two persons fell ill, seven individuals developed a

severe hemorrhagic fever which led to death (Slenczka & Klenk, 2007).

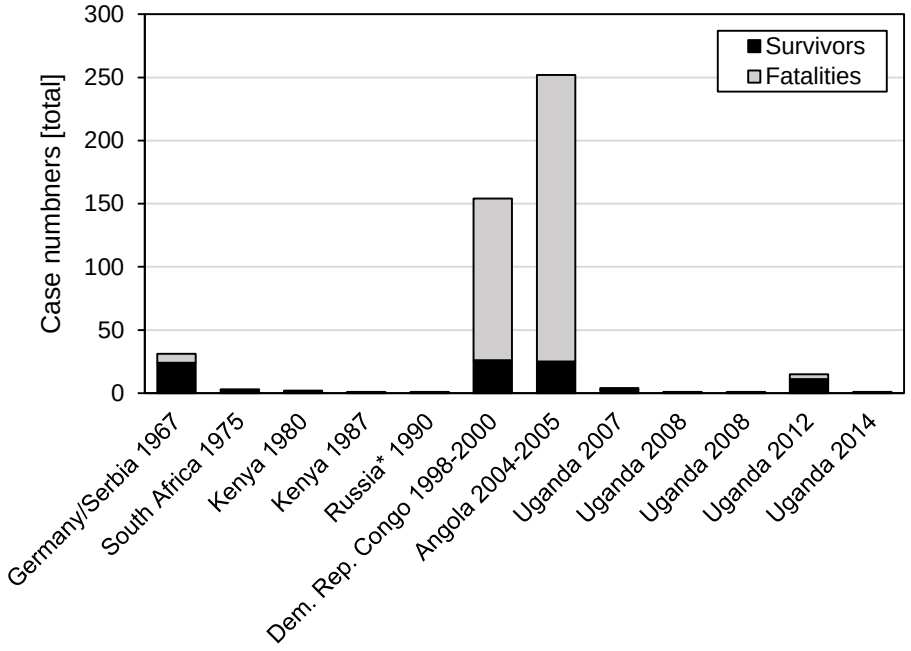

Figure 1: History of Marburg virus cases and outbreaks

Height of the column indicates the total case numbers (survivors of MARV infections are shown in black, lethal MARV cases are shown in grey). * indicates an accidental laboratory exposure**.**

In 1976, the currently much better known and studied member of the *Filoviridae*, the Ebola virus, was discovered in Africa (Bowen *et al.*, 1977). In following years, both viruses caused sporadic outbreaks associated with high lethality rates. Until 1998 it was believed that EBOV had higher lethality rates than MARV. However, the 1998 MARV outbreaks in the Democratic Republic of Congo and the 2004 outbreak in Angola demonstrated the severity of the MARV disease, with lethality rates above 80% (Bausch *et al.*, 2006; Towner *et al.*, 2006). However, the reliability of the case fatality rates is questionable due to significant underreporting. Filoviral outbreaks were considered as self-containing due to the severity of the disease and the predominant occurrence in rural regions of central Africa, affecting either small villages or single tourists (Albariño *et al.*, 2013a; Amman *et al.*, 2014; Bausch *et al.*, 2006; CDC, 2009; Siegert *et al.*, 1967; Towner *et al.*, 2006). An overview of the MARV-induced outbreaks and single cases is shown in figure 1. However, the 2013-2016 EBOV outbreak clearly showed the potential of filoviruses to cause long lasting large-scale outbreaks associated with high lethality rates. 28,616 people became infected of which 11,310 died, resulting in an overall lethality rate of 40% (Acharya, 2014; Carroll *et al.*, 2015; WHO, 2016b). Despite the biological threat to mankind, this outbreak massively

affected the local and regional economy, and highlights the importance of filovirus research (Bartsch *et al.*, 2015).

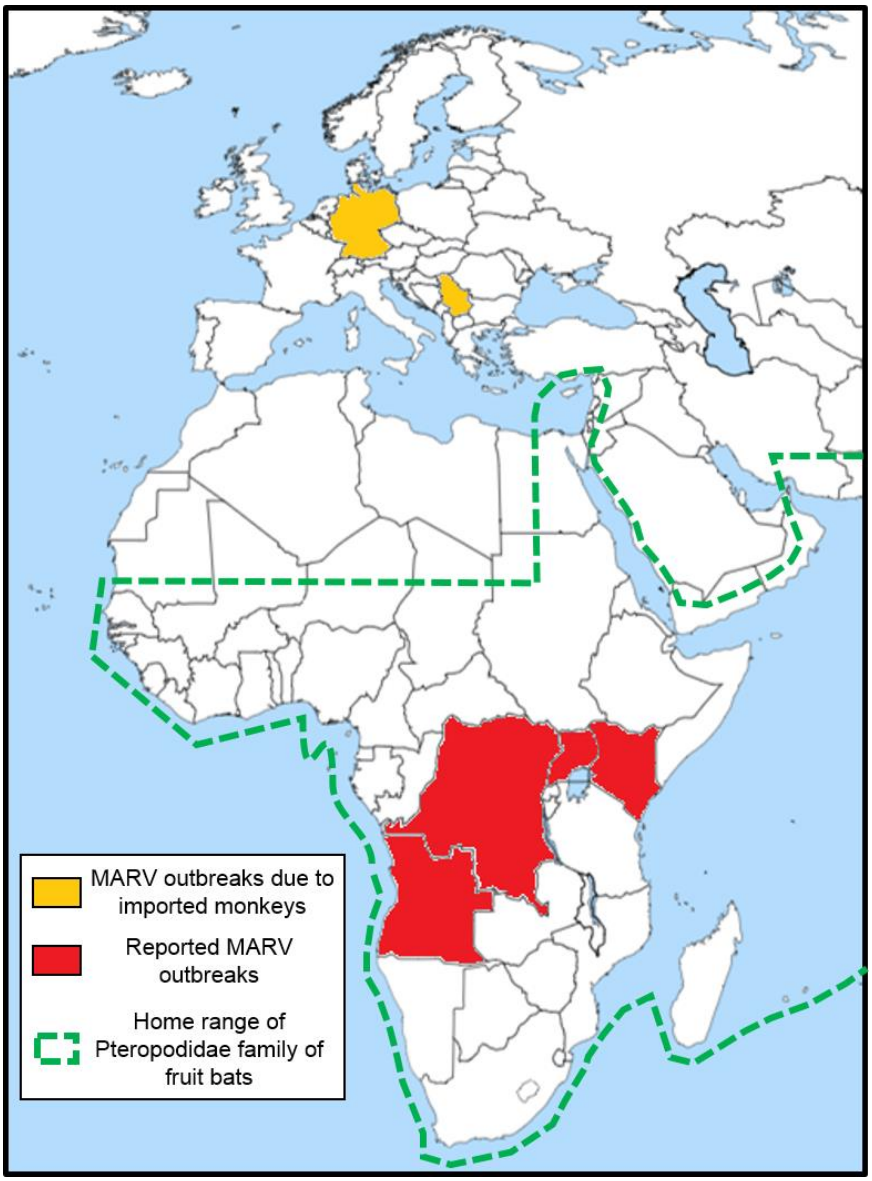

Figure 2: Geographic distribution of Marburg fever outbreaks and habitats of fruit bats from the *Pteropodidae* family

MARV outbreaks caused by contact to tissues of imported and infected monkeys shown in yellow. Countries with reported MARV outbreaks, shown in red. The green line indicates the presence of bats from the *Pteropodidae* family reported as known reservoirs for MARV. Graphic modified from WHO 2009.

Previous zoonotic MARV infections were regularly traced back to the entry of humans into bat caves (Brauburger *et al.*, 2012). In 2007, MARV was isolated from Egyptian fruit bats (*Rousettus aegyptiacus*) which belong to the family of *Pteropodidae,* and soon after, fruit bats were confirmed as natural MARV

reservoir (Pourrut *et al.*, 2009; Swanepoel *et al.*, 2007; Towner *et al.*, 2009; Towner *et al.*, 2007). The distribution of fruit bats from the *Pteropodidae* family, including *Rousettus aegyptiacus*, and human MARV outbreaks overlaps (Fig. 2).

1.2 Clinical appearance

Transmission of MARV to humans occurs either via direct contact to infected animals, such as bats or primates, or may occur by consumption of contaminated bush meat (Beeching *et al.*, 2014; Martini & Siegert, 1971). Human to human transmission of MARV is a result of contact to bodily fluids (such as blood, feces, urine, vomit or sweat) of an infected person.
The onset of symptoms occurs after an incubation period of 2 to 21 days, depending on several factors, such as the infectious dose and transmission route (Martini & Siegert, 1971; WHO, 2012). In addition, individual factors, for instance, the genetic background or an existing immune suppression might play a role in the disease outcome (Martini & Siegert, 1971; Rosenke *et al.*, 2016; WHO, 2012).

The initial phase of the disease is characterized by unspecific symptoms, e.g., high fever, headaches, muscle pain, nausea and gastrointestinal symptoms, such as diarrhea and vomiting. Especially in the initial phase MARV disease is hard to distinguish from other diseases such as the flu, dengue fever, malaria, yellow fever and Lassa fever (Drosten *et al.*, 2002; WHO, 2014). The first MARV disease symptom that allows distinction from the flu is a frequently observed maculopapular rash (Martini & Siegert, 1971; Mehedi *et al.*, 2011). During disease progression the medical condition quickly worsens, many patients display abnormal vascular permeability, edema, dyspnea and some develop hemorrhagic symptoms such as petechiae, mucosal bleedings and bloody diarrhea, neurological symptoms can appear, such as confusion, aggression or disorientation (Mehedi *et al.*, 2011). Death occurs by shock due to multi-organ failure, on average between day eight and nine after the onset of symptoms (WHO, 2012).

The large 2013-2016 Ebola outbreak helped to increase the understanding of filoviral disease in humans significantly. Now it is well accepted that survival

frequently leads to the post-Ebolavirus disease-syndrome accompanied by chronic muscle aches, joint pain, temporary memory loss, exhaustion and impairment of sight and/or hearing (Hunt & Knott, 2016; Mattia *et al.*, 2016; Nanyonga *et al.*, 2016). Viral RNA or infectious virus can persist up to nine months in the semen or the ocular fluid of infected individuals (Deen *et al.*, 2015; Varkey *et al.*, 2015). Sexual transmission of MARV has been observed first during the initial Marburg virus outbreak and multiple sexual transmissions of EBOV confirmed that transmission of filoviruses can occur by sexual contact, even when patients were in convalescence (Christie *et al.*, 2015; Martini & Schmidt, 1968; Mate *et al.*, 2015). Persistence of infectious virus and sexual transmission has to be considered as a possible source of disease flare-ups after an outbreak.

1.3 Vaccines and antivirals

Currently, neither licensed vaccines nor therapeutics against filoviral diseases are available. Numerous different approaches have been made to create an efficient vaccine. Approaches with inactivated virus produced contrary results and full protection was not observed in non-human primates (NHPs) (Ignatyev *et al.*, 1996). Due to the ease of use and production, viral glycoprotein (GP) containing virus-like particles (VLPs) were used for vaccination and showed promising results in both rodents and NHPs (Swenson *et al.*, 2008; Swenson *et al.*, 2005). However, the most promising approaches are vaccine platforms based on reverse genetic systems of low pathogenic viruses like the vesicular stomatitis virus (VSV) or adenoviruses (Wang *et al.*, 2006). A VSV based vaccine which lacks the VSV glycoprotein and contains the MARV-GP instead (VSVΔG/MARV-GP) has been 100% protective in NHPs and was successful as post exposure treatment in NHPs (Daddario-DiCaprio *et al.*, 2006; Geisbert *et al.*, 2009). During the 2013 EBOV outbreak, a VSVΔG/EBOV-GP has been shown as efficient in preventing infection in humans (Henao-Restrepo *et al.*, 2016). However, neither VSVΔG/MARV-GP nor VSVΔG/EBOV-GP are licensed to date.

Generally, supportive treatment takes place upon the course of disease such as replenishing blood, fluids and administration of antibiotics, which reduces overall lethality (Baseler *et al.*, 2016; WHO, 2016a). Despite the lack of licensed

antivirals, effective treatment options have been demonstrated in NHPs, such as siRNA based therapeutics and small molecules (Heald *et al.*, 2015; Thi *et al.*, 2014; Ursic-Bedoya *et al.*, 2014).

1.4 The importance of animal models in filoviral research

1.4.1 Animal models for filovirus research

Due to the high lethality of the Marburg virus disease and the potential to cause prolonged large-scale outbreaks, it is necessary to develop antivirals and vaccines. In order to test the efficacy of treatment and prophylaxis options, relevant animal models are essential (Acharya, 2014; Carroll *et al.*, 2015). Experimental infection of NHPs with human MARV isolates results in lethal disease displaying all hallmarks of a human infection (Banadyga *et al.*, 2016; Nakayama & Saijo, 2013; Sanchez *et al.*, 2006). Disadvantages of NHPs as animal model are ethical issues, high costs and maintenance, the restricted availability of laboratories with the expertise and capacities to work with NHPs under BSL-4 conditions (Banadyga *et al.*, 2016; Bente *et al.*, 2009). Small animal models (mice, hamsters, guinea pigs) allow to overcome some of these issues and could provide general insights into the potentials of treatments and vaccines (Banadyga *et al.*, 2016; Nakayama & Saijo, 2013). However, experimental infection of rodents with human wildtype filovirus isolates does not induce a lethal disease (Cross *et al.*, 2015; Ebihara *et al.*, 2006; Lofts *et al.*, 2007; Lofts *et al.*, 2011; Marzi *et al.*, 2016; Mateo *et al.*, 2011; Qiu *et al.*, 2014; Volchkov *et al.*, 2000a; Warfield *et al.*, 2007; Warfield *et al.*, 2009). Filoviruses requires several passages in rodents for the selection of virus inducing a lethal disease (Cross *et al.*, 2015; Lofts *et al.*, 2007; Lofts *et al.*, 2011; Marzi *et al.*, 2016; Qiu *et al.*, 2014; Warfield *et al.*, 2009).

1.4.2 Adaptation of MARV to rodents

Passaging of MARV in rodents, so called adaptation of MARV to rodents, is accompanied by mutations in the viral genome (Lofts *et al.*, 2007; Lofts *et al.*, 2011; Mateo *et al.*, 2011; Qiu *et al.*, 2014; Volchkov *et al.*, 2000a; Warfield *et al.*, 2007; Warfield *et al.*, 2009). A previously published study by Lofts and colleagues was devoted to adaption of MARV Musoke, an isolate from a human case (Kenia, 1980), to guinea pigs (Lofts *et al.*, 2007). Eight passages of MARV in guinea pigs resulted in selection of a virus variant which induces a lethal disease in guinea pigs (Lofts *et al.*, 2007). Much more passages, 23 to 28, were necessary for adaptation of MARV to mice (Lofts *et al.*, 2007; Lofts *et al.*, 2011; Qiu *et al.*, 2014; Warfield *et al.*, 2009). Mouse-adapted MARV (MA-MARV) had up to 19 amino acid substitutions, while the guinea pig-adapted MARV contained only four mutations (Lofts *et al.*, 2007; Lofts *et al.*, 2011; Qiu *et al.*, 2014; Warfield *et al.*, 2009). Thus, the increase of MARV pathogenicity in guinea pigs occurred earlier during passaging and was accompanied by lower number of mutations in viral genome in comparison with adaptation of MARV to mice (Fig. 5) (Lofts *et al.*, 2007; Lofts *et al.*, 2011; Qiu *et al.*, 2014; Warfield *et al.*, 2009). Adaptation of EBOV to guinea pigs took less passages, as well as, less adaptive mutations were observed than in mice-adapted EBOV (Banadyga *et al.*, 2016). Remarkably, it has been shown by using the reverse genetics approach that not all mutations detected in rodent-lethal EBOV are necessary for the increased pathogenicity (Ebihara *et al.*, 2006; Mateo *et al.*, 2011). For example, 10 non-silent mutations were detected in 5 genes of MA-EBOV, but only two mutations (one mutation in VP24 and one in NP) introduced into recombinant EBOV were sufficient to induce lethal disease in mice (Ebihara *et al.*, 2006). Whether this is the case for rodent-lethal MARV (RL-MARV) is unknown because there are no studies on molecular determinants of RL-MARV using a reverse genetics approach.

How rodent-lethal MARV mutations influence the function of viral proteins in a new host remains mostly unknown, so far only the impact of mutations in VP40 of MA-MARV on the VP40 interferon antagonistic function in mouse cells has been analyzed (Feagins & Basler, 2014; 2015; Valmas & Basler, 2011).

1.5 Morphology and genome organization

Electron microscopic (EM) analysis of Marburg virus particles revealed that the virions can have filamentous, six-shaped, crooked- or donut-like shapes (Bharat *et al.*, 2011; Geisbert & Jahrling, 1995; Siegert *et al.*, 1967; Welsch *et al.*, 2010). Interestingly, a link between particle shape and infectivity has been suggested, for instance, donut-shaped particles are considered as non-infectious (Welsch *et al.*, 2010). Virions are variable in length and can reach up to 1400 nm (Bharat *et al.*, 2011). The diameter of virions is 80 nm (Bharat *et al.*, 2011; Geisbert & Jahrling, 1995). The core of the particle consists of the viral RNA encapsidated by the nucleocapsid proteins NP, VP30, VP35, VP24 and L (Fig. 3) (Becker *et al.*, 1998; Feldmann *et al.*, 1993; Martini & Siegert, 1971). The nucleocapsid complex is covered by a host derived lipid bilayer containing the matrix protein VP40 on the inner side of the envelope and the homotrimeric glycoprotein GP inserted into the envelope (Fig. 3) (Bamberg *et al.*, 2005; Bharat *et al.*, 2011; Feldmann *et al.*, 1991; Noda *et al.*, 2002).

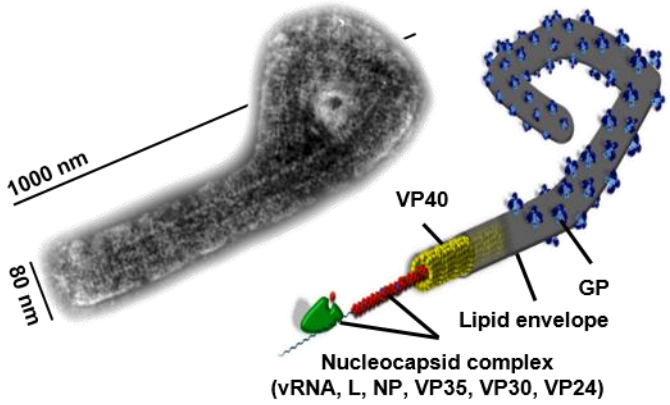

Figure 3: Marburg Virus particle morphology and composition
Representative electron microscopic picture of a MARV particle (left), kindly provided by Dr. Larissa Kolesnikova. Schematic picture of a MARV particle and its protein composition (right), kindly provided by Dr. Gordian Schudt.

The non-segmented RNA genome is 19.1 kb long and of negative orientation. It encodes seven proteins NP, VP35, VP40, GP, VP35, VP24 and L (Fig. 4) (Feldmann *et al.*, 1992; Kiley *et al.*, 1988; Mühlberger *et al.*, 1992). Due to its orientation, the genome itself is not infectious and the nucleocapsid proteins are mandatory to run viral replication and transcription.

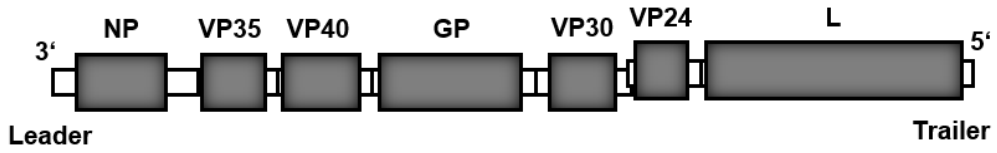

Figure 4: Genome organization of the Marburg virus

The non-segmented negative strand virus genome starts with the 3‘ leader followed by the sequences coding for the viral proteins NP, VP35, VP40, GP, VP30, VP24 and the L protein (gray boxes) and ends with the 5’ trailer sequence. Between the protein encoding sequences are non-transcribed intergenic sequences (white boxes) containing an overlap between VP30 and VP24.

The genome is flanked by non-transcribed regions (3’ leader and 5’ trailer) that contain signals for replication initiation as well as for packaging by the nucleoprotein NP (Mühlberger, 2007). The open reading frames (ORF) are separated by non-transcribed intergenic regions, which overlap between the VP30 and VP24 genes, and are known to contain highly conserved signals for the transcription–initiation and –termination (Feldmann *et al.*, 1992; Mühlberger *et al.*, 1996; Sanchez *et al.*, 1993; Weik *et al.*, 2005). Transcription-re-initiation is prone to failure at every gene border, resulting in a constant decline of transcription of the following gene (Shabman *et al.*, 2013; Shabman *et al.*, 2014). Therefore, the quantity of viral mRNAs forms a gradient, with NP as the most abundant and L as the least transcribed gene (Shabman *et al.*, 2013; Shabman *et al.*, 2014).

1.6 Functions of Marburg virus proteins and mutations detected in rodent-lethal Marburg virus

1.6.1 Nucleoprotein (NP)

This chapter will briefly introduce the MARV proteins. The aim is to give an insight into the main functions of the viral proteins for the viral life cycle and to provide informations about the presence, of mutations that were detected in RL-MARV. In addition, information about studies devoted to the impact of RL-MARV mutations on the viral protein function in a new species will be shown.

The nucleoprotein (NP) encapsidates the genomic and antigenomic viral RNAs and serves as the structural basis of the nucleocapsid complex necessary for transcription and replication (Mühlberger *et al.*, 1998). During virus infection or single ectopic expression, NP accumulates in perinuclear inclusion bodies. Viral inclusion bodies represent the site of viral transcription and replication (Becker *et al.*, 1998; Hoenen *et al.*, 2012). NP directly interacts with VP30, VP35 and shows weak interactions with VP40 (Becker *et al.*, 1998; Bharat *et al.*, 2011; Dolnik *et al.*, 2008; Dolnik *et al.*, 2010; Liu *et al.*, 2011; Spiegelberg *et al.*, 2011).

In total only three mutations, T14S, Y210H and Y536H have been observed in NP from four RL-MARV strains (Cross *et al.*, 2015; Lofts *et al.*, 2007; Lofts *et al.*, 2011; Warfield *et al.*, 2009) (Fig. 5). Interestingly the mutation T14S was observed twice in a guinea pig- and a mouse-lethal Marburg Ravn virus (Cross *et al.*, 2015; Warfield *et al.*, 2009). The effect of these mutations in NP on the virulence of the rodent-lethal viruses has not been investigated to date.

1.6.2 Viral protein 35 (VP35)

The viral protein 35 (VP35) acts as a polymerase cofactor and is mandatory for efficient viral replication and transcription (Mühlberger *et al.*, 1998; Mühlberger *et al.*, 1999). VP35 binds to L and leads to a re-localization of L into NP-derived inclusions (Becker *et al.*, 1998). Besides these functions VP35 blocks the interferon (IFN) production, by prevention of the activation of retinoic acid inducible gene I (RIG-I) through binding to dsRNA (Bale *et al.*, 2012; Ramanan *et al.*, 2012).

In total nine amino acid substitutions were observed in VP35 from four different strains of RL-MARV (Lofts *et al.*, 2007; Marzi *et al.*, 2016; Qiu *et al.*, 2014; Warfield *et al.*, 2009) (Fig. 5). All mutations were located in the N-terminal region of VP35 (Lofts *et al.*, 2007; Qiu *et al.*, 2014; Warfield *et al.*, 2009). No studies were performed to analyze the importance of these mutations in VP35 for the virulence of MARV in rodents. An effect of these mutations on the IFN antagonistic function of VP35 has not been analyzed, perhaps, because the IFN inhibitory domain is located in the C-terminal domain of VP35 (Albariño *et al.*, 2015; Ramanan *et al.*, 2012).

1.6.3 Viral protein 40 (VP40)

The viral protein 40 (VP40) is encoded by the third MARV gene, contains 303 amino acids, and fulfils many functions in the viral life cycle: assembly, budding, IFN antagonist, regulator of transcription and replication. VP40 consists of an N-terminal domain important for homo-oligomerization and an containing an interferon antagonistic function, and a C-terminal domain vital for membrane binding (Oda *et al.*, 2015). VP40 is synthesized as cytosolic protein and associates rapidly after synthesis with membranes (Kolesnikova *et al.*, 2004a). VP40 is the driving force of particle assembly and budding, single ectopic expression of VP40 results in production and release of filamentous virus-like particles (VLPs), resembling virions (Kolesnikova *et al.*, 2004b; Noda *et al.*, 2002; Swenson *et al.*, 2004). Co-expression of VP40 and nucleocapsid proteins results in redistribution of nucleocapsid proteins from the perinuclear region to the

plasma membrane and incorporation of nucleocapsid-like complexes into VLPs (Dolnik *et al.*, 2008; Kolesnikova *et al.*, 2007b; Mittler *et al.*, 2007; Wenigenrath *et al.*, 2010). Remarkably, not only nucleocapsid proteins, but also GP can be redistributed by VP40 to the site of budding, for example, in polarized cells apically located GP is redistributed to the basolaterally located VP40-enriched membrane clusters (Kolesnikova *et al.*, 2007b). Due to an unknown mechanism co-expression of VP40 and GP enhances the release of VP40-induced VLPs (Han & Harty, 2005; Kolesnikova *et al.*, 2004b; Swenson *et al.*, 2004).

In MARV infected cells, VP40 is detectable in multivesicular bodies and to a lesser extent in inclusion bodies and in the nuclei (Kolesnikova *et al.*, 2004b). A role of VP40 in regulation of transcription and replication has been observed, but is poorly understood (Hoenen *et al.*, 2010). VP40 has a regulatory role on minigenome replication and transcription and substantially suppresses the reporter gene activity upon co-expression in the minigenome system (Hoenen *et al.*, 2010; Koehler *et al.*, 2016; Koehler *et al.*, 2015).

MARV VP40 is a potent IFN antagonist. It inhibits the activation of the Jak-STAT pathway by inhibiting the phosphorylation of Janus kinase 1 (Jak1) (Valmas *et al.*, 2010). Regulation of the different VP40 functions remains poorly understood, it might be mediated through specific structural states of VP40 such as monomers, dimers and higher oligomers (Dolnik *et al.*, 2008; Lenard, 1996; Oda *et al.*, 2015).

Almost all so far developed RL-MARVs contain mutations in VP40 (Fig. 5). Up to ten mutations (Y7H, Y19H, Y27S, L34P, V57A, Q112L, T165A, D184N, N189S, T190A) in VP40 have been detected in mouse-lethal MARV Ravn, and from one to three mutations have been observed in VP40 of guinea pig-lethal MARV (Cross *et al.*, 2015; Lofts *et al.*, 2007; Lofts *et al.*, 2011). Analysis of MA-MARV mutations in VP40 was devoted to the interferon antagonistic function of VP40 in a new host (Fig. 5) (Feagins & Basler, 2015; Valmas & Basler, 2011). It has been shown that the mutations V57A, T165A and G79S are important while, D184N, Y7H, Y19H, Y27S, L34P, Q112L, N189S and T190A are not important for the inhibition of the interferon signaling in mouse cells (Feagins & Basler, 2015; Valmas & Basler,

2011).

The D184N mutation is of special interest due to its repeated occurrences in VP40 of rodent-lethal MARV strains (Lofts *et al.*, 2007; Lofts *et al.*, 2011; Marzi *et al.*, 2016; Warfield *et al.*, 2009). The D184N mutation in VP40 appeared at early passages in two MA-MARV strains suggesting its necessity for adaption of MARV to rodents (Lofts *et al.*, 2011). In addition, the D184N mutation is present in the reference sequence of MARV Ci67, obtained after several passages in hamsters (Lofts *et al.*, 2011). However, the impact of the D184N mutation in VP40 for the MARV pathogenicity in rodents remains unclear.

1.6.4 Glycoprotein (GP)

The single surface glycoprotein GP, is the only MARV protein which is synthesized at the endoplasmatic reticulum (Feldmann *et al.*, 1991). Following synthesis, GP is post-translationally modified by glycosylation, phosphorylation and acylation (Becker *et al.*, 1996; Feldmann *et al.*, 1991; Funke *et al.*, 1995; Sänger *et al.*, 2002). GP is cleaved in the *trans* Golgi network into GP_1 and GP_2 by either furin or furin-like proteases (Volchkov *et al.*, 2000b). The subunits remain linked via two disulfide bonds (Volchkov *et al.*, 2000b). Trimers of filoviral GP are present in the viral envelope, necessary for virus attachment and cell entry through binding to the endosomal/lysosomal receptor Niemann-Pick C1 (NPC1) (Carette *et al.*, 2011).

Only four amino acid mutations, F445P, N422D, N283H and G435A have been observed in GP of mouse-lethal MARV (Cross *et al.*, 2015; Lofts *et al.*, 2011; Qiu *et al.*, 2014) (Fig. 5). Whether these mutations in GP improve MARV entry into mouse cells remains to be analyzed.

1.6.5 Viral protein 30 (VP30)

The viral protein 30 (VP30) is a component of the nucleocapsid complex and recruited by NP into perinuclear inclusion bodies (Becker *et al.*, 1998). The role of VP30 in the viral life cycle is not fully understood. MARV VP30 is not essential for replication and transcription in a minigenome based reporter assay, however presence of VP30 is crucial to rescue recombinant MARV (Enterlein *et al.*, 2006; Mühlberger *et al.*, 1998). VP30 has a regulatory role on viral transcription, since siRNA mediated knockdown of VP30 reduced the transcription of all other viral mRNAs (Fowler *et al.*, 2005).

Only one mutation, N103D, has been found in VP30 of a mouse-lethal MARV (Qiu *et al.*, 2014) (Fig. 5). The importance of this mutation for the increased MARV pathogenicity in rodents is unknown.

1.6.6 Viral protein 24 (VP24)

The viral protein 24 (VP24) is the smallest MARV protein. Within the virion, VP24 is in close proximity to the nucleocapsid, supporting the growing evidence that it might act as a condensation factor of the nucleocapsid complex (Bharat *et al.*, 2011; Watt *et al.*, 2014). A role of VP24 as nucleocapsid maturation factor or its importance for viral assembly has been presumed as well (Bamberg *et al.*, 2005). It has been shown that a Flag-tagged MARV VP24 does not suppress viral replication and transcription (Bamberg *et al.*, 2005). The specific role of VP24 remains enigmatic.

Three amino acid changes in VP24 were found in mouse-lethal MARV, V157M, V66I and L216S (Fig. 5) (Cross *et al.*, 2015; Qiu *et al.*, 2014). The relevance of these mutations for the higher MARV virulence in rodents remains unknown.

1.6.7 Polymerase L protein (L)

The polymerase L protein (L) is the largest of the seven MARV proteins. It consists of 2331 amino acids and has an apparent molecular weight of 267 kDa (migrates at ~220 kDa in SDS-PAGE) (Mühlberger *et al.*, 1992). L together with VP35 forms the RNA-dependent RNA polymerase (RdRp) complex essential for viral transcription and replication of the viral genome (Becker *et al.*, 1998; Mühlberger *et al.*, 1998). The MARV L protein has six conserved regions (CR I - VI) which show a high degree of sequence homologies with L proteins of other non-segmented negative strand (NNS) RNA viruses (Mühlberger *et al.*, 1992; Poch *et al.*, 1990). The CR I - IV of MARV L are presumed to be part of the predicted RNA-dependent RNA polymerase domain (Liang *et al.*, 2015; Poch *et al.*, 1990). CR III contains the highly conserved GDN motif which is present in all L proteins of NNS RNA viruses (Liang *et al.*, 2015; Poch *et al.*, 1990). Mutations in or in close proximity to the GDN motif severely abolish the polymerase function, supporting the idea that CR III represents the active site of the L protein (Magoffin *et al.*, 2007; Malur *et al.*, 2002; Noton *et al.*, 2012; Schnell & Conzelmann, 1995; Sleat & Banerjee, 1993; Smallwood *et al.*, 2002). CR IV most likely encodes the mRNA capping domain necessary for production of mRNAs. CR VI is suggested to encode a methyltransferase domain important for regulation of viral transcription (Poch *et al.*, 1990). While CR I - IV are highly conserved among L proteins of NNS, CR V and CR VI are more variable and considered as regions that interact with host cell cofactors (Dortmans *et al.*, 2011; Poch *et al.*, 1990; Sidhu *et al.*, 1993).

Adaptive mutations in the L protein of MARV upon passaging in rodents were observed only once, in a guinea pig-adapted MARV. All three detected mutations were located in the active site of the L protein (Fig. 5) (Lofts *et al.*, 2007). The functional relevance of these guinea pig-adaptive mutations in L is unknown.

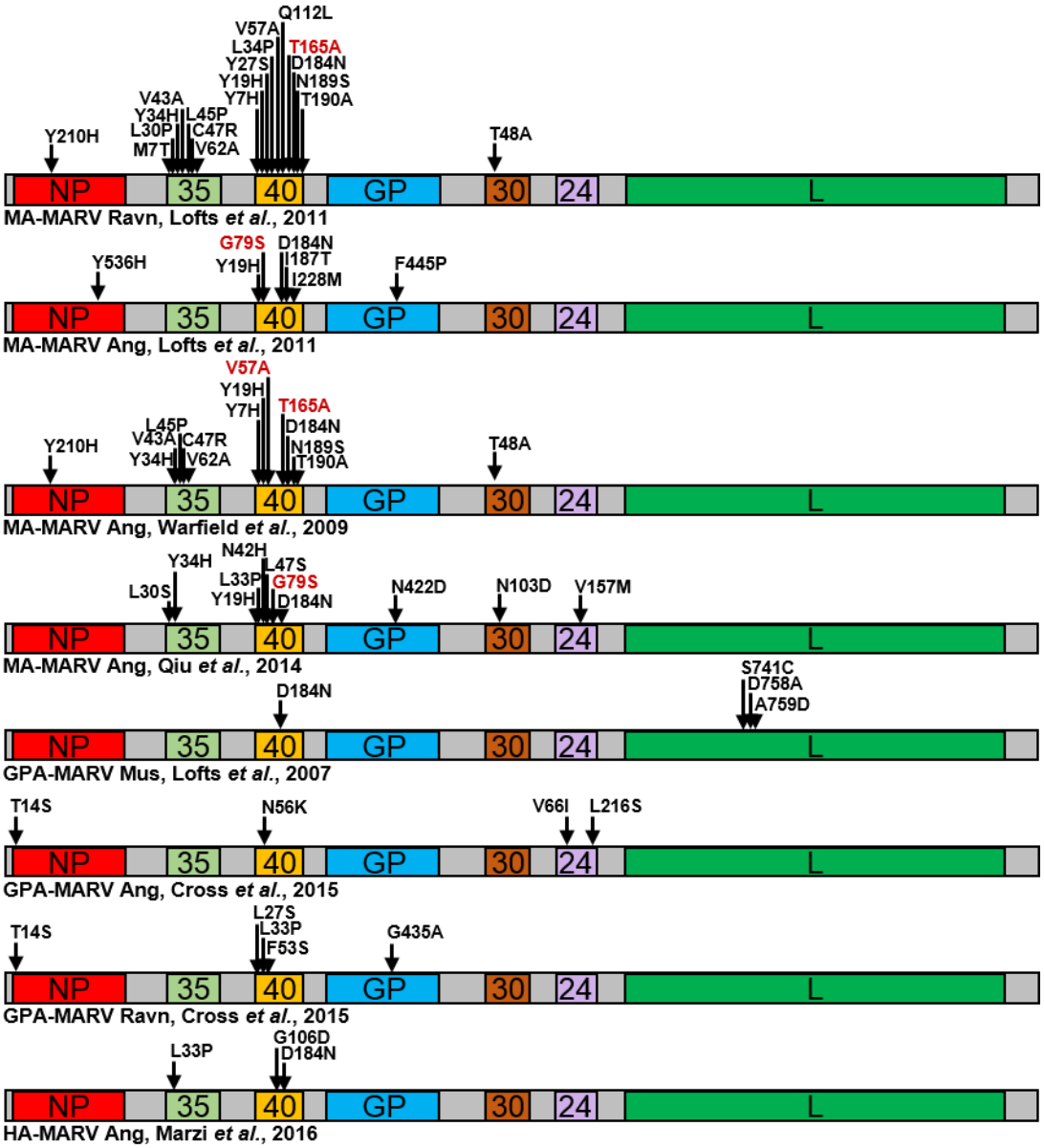

Figure 5: Scheme representing amino acid substitutions in rodent-lethal MARVs

Amino acid substitutions are indicated by the one letter amino acid code and the position of the substitution within each gene is marked by arrows. Red colored substitutions indicate mutations which have been demonstrated to have an impact on the species-specific protein function. MA (Mouse-adapted), GPA (Guinea pig-adapted), HA (Hamster-adapted), Ravn (Marburg virus Ravn isolate), Mus (Marburg virus Musoke isolate), Ang (Marburg virus Angola isolate). Figure modified from (Banadyga *et al.*, 2016).

1.7 The viral replication cycle

In a simplistic view virus replication can be divided into three phases. First, virions attach to the host cell and enter via macropinocytosis (Mulherkar *et al.*, 2011; Nanbo *et al.*, 2010). Second, transcription and replication of the viral genome takes place. Third, newly produced viruses assemble and bud from the infected cell.

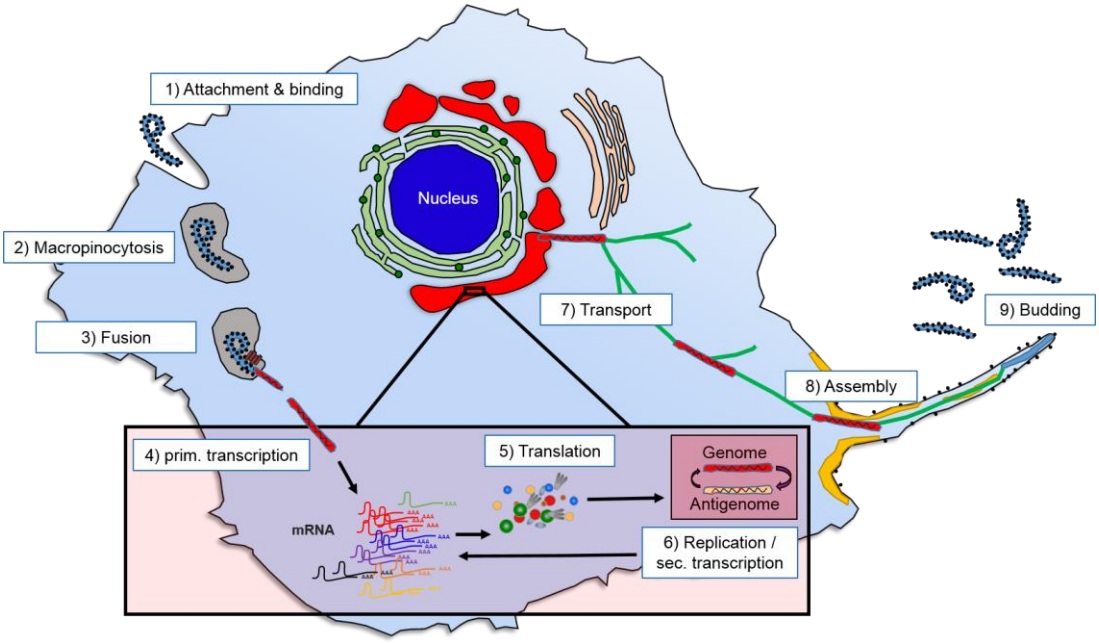

Figure 6: The viral replication cycle

Attachment and binding of MARV virions to the host cells can be facilitated through several surface molecules such as DC-SIGN or TIM-1 (1). MARV particles enter the cell predominantly via macropinocytosis (2). By interaction of GP with NPC1 the viral envelope fuses with the endosomal membrane, leading to entry of the nucleocapsid into the cytoplasm (3). Steps 4-6 are processes that are carried out in inclusion bodies, they are shown in the transparent red box. Once the nucleocapsid entered the cell, primary transcription is initiated and production of viral mRNAs starts (4). The viral mRNAs are translated into the corresponding proteins (5). Production of the viral proteins supports secondary transcription and finally leads to replication of the viral genome via the intermediate antigenome (6). Maturation of the nucleocapsids takes place in the inclusion bodies (red), the mature nucleocapsids are transported to the plasma membrane via polymerization of actin (7). In close proximity to the membrane the mature nucleocapsid comes in close contact to VP40 (yellow) and GP (black speckles) leading to assembly of the viral particles (8). The virus particle is released into the supernatant via filopodia (9).

Research on the attachment and entry mechanisms of MARV are limited compared to EBOV. However, due to high structural similarities of the filoviral glycoproteins, it is assumed that cell entry is achieved in a similar manner (Hashiguchi *et al.*, 2015; Koellhoffer *et al.*, 2012).

Filoviral attachment and entry is provided by interactions with one or multiple cellular receptors e.g. T-cell immunoglobuline and mucin domain 1 (TIM-1), Ax1, Mer and several C-type lectins including DC-SIGN and LSECtin (Fig. 6, step 1) (Becker *et al.*, 1995; Brindley *et al.*, 2011; Gramberg *et al.*, 2005; Kondratowicz *et al.*, 2011; Marzi *et al.*, 2004; Shimojima *et al.*, 2006). However, cells lacking these molecules are still susceptible to filoviral infection, suggesting the presence of additional mechanisms for viral attachment and entry (Kondratowicz *et al.*, 2011; Matsuno *et al.*, 2010). Existence of such mechanisms would explain the wide cell tropism of filoviruses (Kondratowicz *et al.*, 2011; Sinn *et al.*, 2003). The major entry route of filoviruses into target cells is considered to be macropinocytosis, the macropinosome fuses subsequently with endosomes (Fig. 6, step 2) (Aleksandrowicz *et al.*, 2011; Bhattacharyya *et al.*, 2011; Mulherkar *et al.*, 2011; Nanbo *et al.*, 2010; Saeed *et al.*, 2010). GP1 is proteolytically activated by endosomal host proteases (Chandran *et al.*, 2005; Misasi *et al.*, 2012). Activation of GP1 allows binding to the filovirus specific endosomal receptor Niemann-Pick 1 (NPC1), while GP2 mediates fusion between the viral and the endosomal membrane (Fig. 6, step 3) (Carette *et al.*, 2011; Markosyan *et al.*, 2016). Enzymes that proteolytically activate GP1 are unknown for MARV, but it has been shown that EBOV GP is activated by Cathepsin B and L (Gnirss *et al.*, 2012). Upon fusion of the viral envelope and the endosomal membrane the viral nucleocapsid is released into the cytoplasm (Koellhoffer *et al.*, 2012; Markosyan *et al.*, 2016).

Primary transcription and production of viral mRNAs starts soon after the entry of the nucleocapsid into the cytoplasm and is detectable 2-4 h post EBOV infection (p.i.) (Fig. 6, step 4) (Hoenen et al., 2012; Nanbo et al., 2013). Transcription is carried out by the polymerase complex consisting of NP, VP35 and L (Mühlberger *et al.*, 1998). MARV VP30 seems to have a supportive role (Mühlberger et al., 1998). Initiation of transcription occurs at the 3'-leader region of the genome exclusively (Mühlberger et al., 1999). The transcribed mRNAs follow a gradient as previously explained, see chapter 1.4 (Shabman et al., 2013; Shabman et al., 2014).

Translation of viral mRNAs is facilitated by the host translational machinery (Fig. 6, step 5). Except GP, all viral mRNAs are translated by free ribosomes in close proximity to the perinuclear region. Translation of the NP mRNA, which is the

most abundant, results in formation of perinuclear inclusion bodies (Kolesnikova *et al.*, 2000). GP is synthesized on ER associated ribosomes, it is processed and transported to the cell surface via the secretory pathway (Volchkov *et al.*, 2000b).

Replication of viral genomes occurs in perinuclear inclusion bodies and can be detected 12-16 h p.i. by reverse transcription quantitative PCR (RT-qPCR) and in-situ hybridization (Fig. 6, step 6) (Hoenen *et al.*, 2012; Nanbo *et al.*, 2013). During replication, the 5'-3' antigenome is synthesized, which then serves as template for the synthesis of negative sensed viral 3'-5' genomes (Fig. 6, step 6). Both, the 3'- and the 5'- end contain short complementary sequences of 13 nucleotides, which most likely provide binding sites for the polymerase complex (Enterlein *et al.*, 2009; Whelan *et al.*, 2004). The viral antigenome and viral genome are encapsidated by the nucleoprotein, preventing viral RNA from degradation by cellular RNases (Mühlberger *et al.*, 1998; Mühlberger *et al.*, 1999).

Mature nucleocapsids assemble and accumulate in inclusion bodies, their transport to the plasma membrane depends on polymerization of actin (Fig. 6, step 7) (Schudt *et al.*, 2013). Envelopment of nucleocapsids with VP40- and GP-enriched membrane and fission of viral particle from plasma membrane leads to the formation of infectious virions. Budding of infectious virions occurs at the tip of filopodia and to a lesser extent at the flat surfaces of the plasma membrane (Fig. 6, step 8-9) (Bharat *et al.*, 2011; Kolesnikova *et al.*, 2007a; Kolesnikova *et al.*, 2007b; Welsch *et al.*, 2010). Filopodia are known as dynamic, actin enriched, filamentous cellular protrusions, which are hijacked by filoviruses, and most likely provide efficient transfer of virus particles to neighboring cells (Faix & Rottner, 2006; Kolesnikova *et al.*, 2007a).

1.8 BSL-2 models as a tool to study the function of viral proteins in a new host

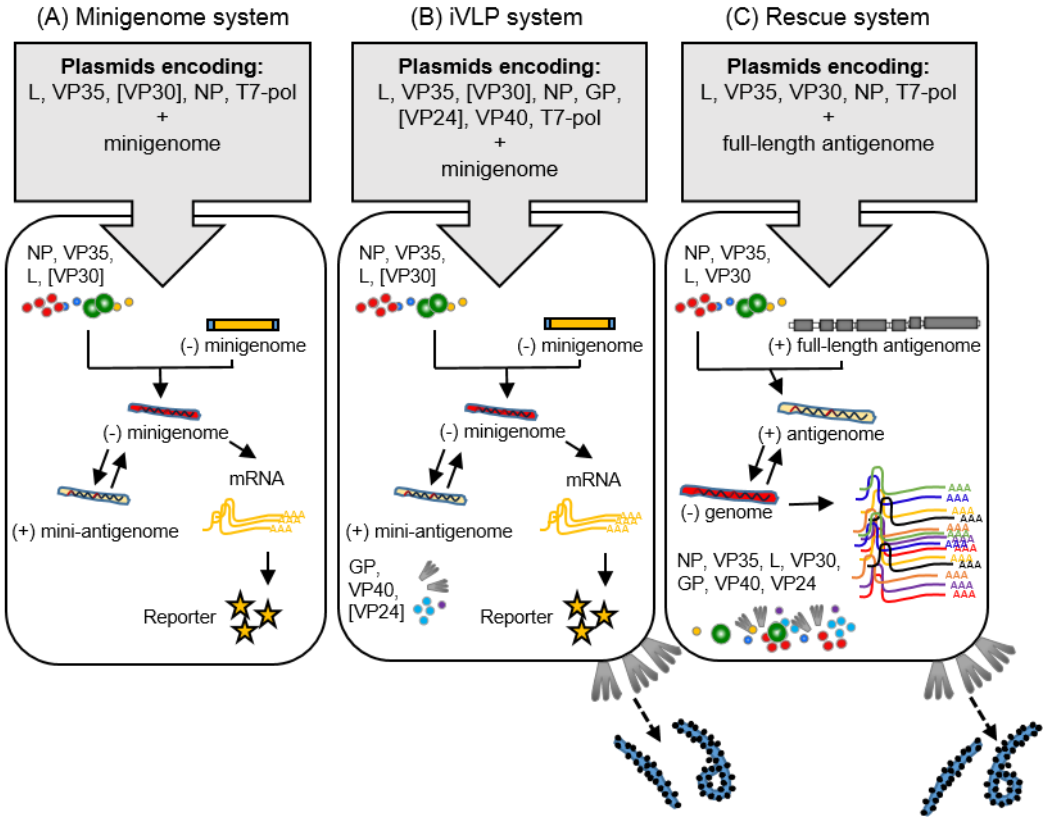

Figure 7: MARV reverse genetic systems

(A) Minigenome system, (B) infectious virus-like particle system and the (C) Rescue system for recombinant viruses. In the minigenome system viral replication and transcription process is simulated by transfection of plasmids encoding NP, VP35, VP30, L and the minigenome (A). In the iVLP system additional transfection of VP24-, GP- and VP40-encoding plasmids leads to production of infectious virus-like particles (B). All systems require transfection of the T7 polymerase (T7-pol) facilitating efficient expression of the negative orientated RNA minigenome or the full-length RNA genome. Viral RNA minigenomes or the full-length genomes are encapsidated by the expressed nucleocapsid proteins. Transcription of the minigenome leads to reporter gene expression in the minigenome and iVLP system (A, B). iVLPs can be used for infection of indicator cells (B). Plasmids in brackets are not crucial for efficient replication and transcription but enhance the reporter gene activity. Figure modified from (Schmidt & Mühlberger, 2016).

Reverse genetics are commonly used for BSL-3/4 viruses to develop powerful BSL-2 compatible tools able to simulate multiple steps of the viral life cycle (Schmidt & Mühlberger, 2016; Wenigenrath *et al.*, 2010). These model systems are useful for the analysis of functional changes in viral proteins induced by mutations, e.g., adaptive mutations occurring in rodent-lethal filoviruses. Reverse genetics are defined by the directed introduction of nucleotide changes

within a specific gene, for example, into viral genes, and the subsequent characterization of the resulting phenotype. Application of plasmids encoding mutated proteins and relevant assays in cell lines of different species might help to understand whether mutations can provide rodent-lethal MARV with species-specific advantages.

1.8.1 Minigenome system

The first minigenome system was developed in the early 90s for the vesicular stomatitis virus (Pattnaik *et al.*, 1992; Pattnaik & Wertz, 1990; 1991). The minigenome systems for filoviruses were developed in 1998 (Mühlberger *et al.*, 1998; Mühlberger *et al.*, 1999). The MARV minigenome contains the 3'- and 5'-sequences of the viral genome which contain the *cis*-acting signals for initiation of replication, transcription and encapsidation under the control of the T7 promoter, as well as the sequence encoding a reporter gene (Mühlberger *et al.*, 1998). Transfection of cells with the minigenome encoding plasmid, plasmids encoding the T7 polymerase (T7-pol) and the viral proteins NP, VP30, VP35 and L allows synthesis of the T7-pol-derived minigenomic RNA (Mühlberger *et al.*, 1998; Schmidt & Mühlberger, 2016). The negative-sensed RNA minigenome is then encapsidated by NP. The resulting mininucleocapsid is transcribed by the ectopically expressed viral polymerase complex to generate the reporter mRNA, which is subsequently translated to the reporter protein (Fig. 7A). While the original MARV minigenome contained a chloramphenicol acetyltransferase as reporter, the minigenome used in this study encoded the *Renilla* luciferase. Thus, measurement of the luciferase reporter gene activity allowed to determine and compare the transcription and replication activity in cells derived from different species, as well as for wild type and mutated nucleocapsid complex proteins.

1.8.2 Infectious virus like particle (iVLP) assay

The expression of all plasmids required for the minigenome assay together with the expression of plasmids encoding VP40, GP and VP24 results in production of infectious virus-like particles (iVLP) (Wenigenrath *et al.*, 2010). The iVLP assay allows to study the assembly, budding and infectivity of iVLP (Fig 7B). Application of this assay can clarify e.g., which step of virus assembly is influenced by adaptive mutations in viral proteins.

1.8.3 Rescue system of recombinant MARV

Rescue systems of NNS viruses are available since the mid-90s and have greatly improved the understanding of the viral life cycle and functions of viral proteins (Schnell *et al.*, 1994). Rescue of recombinant full-length viruses is based on a DNA plasmid that encodes the full length viral genome under the control of the T7-pol (Albariño *et al.*, 2013b; Enterlein *et al.*, 2006; Krähling *et al.*, 2010). Presence of the T7-pol allows the generation of the full-length genome template which is then replicated and packaged into infectious virus particles by the ectopically expressed viral nucleocapsid proteins (Schmidt & Mühlberger, 2016). Recombinant MARVs have been used in several studies to determine the effect of mutations in the viral genome on virus production (Albariño *et al.*, 2015; Dolnik *et al.*, 2014; Mittler *et al.*, 2013). Addition or deletion of genes in a new ORF or tagging of viral proteins have been successfully performed (Fig. 7C) (Enterlein *et al.*, 2006; Halfmann *et al.*, 2008; Schmidt *et al.*, 2011; Schudt *et al.*, 2013).

1.9 Aim of the study

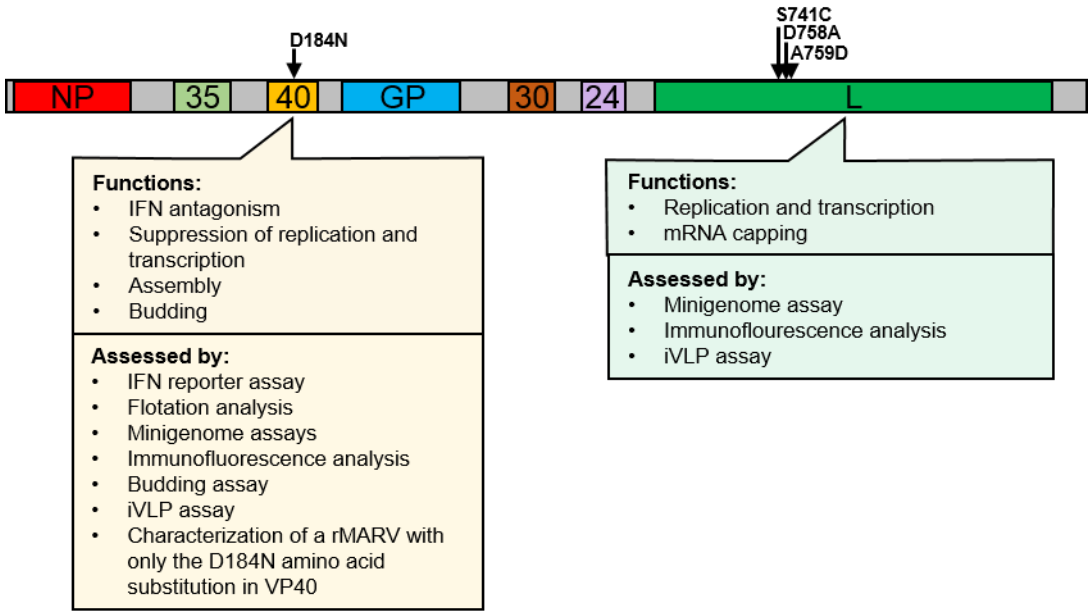

Figure 8: Schematic presentation of the aims of the study

Mutations present in viral proteins of the guinea pig-lethal MARV (Lofts *et al.* 2007) are indicated by arrows above the schematic viral genome. The boxes show the single functions of the viral proteins VP40 (yellow) and L (green) and the approaches that will be used to determine the impact of these mutations on the protein functions in human and guinea pig cells.

The virulence of MARV is species-specific. While being highly pathogenic in humans and non-human primates, MARV is non-virulent for rodents. An increase in pathogenicity of MARV in rodents can be induced by multiple passages of the virus in rodents. Those rodent-lethal MARVs harbor several mutations in the viral genome (Fig. 5). A guinea pig-lethal MARV established by Lofts et al. in 2007 harbors four amino acid changes, a D184N mutation in VP40 and three mutations, S741C, D758A and A759D, in the L protein (Fig.5). How these mutations influence the function of viral proteins in the guinea pig cells remains obscure.

VP40 is a multifunctional protein that fulfills many important functions in the viral life cycle (Fig. 8) (Kolesnikova *et al.*, 2012). This work aims to determine the effect of the D184N mutation in VP40 on the different functions of VP40, such as virus assembly, budding, inhibition on replication and transcription and the VP40-mediated interferon antagonism in guinea pig and human cells (Dolnik *et al.*, 2008; Hoenen *et al.*, 2010; Kolesnikova *et al.*, 2004a; Kolesnikova *et al.*, 2004b; Valmas *et al.*, 2010). This will be clarified using different methods to investigate

the influence of the D184N mutation on the multiple functions of VP40 in human and guinea pig cells (Fig. 8).

The viral polymerase L is essential for transcription and replication (Fig. 8) (Becker *et al.*, 1998; Mühlberger *et al.*, 1998; Mühlberger *et al.*, 1999). There are no antibodies that detect the MARV polymerase L, therefore, to allow efficient detection of the L protein by Western blotting and immunofluorescence a functional L protein containing a mCherry-tag will be created. Furthermore, we plan to insert all possible combinations of the guinea-pig lethal mutations into the fluorescently tagged L protein to characterize the effect of these mutations on replication and transcription activity (Fig. 8). This will be addressed by analysis of the wildtype L protein or the L mutants in minigenome reporter assays in human and guinea pig cells (Fig. 8). Additionally, a possible additive effect of the single D184N mutation in VP40 and relevant L mutations on replication and transcription will be analyzed using the minigenome assay. It is expected that these studies will elucidate the role of the mutations present in the guinea pig-lethal MARV for the species-specific improvement of the viral protein functions and increase of viral fitness. This study could lead to a better understanding of factors that modulate MARV virulence.

The aim of this study was to analyze the species-specific effects of these guinea pig-adaptive mutations on the function of VP40 and L (Fig. 8).

2 Methods

2.1 Molecular biological and biochemical methods

2.1.1 Polymerase chain reaction (PCR), amplification of specific DNA sequences

The polymerase chain reaction (PCR) is a method used to amplify specific DNA sequences in vitro. Short complementary DNA sequences (15-25 bp), so called primers, provide the sequence specificity of the reaction. The primer pair binds to the target sequence and is recognized by DNA dependent DNA polymerases, leading to synthesis and amplification of the desired fragment. Depending on the aim and strategy of the cloning project, the 5'- end can be modified to introduce additional restriction enzyme cutting sites or small tags (e.g. myc-tag). DNA polymerases contain a 5'-3' polymerase activity as well as a proofreading activity carried out by the 3-5' exonuclease activity able to correct mismatches of the newly synthesized DNA strand. Polymerases can differ in their replication and error rate. The commonly used *Pwo* polymerase has a low error rate (McInerney *et al.*, 2014). PCR products were purified via agarose gel electrophoresis and subsequent gel extraction with the E.Z.N.A Gel Extraction Kit. A reaction for a PCR was set up as following according to the manufacturer's manual:

Reagent	Amount
DNA sample	25-100 ng
dNTPs	each 10 mM
Forward primer	12.5 µM
Reverse primer	12.5 µM
10x buffer, Peqlab	5 µL
Pwo Polymerase (1 U/ µL), Peqlab	0.125 µL
dH_20	Ad 50 µL

	Temperature	Time	Cycles
Denaturation	94°C	2 min	1
Denaturation	94°C	15 sec	30-40
Annealing	50-65°C	30 sec	
Elongation	72°C	1 min/kb	
Elongation	72°C	2 min	1
Storage	4°C	∞	1

2.1.2 Separation and visualization of DNA via gel electrophoresis

DNA has a negative charge provided by the phosphate groups. DNA fragments of different size are separated, depending on the agarose concentration of the agarose gels, by their physicochemical properties. The concentration of agarose in the gels varies depending on the size of the desired fragments but is usually between 0.5 and 2 %. The agarose was solved by heating in 1x TAE buffer and poured into an agarose gel chamber. 10-30 µL of sample were mixed with 6x Gel Loading Dye (NEB). As a marker for the fragment size 5 µL of the O'GeneRuler 1 kb Plus DNA Ladder (Thermo Scientific) were used. The gel electrophoresis ran at 100 V at maximum current for ~1 h with 1x TAE-buffer, pH 8.0 (chapter 7.5). DNA was stained with an aqueous ethidium bromide solution (1 µg/mL) for at least 15min. The ethidium bromide stained DNA was visualized with the GelDoc 2000 system (BioRad).

2.1.3 DNA digestions via restriction enzymes

Restriction enzymes can hydrolytically cleave double stranded DNA (dsDNA) via specific, often palindromic, nucleotide motifs. Restriction enzymes are used to generate DNA fragments for insertion into a plasmid. Alternatively, restriction enzymes can be used as a diagnostic tool, digestion of a plasmid at specific sites will result in a distinct band pattern upon agarose gel electrophoresis. Different DNA molecules, which differ in the number or position of restriction sites generate different DNA band patterns upon agarose gel electrophoresis. The used enzyme

buffers and reaction conditions may vary between enzymes. 1-20 µg of DNA were used for one reaction. The reactions were performed according to the NEB manufacturers guide or for double digestions according to the DoubleDigest finder tool available at the NEB homepage (www.neb.com/tools-and-resources/interactive-tools/double-digest-finder). The purification of the digested DNA fragment was performed with the E.Z.N.A DNA Probe Purification Kit or by separation of the fragment of interest on an agarose gel and consecutive sample purification with the E.Z.N.A. Gel Extraction Kit.

Set up for a diagnostic digestion:	100-500 ng of DNA 1 µL 10x buffer according to the manufacturers guide (1 µL of 10% BSA, optional) 1-5 U restriction enzyme ad 10 µL dH_2O
Set up for digestion of DNA for cloning:	5-20 µg of DNA 10 µL 10x buffer according to the manufacturers guide (10 µL of 10% BSA, optional) 10-20 U restriction enzyme ad 100 µL dH_2O

2.1.4 DNA purification

DNA fragments resulting from PCR amplification or restriction digests were purified using the E.Z.N.A. DNA Probe Purification Kit according to the manufacturer's protocol. The purification of specific fragments from agarose gels was done using the E.Z.N.A Gel Extraction Kit. The fragment of interest was removed from the agarose gel using a scalpel and a UV-light table (λ=302 nm). Purified DNA was stored at -20°C.

2.1.5 Dephosphorylation of DNA

In commonly used cloning strategies fragments of interest are inserted into linearized plasmids. Dephosphorylation via e.g. alkaline phosphatases are routinely used to restrict the religation of the linearized plasmid reducing the background of the ligation reaction. 1-20 µg of DNA (chapter 2.1.3) were used in a volume of 87 µL dH_2O for one reaction. The calf intestine phosphatase (CIP) and the dephosphorylation buffer (CIP buffer) were purchased from Roche. The dephosphorylation was performed according to the manufacturer's instructions.

Reagent	Volume [µL]
Linearized vector (1-20 µg)	87
10x CIP buffer, Roche	10
CIP (1 U/ µL), Roche	3

The reaction was incubated for 75 min at 37°C. The dephosphorylated DNA was purified via the E.Z.N.A DNA Probe Purification kit.

2.1.6 Ligation of DNA fragments into linearized vector

DNA ligases catalyze binding of phosphodiester bonds between a free 5'-phosphate from a DNA strand and a free 3'-OH of another adjacent DNA strand. This allows to clone DNA fragments into a linearized dephosphorylated vector. The ligation reaction was performed using the T4 DNA ligase (NEB) for at least 1 h at RT according to the manufacturer's protocol. The reaction mix was then transformed into competent bacteria (chapter 2.1.7). Due to their size (>19 kb) full-length plasmids were ligated overnight at 16°C.

Reagent	Volume [µL]
Fragment of interest	100-200 ng
Vector DNA	25-50 ng
Ligation buffer 10x, NEB	2
T4 DNA Ligase, NEB	0.5
dH_20	Ad 20

2.1.7 Transformation and selection of plasmids in bacteria

Upon transformation plasmid DNA is transferred into competent bacteria. Competent bacteria were prepared by treating *E.coli* (XL1 blue) according to the Z-Competent™ E.coli Transformation Kit (ZymoResearch). The transformation was carried out by thawing 100 µL of competent bacteria on ice and addition of DNA (e.g. 10 µL ligation reaction, 100 ng of plasmid DNA). The mixture of competent bacteria and DNA was incubated on ice for 20 min. After the transformation 100 µL of the bacteria were added to the LB plates (chapter 7.7.1) and incubated for >16 h at 37°C. LB plates contained 100 µg/mL of ampicillin, allowing efficient and selective growth of successfully transformed bacteria. PCR products from the QuikChange™ Multi Site Directed Mutagenesis Kit (Agilent) were transformed according to the protocol provided by the manufacturer.

2.1.8 DNA preparation from bacteria (mini-/ maxi-prep)

Plasmids were isolated from bacteria either from small scale 5 mL (mini prep) or large scale cultures 150 mL (maxi prep). The LB media (chapter 7.7.1) containing 100 µg/mL of ampicillin, for specific selection of the plasmid, was inoculated with a single bacterial colony. The inoculated media was incubated overnight (>16 h) at 37°C. Isolation of the plasmid DNA was performed using the manufacturer's protocol of either the E.Z.N.A Plasmid DNA Mini Kit I for mini preps or the E.Z.N.A FastFilter Plasmid DNA Maxi Kit for maxi preps. The isolated plasmid DNA was eluted in 50 µL (mini preps) or 1.5 mL (maxi preps) of elution buffer. The quality and concentration of the DNA was controlled using a photometer (NanoDrop Lite, Thermo Scientific). The sequence integrity was controlled via sequencing.

2.1.9 DNA quantification via the NanoDrop

DNA can be quantified directly in aqueous solutions due to the direct relation of the optical density and the DNA concentration at a wavelength of 260 nm (OD 260). The calculation for the concentration of double stranded DNA is based on the following equation:

OD 260 x dilution x 50 = DNA concentration [µg/ µL]

The quotient of the OD 260 to the OD 280 indicates the purity of the DNA. Quotients from 1.7 to 2.0 are considered as pure DNA preparations. Values <1.6 indicate contaminations by proteins or RNA. All samples were measured with the NanoDrop Lite, Thermo Scientific.

2.1.10 Site directed mutagenesis

The QuikChange™ Multi Site Directed Mutagenesis Kit (Agilent) was used to insert single mutations, deletions or insertions into plasmids of interest. Mutagenic primers were designed with the online tool: QuikChange Primer Design, the mutagenesis of the plasmids was accomplished using the manufacturer's protocol.

2.1.11 One step quantitative real-time PCR (RT-qPCR)

RT-qPCR is a very sensitive tool to detect and quantify a specific target sequence within a RNA pool. RT-qPCR can detect changes in the expression of target genes or determine the number of viral genome copies in a sample. RT-qPCR was performed according to the manufacturer's protocol of either the QuantiTect® Probe RT-PCR Kit to determine the number of viral genomes or the QuantiTect® SYBR® Green RT-PCR Kit to detect minigenomes present in the supernatants of virus-infected cells or iVLP preparations. Viral genomes were detected by primers and probes specifically designed to detect a unique region of the MARV polymerase L gene. Minigenomes were detected by primers directed against unique regions in the minigenome. The viral genome copies were calculated via

a standard curve and the minigenome copies based on their CT value. One reaction for the QuantiTect® Probe RT-PCR Kit consisted of:

Reagent	Conc. Stock	Volume [µL]
5x QuantiTect™ RT-PCR buffer, Qiagen	5x	6
QuantiTect™ RT Mix, Qiagen		1.2
dNTPs	10 mM	1.2
MARV rev	10 µM	0.6
MARV Probe	10 µM	0.6
DEPC H_2O		7.28
Template		10

	Temperature	Time	Cycles
Reverse transcription	50°C	30min	1
Denaturation	95°C	15min	1
Denaturation	94°C	20sec	46
Annealing	58°C	45sec	
Elongation	72°C	15sec	

One reaction for the QuantiTect® SYBR® Green RT-PCR Kit was composed of:

Reagent	Conc. Stock	Volume [µL]
2x QuantiTect® SYBR Green RT PCR Master Mix, Qiagen	2x	25
Forward primer	0.5 µM	2.5
Reverse primer	0.5 µM	2.5
QuantiTect® RT Mix, Qiagen		0.5
dH_20		14.5
Template		5

	Temperature	Time	Cycles
Reverse transcription	50°C	30 min	1
Denaturation	95°C	15 min	1
Denaturation	94°C	15 sec	45
Annealing	55°C	30 sec	
Elongation	72°C	30 sec	

2.1.12 DNA sequencing

Sanger sequence analyses were carried out by Seqlab laboratories. Samples were prepared as follows: 700-1500 ng of plasmid DNA and 30 pmol of the according primer were filled up to 15 µL with dH_2O. Plasmids containing the full genomic sequence of MARV were linearized by restriction digest with the enzyme NaeI and PvuI and subsequently purified via the E.Z.N.A. DNA Probe Purification Kit and sequenced.

2.1.13 Sodium dodecyl sulfate-polyacrylamide gel-electrophoresis (SDS- PAGE)

Sodium dodecyl sulfate-polyacrylamide gel electrophoresis (SDS-PAGE) is a commonly used method for separation of proteins based on their electrophoretic mobility. SDS serves as anionic detergent which denatures proteins and puts a negative charge on them. When an electric current is applied the proteins move towards the anode into an SDS containing polyacrylamide gel where the proteins will be separated predominantly by sheer size. The Tris-glycine or Tris-acetate-gel consists of a 5% polyacrylamide stacking gel followed by a separation gel with a higher concentrations of polyacrylamide. 4x loading buffer was added to the samples and the samples were denatured for 10 min at 100°C. The samples and a marker protein mixture, PageRuler™ Prestained Protein Ladder Plus, containing proteins with a specific molecular weight, were loaded on a 12% gel and separated in a SDS chamber filled with SDS running buffer at 25 mA at maximum voltage for 45-60 min for detection of VP40. After separation the SDS gel was either used for silver staining or Western blot analysis. The chemicals

used for preparation of four Tris- glycine SDS gels shown in the Table below. For SDS-PAGE of samples aiming to detect the mCherry-tagged L, commercially available 7% Tris-acetate gels were purchased from BioRad, and the separation ran 1-2 h at constant 150 V.

Chemical	Stacking gel 5%	Separation gel 12%
dH_20	6.8 mL	6.6 mL
30% polyacrylamide solution (Rotiphorese® 30)	1.7 mL	8 mL
SDS PAGE Stacking gel buffer	1.25 mL	---
SDS PAGE Separation gel buffer	---	5.3 mL
APS 10% in dH_20	0.1 mL	0.2 mL
TEMED	0.01 mL	0.01 mL

2.1.14 Silver Staining

Silver staining is a fast and sensitive method for detection of proteins within a SDS gel. Silver staining of SDS gels was used to compare the protein composition of virus stocks between wildtype and mutant viruses. The silver staining was carried out according to the manufacturer's instructions from the Pierce® silver stain kit. The gel was scanned and the band intensities where measured with the Image Lab software.

2.1.15 Western Blot

Western blotting allows the specific detection of proteins transferred from an SDS gel to a polyvinyldifluoride (PVDF) membrane using antibodies. Different variants of Western blotting techniques exist such as semi-dry and wet blotting. Semi-dry blotting works fast and is well suited for the detection of proteins with a low molecular weight. Semi-dry blotting was used for the blots shown in chapter 3.1-3.7. Detection of large proteins is complicated using the semi-dry blotting approach, therefore for efficient detection of the mCherry-tagged polymerase (size of ~250 kDa) a wet blot protocol was used.

2.1.15.1 Semi-dry blotting

Initially, the PVDF membrane was activated by incubation of the membrane in 100% methanol and then transferred into 1x transfer buffer. Per SDS gel a total of 8 Whatman papers (6.3 x 9.1 cm) where wetted in 1x transfer buffer. The components were arranged onto the anode of a blotting chamber in the following order. 4 pieces of Whatman paper followed by the PVDF membrane and the SDS gel covered by 4 additional pieces of Whatman paper. Bubbles were removed by rolling of a glass pipette over the SDS gel layers. The blotting chamber was closed and the transfer from the SDS gel onto the PVDF membrane takes place at 20 V with a maximal current for 25 min.

2.1.15.2 Wet blotting

The PVDF membrane was activated by incubation in 100% methanol and then washed with 1x transfer buffer. A total of 8 Whatman papers (6.3 x 9.1 cm) where wetted in 1x transfer buffer. The components were arranged facing the anode of a blotting chamber in the following order. First a sponge followed by 4 pieces of Whatman paper then the PVDF membrane and then the SDS gel covered by 4 additional pieces of Whatman paper and another sponge. A glass pipette was rolled over the SDS gel layers to remove bubbles. The blotting chamber, containing an ice pack, was closed and the transfer from the SDS gel onto the PVDF membrane was performed at 40 mA at 4°C over night.

2.1.15.3 Staining of PVDF membranes

Detection of the proteins by Western blotting relies on the ability of primary antibodies to bind specific proteins on the PVDF membrane, which in turn can be detected by secondary antibodies. The secondary antibody is commonly conjugated with fluorophores or horseradish peroxidase (HRP). HRP cleaves its substrate resulting in the emission of light. The emitted light is detected via the BioRad ChemiDoc system and stands in direct relation to the amount of protein

present on the PVDF membrane. Unspecific signals were blocked by incubation of the membrane in 10 % milk powder in PBS_{def} for 1 h at RT. The primary antibody was incubated on the membrane for 1h at RT. Unspecific bound antibodies were removed by three consecutive 5 min washes of the membrane with PBS_{def} + 0.1% Tween20. The secondary antibody was incubated for 1 h at RT followed by three 5 min washes with PBS_{def} + 0.1 % Tween20 and two washes with PBS_{def}. After addition of 1 mL of the SuperSignal™ West Femto Maximum Sensitivity Substrate per membrane, proteins were detected with the BioRad ChemiDoc system.

Primary antibody	Species	Dilution
α-VP40 (40-2-2)	Mouse	1:500
α-NP (59-9-10)	Mouse	1:1.000
α-GP (50-6-10)	Mouse	1:10
α-mCherry	Mouse	1:1.000
α-Tubulin	Mouse	1:3.000
α-Vinculin	Mouse	1:5.000

Secondary antibody	Conjugate	Species	Dilution
α-mouse	HRP	Mouse	1:30.000

2.2 Cell biological and virological methods

2.2.1 Cultivation of mammalian cells

The following cell lines were used in the present study: human Huh-7 cells, derived from a hepatoma and HEK293 derived from embryonic kidney cells; guinea pig cells derived from an adenocarcinoma (GPC16) and from fetal tissue (104C1) as well as cells from African green monkeys (VeroE6). The cells were grown in 75 cm² tissue culture flasks at 37°C and 5% CO_2. DMEM+++ which contains 10% fetal calf serum (FCS), penicillin and streptomycin (P/S) and L-Glutamine (Q) was used for cultivation of all cell lines, except 104C1 cells which were cultivated in RPMI+++ media. Passaging was performed under sterile conditions every 3-4 days once the cells reached confluency. Initially, media was removed from the cells and the cells were washed with pre-warmed PBS_{def} (37°C). This step removes Ca^{2+}/Mg^{2+} allowing efficient cleavage of surface proteins by trypsin. PBS_{def} was removed and 2 mL of 0.05 % trypsin/EDTA was added and incubated until the cells detached from the surface. Trypsinization was stopped by adding 8 mL of pre-warmed DMEM+++ or RPMI+++. The desired number of cells was seeded into new tissue culture flasks or plates.

2.2.2 Transient transfection of mammalian cells with TransIT©

Plasmid DNA was delivered into eukaryotic cells by usage of cationic lipids which interact with the negative charged phosphates of the DNA backbone. In aqueous solutions these complexes form liposomes containing the plasmid DNA of interest. These liposomes interact and fuse with cellular membranes allowing recognition of the DNA in the cells and subsequent expression of the gene of interest. Transfection is performed on a 60-80% confluent monolayer of cells. The transfection mix of TransIT© and OptiMEM is prepared as recommended by the supplier (3 µL TransIT©/µg DNA).

For example for a transfection of a 12 well plate:

	Mixture of	Volume [µL]
Mix 1	OptiMEM + DNA	50
Mix 2	OptiMEM + TransIT	50

Mix 1 and 2 are incubated separately for 5 min at RT, then thoroughly mixed and incubated at RT for additional 15 min. During that time period the cells are washed once with OptiMEM and then 900 µL of OptiMEM was added. After the incubation time the transfection mix was added carefully to the well and then incubated at 37°C and 5% CO_2. 4-6 h post transfection the media was changed to 2 mL DMEM+++ or RPMI+++ depending on the transfected cell line. Depending on the assay the amount of DNA and TransIT© were adjusted accordingly.

2.2.3 MARV specific minigenome reporter assay

The MARV specific minigenome reporter assay was used to mimic and determine the transcription and replication capacity of the MARV nucleocapsid complex in cell lines from different species. Detailed information for the minigenome assay is available in chapter 1.8.1. The minigenome was essentially performed as described by (Koehler *et al.*, 2016; Koehler *et al.*, 2015; Mühlberger *et al.*, 1998; Mühlberger *et al.*, 1999) briefly, HEK293 cells or 104C1 cells (60-80% confluent) were transfected with all plasmids necessary for formation of the MARV nucleocapsid complex (L, NP, VP30, and VP35, a MARV-specific minigenome carrying the *Renilla* luciferase reporter gene) and the T7-pol. A pGL4 construct encoding *Firefly* luciferase was added to normalize the transfection efficiency. To test the effect of mutations in viral proteins, the wildtype encoding plasmids were substituted by plasmids containing mutations at specific sites, e.g. plasmids containing mutations in the active site of the L protein. In addition, other plasmids encoding viral proteins, such as VP40, were transfected and their impact on replication and transcription was analyzed in cell lines of different species. The mixture for one reaction in a 12 well plate was as follows:

Plasmids		Promotor	Amount [ng]
1	pCAGGS-L_{WT} resp. -$L_{Mutants}$	β-actin (chicken)	400
2	pCAGGS-NP	β-actin (chicken)	100
3	pCAGGS-VP30	β-actin (chicken)	20
4	pCAGGS-VP35	β-actin (chicken)	20
5	pAndy-3M5M (*Renilla* luciferase minigenome)	T7	200
6	pCAGGS- T7-pol	β-actin (chicken)	100
7	pCAGGS-pGL4	SV40	40

A master mix is prepared from plasmids 2-7, resulting in the negative control without the L protein. Afterwards plasmid 1 is added. In chapter 3.5 increasing amounts of wildtype or VP40 mutant encoding plasmids were added. The transfection mix was removed after an incubation period of 4-6 h and 2 mL of DMEM+++ or RPMI+++ was added for 24 h to 48 h p.t at 37°C and 5% CO_2. The cells were washed with 1 mL PBS_{def} and then harvested by scraping in 1 mL $PBS_{def.}$ The cells are pelleted by 5000 rpm for 5 min. The supernatant was aspirated and the pellet was resuspended with 100 µL lysis buffer (2x Dual Lysis Juice, PJK GmbH) and incubated for 20 min at RT. Cellular debris was removed by centrifugation for 10 min at 13.000 rpm. The *Renilla* and *Firefly* luciferase activity of 5 µL from the supernatant was measured in a luminometer. The values of *Renilla* luciferase activity reflect minigenome specific transcription and replication and *Firefly* luciferase reflects cellular transcription and transfection efficiency used for normalization. The minigenome assays were performed in triplicates in at least three independent experiments.

2.2.4 Marburg virus specific infectious virus like particle assay (iVLP assay)

The infectious virus-like particle assay (iVLP assay) allows the production of virus-like particles resembling authentic virions with the difference that they contain a minigenome encoding *Renilla* luciferase instead of the viral genome. The iVLP assay was carried out as described in (Koehler *et al.*, 2016; Koehler *et al.*, 2015; Wenigenrath *et al.*, 2010) briefly, either HEK293 or 104C1 cells (80% confluent) were transfected in 6 cm dishes as follows for one reaction:

Plasmids		Promotor	Amount [ng]
1	pCAGGS-NP	β-actin (chicken)	1000
2	pCAGGS-VP30	β-actin (chicken)	200
3	pCAGGS-VP35	β-actin (chicken)	200
4	pCAGGS-VP24	β-actin (chicken)	140
5	pCAGGS-GP	β-actin (chicken)	200
6	pAndy-3M5M (*Renilla luciferase* minigenome)	T7	2000
7	pCAGGS- T7-pol	β-actin (chicken)	1000
8	pCAGGS-pGL4	SV40	1000
9	pCAGGS-VP40 resp. $VP40_{D184N}$	β-actin (chicken)	500
10	pCAGGS-L_{WT} resp. -$L_{Mutants}$	β-actin (chicken)	2000

The transfected cells were named p0 cells. These p0 cells were used for the production of VLPs, the minigenome reporter gene activity in these cells reflected transcription and replication in the presence of all viral proteins. Plasmids 1-9, or 1-8 and plasmid 10, were prepared as a master mix and the corresponding L_{Mut} or $VP40_{Mut}$ plasmid was added and substituted the wildtype protein encoding plasmid. The transfection mix was removed after an incubation period of 4-6 h and 6 mL of DMEM+++ or RPMI+++ was added to the cells for further incubation until 72 h post transfection (p.t.) at 37°C and 5% CO_2.

Harvesting and analysis of iVLPs

Supernatants were collected 72 h p.t. and cellular debris was removed by centrifugation at 3.000 rpm for 10 min. The supernatant was transferred into Ultra-Clear™ ultra-centrifuge tubes for SW41 ultracentrifuge rotors and was under laid with 2 mL of 20% sucrose in TNE, which allows to purify membranous particles from cellular supernatants. The tubes were filled with sterile PBS_{def}, tared and centrifuged at 36.000 rpm for 2 h at 4°C. The supernatant was removed and the pellet resuspended in 220 µL of sterile PBS_{def}. 200 µL of the resuspended iVLPs were mixed with either 1 mL of DMEM++ (lacking FCS) or RPMI++ (lacking FCS) and used for subsequent infection of indicator (p1 cells). 20 µL of iVLPs and were added to 7 µL of 4x loading Buffer and used for SDS-PAGE and Western blot analysis.

Minigenome RNA extraction from iVLPs

72 h p.t. the iVLPs were harvested in 200 µL of PBS_{def} and the RNA from the minigenome containing iVLPs was isolated using the QIAamp Viral RNA Mini Kit (Qiagen) according to the manufacturer's instructions. The eluted RNA was digested with RNase-free DNase using the RNeasy mini kit and eluted in 50 µL of RNase-free water. Equal amounts of purified RNA were used for QuantiTect® one-step RT-qPCR using primers against the minigenome.

Measurement of MARV specific minigenome transcription and replication in p0 cells

72 h p.t. the cells were washed once with PBS_{def} and then scraped in 1 mL of PBS_{def}. Cells were pelleted by centrifugation at 5.000 rpm for 5 min. The supernatant was aspirated and the pellet was resuspended with 200 µL lysis buffer (2x Dual Lysis Juice, PJK GmbH) and incubated for 20 min at RT. Cell debris was pelleted by centrifugation of the cell lysate at 13.000 rpm for 10 min. The *Renilla*- and *Firefly* luciferase activity was measured in 5 µL of cleared cell lysate.

Infection of indicator p1 cells with iVLPs

From p0 cells purified iVLPs were used to infect either Huh-7 or 104C1 cells. Up to 400 µL of the iVLPs were resuspended in DMEM or RPMI used for infection of p1 cells per well in a 12 well plate. The amounts of iVLPs used for infection were normalized by the amount of VP40 measured by Western blot. The infection of p1 cells was performed for 2 h at 37°C and 5% CO_2. After that time period 1.6 mL of DMEM+++ or RPMI+++ were added and incubation of cells was continued for 48h p.i.. Indicator p1 cells were either pre-transfected with plasmids encoding L, NP,VP30, VP35 and pGL4, see table below (reflecting the ability of iVLPs to induce reporter gene activity, namely replication and transcription in target cells) or remained naïve (reflecting the capability of the iVLPs to induce primary transcription in target cells). Depending on the goal of the experiment L_{WT} or one of the L_{Mut} was pre-transfected 24 h before infection with iVLPs. The pre-transfection mix containing following plasmids was added to one well of a 12 well plate:

Plasmids		Promotor	Amount [ng]
1	pCAGGS-L_{WT} resp. $L_{Mutants}$	β-actin (chicken)	400
2	pCAGGS-NP	β-actin (chicken)	200
3	pCAGGS-VP30	β-actin (chicken)	40
4	pCAGGS-VP35	β-actin (chicken)	40
5	pCAGGS-pGL4	SV40	40

Cell lysates from minigenome, VLPs, and iVLPs assay were used for measurement of minigenome reporter gene activity and analyzed by Western blotting. The cell lysates were harvested by washing the cells once with PBS_{def} and then scraped in 1 mL of PBS_{def}. The cells were pelleted by centrifugation at 5000 rpm for 5 min. The supernatant was aspirated and the pellet was resuspended in 50 µL of lysis buffer (2x Dual Lysis Juice, PJK GmbH) and incubated for 20 min at RT. Cell debris was pelleted by centrifugation of the lysate at 13.000 rpm for 10 min The *Renilla*- and *Firefly* activity in 10 µL of the cleared cell lysate was measured.

2.2.5 Interferon signaling assay

The Mx1 reporter gene assay was performed as described previously (Hug *et al.*, 1988; Jorns *et al.*, 2006; Koehler *et al.*, 2015)**.** Briefly, HEK 293 cells or GPC16 cells were co-transfected with a reporter plasmid encoding a *Firefly* luciferase under the control of the Mx1 promoter, a pGL 4.73 encoding *Renilla* luciferase reporter construct, and either VP40 or $VP40_{D184N}$. At 24 h p.t., cells were washed with PBS and incubated for additional 24 h in presence or absence of a recombinant interferon (IFN) hybrid (interferon-α/β B/D hybrid, 500 U/ml), shown to have a broad host-range activity in antiviral assays (Horisberger & de Staritzky, 1987). After the IFN treatment, cells were harvested using Dual Passive lysis buffer (Promega, Madison, WI), and the *Firefly* and *Renilla* luciferase activities were measured.

2.2.6 Flotation assay

VP40 is a peripheral membrane protein synthesized as cytosolic protein and associates to membranes shortly after synthesis. Flotation analysis allows to characterize the capability of proteins to interact with cellular membranes. Flotation analysis was performed as described in (Kolesnikova *et al.*, 2012). Briefly, Huh-7 or 104C1 cells were transfected with plasmids encoding either only one of the VP40 constructs, or NP, or combination of these plasmids. To maintain comparable DNA amounts for the single expression of NP or VP40 an empty vector construct was used to ensure equal DNA amounts upon transfection.

Plasmids		Amount [ng]
1	pCAGGS-VP40 or -$VP40_{D184N}$	500
2	pCAGGS-NP	500
3	pCAGGS (empty vector)	500

At 24 h p.t. the cells were washed three times with lysis buffer for flotation assay for 10 min at 4°C. Cells were harvested in 300 µL of lysis buffer and mechanically destroyed by passing the lysate through a 26 gauge needle for ten times. 60% Nycodenz in TNE were added to the cell lysates to reach a final concentration of 40% Nycodenz. The cell lysate in 40% Nycodenz was transferred into Ultra-

Clear™ ultra-centrifuge tubes for SW60 ultracentrifuge rotors and then carefully overlaid with 3 mL 30% Nycodenz solution and 500 µL 5% Nycodenz solution. The samples were centrifuged overnight at 4°C with 36.000 rpm. After the centrifugation the membrane-associated proteins were visible as a small band between the 5% and 30% layers. For analysis 5 fractions of 900 µL each were taken from the sample, the last fraction was thoroughly resuspended. 50 µL of each fraction were mixed with 12.5 µL of 4x loading buffer. The samples were analyzed via SDS-PAGE and Western blot analysis.

2.2.7 Budding assay

Single ectopic expression of VP40 leads to the release of VLPs into the supernatant, these VLPs can be quantified by Western Blot analysis (Swenson *et al.*, 2004). Either HEK293 or 104C1 cells were transfected with plasmids encoding VP40 or $VP40_{D184N}$ and 24 h p.t. the supernatants were harvested.

Plasmids		Amount [ng]
1	pCAGGS-VP40 or -$VP40_{D184N}$	500
2	pCAGGS-NP	500

Cellular debris was removed by centrifugation for 10 min at 3.000 rpm. To purify the VLPs the supernatant was transferred into Ultra-Clear™ ultra-centrifuge tubes for SW41 ultracentrifuge rotors and was under laid with 2 mL of 20% sucrose in TNE. The tubes were filled up with sterile PBS_{def} tared and centrifuged at 36.000 rpm for 2 h at 4°C. The supernatant was removed and the pellet was resuspended in 50 µL of 4x loading buffer, similar amounts of sample were used for SDS-PAGE and consecutive Western blot analysis.

2.2.8 Indirect immunofluorescence microscopy analysis (IFA)

Immunofluorescence analysis allows to study the intracellular localization of proteins. Indirect immunofluorescence analysis is based on efficient binding of two antibodies, a primary antibody recognizing the target protein and a secondary antibody, conjugated with a fluorophore, and reacting with the primary antibody. The UV light excites the fluorophore which leads to emission of light followed by detection. Huh-7, VeroE6 or 104C1 cells were seeded on coverslips (12 mm diameter) and either transfected with plasmids encoding the desired proteins or infected in the BSL-4 laboratory with recombinant MARV. Transfected cells were fixed with 4% PFA in DMEM for 30 min at RT. Infected cells were fixed with 4% PFA in DMEM for at least 16 h, the fixed coverslips where then transferred into 4% PFA in DMEM in a new 12 well plate and the samples were exported from the BSL-4 laboratory. For the immunofluorescence staining 4% PFA in DMEM was removed and the coverslips were washed three times for 3 min in PBS_{def}. To reduce the background and to quench free aldehyde groups from residual PFA, coverslips were incubated for 5 min in PBS_{def} + 100 mM glycine. Afterwards, cells were permeabilized using PBS_{def} + 0.1% Triton X-100 for 5 min. Then, unspecific antibody binding was blocked by incubation of the cells in blocking buffer for 10 min. Coverslips were incubated with the primary antibodies diluted in blocking buffer for 1 h at RT in a wet chamber. After the incubation period the coverslips were washed three times for 3 min with PBS_{def} and then incubated for 1 h at RT with the secondary antibodies and DAPI, as staining for the nuclei, diluted in blocking buffer. Finally the cells were washed three times for 3 min with PBS_{def}; excess buffer was removed by placing the edge of the coverslip on a Kimtech wipe and then placed into mounting media (Fluoprep) on object slides. After drying of the mounting media the samples were analyzed on the Leica SP5 confocal laser scanning microscope.

Primary antibody	Species	Dilution
α-VP40 (40-2-2)	Mouse	1:50
α-NP 2	Guinea pig	1:200
α-MARV	Goat	1:100

Secondary antibody	Conjugate	Species	Dilution
α-mouse	Alexa 488	Goat	1:300
α-guinea pig	Alexa 594	Goat	1:300
DAPI (4',6-Diamidin-2-phenylindol)		Goat	1:100
Phalloidin	FITC		1:10
Phalloidin	TRITC		1:10
Filipin III			50 µg/ml

2.2.9 Cloning and rescue of recombinant viruses

Cloning and rescue of recombinant MARV (rMARV) was based on an approach developed in the group of Stephan Becker and performed as previously described in (Dolnik *et al.*, 2014; Koehler *et al.*, 2015; Krähling *et al.*, 2010). Briefly, three individual pBlueScript plasmids containing different parts of the MARV genomic sequence have been digested on unique restriction sites. Fragment 1 contains the sequences of (T7- leader-NP-VP35-VP40-GP), fragment 2 (GP-VP30-VP24-L) and fragment 3 contains the (L-Trailer-Ribozyme). The ligation of the three fragments results in the full genomic sequence of MARV Musoke (GenBank accession number: NC_001608) (Mühlberger *et al.*, 1998). Recombinant viruses can be distinguished from wildtype isolates, since they carry two silent nucleotide substitutions at positions 6498 (C→T) and 7524 (A→G). This nucleotide exchanges result in the substitution of a KpnI restriction site with a SacII restriction site.

The D184N mutation was inserted in fragment 1 via multisite-directed mutagenesis by Ulla Welzel as part of her Master studies in 2011, through substitutions of the nucleotides GAC to AAT at the positions 8104 to 8106.

The rescue of the $rMARV_{WT}$ and $rMARV_{VP40(D184N)}$ was performed by Dr. Gordian Schudt in 2012. In detail, Huh-7 cells and VeroE6 cells were equally mixed and seeded into wells of a 6-well plate. Once the cells reached 50% confluency transfection with the helper plasmids, NP, VP30, VP35, L and the T7-pol, and the full-length plasmid was performed as described in (Dolnik *et al.*, 2014; Krähling *et al.*, 2010). The sequence integrity of the rescued $rMARV_{WT}$ and $rMARV_{VP40(D184N)}$ was verified by sequencing.

2.2.10 Infection of Huh-7- and 104C1-cells with rMARVs (BSL-4)

HuH-7, 104C1 or VeroE6 were infected with either $rMARV_{WT}$ or $rMARV_{VP40(D184N)}$. For an infection of a 12 well plate the media on the cells was removed and 1 mL of virus containing media (FCS deficient) was added. Virus was incubated on the cells for 1 h at 37°C, allowing binding and internalization of virions. Virus containing media was removed and cells were washed with PBS_{def} and 2 mL of fresh media DMEM+++ (with 2% FCS) or RPMI+++ (with 2% FCS) were added to every well. The used multiplicity of infection (MOI) for the different experiments is specified for each experiment.

2.2.11 Propagation and concentration of virus stocks (BSL-4)

To produce sufficient amounts of infectious virus, a pre-culture of VeroE6 cells (T25 cm^2 flask, $1x10^6$ cells) were infected with virus an MOI of 0.1. The pre culture cells were incubated 7 days at 37°C, 5% CO_2. The supernatant of the pre-culture was collected into 15 mL falcon tubes and centrifuged at 4°C for 10 min at 2.500 rpm. The supernatant was diluted 1:10 and 10 mL were added to fresh VeroE6 cells (T175 cm^2 flask, $7x10^6$ cells). The virus was propagated for 4-7 days until a clear cytopathic effect (CPE) was apparent. The virus containing supernatant was centrifuged at 4°C for 10 min at 2.500 rpm. For non-concentrated virus stocks 1 mL was aliquoted into 2 mL cryo tubes. For preparation of concentrated virus stocks 25 mL of the supernatant were added into SW32 ultra centrifuge tubes under laid with 5 mL 20% sucrose and filled up with the rest of the supernatant. Virus was pelleted by centrifugation for 2 h at 4°C at 28.000 rpm. The supernatant was discarded and the pellet was resuspended in 1.2 mL PBS_{def}, 35 µL of virus were aliquoted into 1 mL cryo tubes. Non- and concentrated virus stocks were titrated by tissue culture infectious dose 50 (TCID50).

2.2.12 Virus quantification by tissue culture infectious dose 50 (TCID50)

The TCID50 (tissue culture infectious dose 50) is a method to determine the titer of virus from supernatants. This method determines the virus dilution which is able to infect 50% of the cells. VeroE6 cell were seeded to a confluency of ~50% into 96 well plates. The media was removed and 100 µL of DMEM+++ (5% FCS) were added prior to infection in the BSL-4 laboratory. A dilution series of the virus was prepared (10^{-2} to 10^{-7}). 100 µL of the virus dilution were added to the wells via a multi pipette, every dilution is tested in octuple. The cells were incubated for 10-14 days at 37°C and 5% CO_2 until the CPE remained constant. The calculations of the TCID50/mL were carried out according to the Spearman and Kärber method (Spearman & Karber, 1974).

2.2.13 Infectivity assay (BSL-4)

The infectivity of viruses in different cell species can be determined using a single step growth curve, allowing detection of infected cells before newly made virus is released from cells and infects neighboring cells, reflecting only initially infected cells. For the infection equal amounts of TCID50 units/mL were added to either VeroE6, as internal control for titration and infection, Huh-7 or 104C1 cells in the BSL-4 laboratory. The cell numbers were quantified prior to infection and the cells seeded on glass coverslips were infected at an MOI of 1. After a one hour infection the virus containing media was removed and cells were washed with 1 mL PBS_{def} followed by addition of 2 mL fresh DMEM+++ (with 2 % FCS). or RPMI+++ (with 2 % FCS). 19 h p.i. the cells were fixed with 4% PFA in DMEM for at least 16 h, fixed coverslips where then transferred into fresh 4% PFA in DMEM into a new 12 well plate and the samples were exported from the BSL-4 laboratory to the BSL-2 laboratory. Coverslips were stained with antibodies against NP and VP40 as well as DAPI and the percentage of infected cells was quantified.

2.2.14 Preparation of rMARV for electron microscopy (EM) by negative staining

Electron microscopy allows to determine the morphology of virus particles. For preparation of virus for EM, an 1.5 mL microcentrifuge polyallomer tube was filled with 650 µL of virus containing suspension, then 200 µL of 20% sucrose were added to the bottom of the tube and additional 650µL were added to the top of the tube. The samples were centrifuged at 45.000 rpm for 2 h at 4°C. The supernatant was removed and the pellet was fixed in 4% PFA in DMEM for at least 16 h. The 4% PFA in DMEM was removed and the tube was completely filled with fresh 4% PFA in DMEM and exported from the BSL-4 laboratory. The 4% PFA in DMEM was removed and the pellet was resuspended in 100 µL of 4% PFA in DMEM. The following steps including preparation of the samples and the EM analysis was performed by Dr. Larissa Kolesnikova. To improve adherence of viral particles Formvar-coated 400-mesh grids were pretreated with 1% alcian blue, an adherence time of virus samples was constant, 10 min. The grids were negatively stained with 2% phosphotungstic acid. Viral particles were analyzed by using a JEM1400 transmission electron microscope. Indirect immunostaining of GP was performed as described previously (Koehler *et al.*, 2015; Mittler *et al.*, 2007), by using a goat serum anti-GP and a donkey anti-goat IgG coupled with colloidal gold beads, 12 nm in diameter.

2.2.15 Preparation of rMARV infected cells for thin sectioning

The EM analysis of cellular ultrathin sections allows an insight into the ultrastructural changes of cells infected with different viruses. Huh-7 or 104C1 cells were infected with rMARVs and fixed for 30 min at RT by adding an equal volume of double-concentrated fixative solution [120 mM piperazine-N,N′-bis(2-ethanesulfonic acid), 50 mM HEPES, 4 mM MgCl2, 20 mM EGTA, 8% paraformaldehyde, 0.2% glutaraldehyde, pH 6.9] to the culture media in the BSL-4 laboratory. After the fixation the cells were scraped and pelleted at 4°C for 10 min at 13.000 rpm. The pellet was overlaid with 4% PFA in DMEM for at least 16 h. The PFA was exchanged and the tubes completely filled with fresh 4% PFA in DMEM and then removed from the BSL-4 laboratory. The following steps including embedding and the preparation of the samples for thin sectioning and the subsequent EM analysis were performed by Dr. Larissa Kolesnikova. The tubes were processed for embedding in Epon and Araldite as described in (Bharat *et al.*, 2011; Koehler *et al.*, 2015; Welsch *et al.*, 2010). Samples were polymerized at 60°C for 24 h. Ultrathin sections (60 to 90 nm) of virus- and mock-infected cells were prepared using an ultramicrotome (Leica EM UC6) and stained with uranyl acetate and lead citrate. Ultrathin sections were analyzed using a JEM 1400 transmission electron microscope.

3 Results

3.1 Analysis of the impact of the D184N mutation in VP40 on its functions in guinea pig and human cells

Even though the D184N was frequently observed in rodent-adapted MARV strains, the importance and function of this mutation for the increased virulence of rodent-adapted MARV is still unknown (Lofts *et al.*, 2007; Lofts *et al.*, 2011; Marzi *et al.*, 2016; Warfield *et al.*, 2009). The aim of this chapter is to elucidate whether the D184N mutation in VP40 affects any of the known functions of VP40 in a species-specific manner. To determine species-specific effects of the D184N mutation in VP40, all experiments will be performed in human and guinea pig cells comparing wildtype VP40 to $VP40_{D184N}$.

3.1.1 Characterization of the interferon antagonistic function of VP40 and $VP40_{D184N}$

MARV VP40 is a potent suppressor of the innate immune response via inhibition of the Jak-STAT signaling (Valmas *et al.*, 2010). To determine the impact of the D184N mutation on the interferon (IFN) antagonistic function of VP40 the suppression of the IFN signaling pathway by either wildtype VP40 or $VP40_{D184N}$ was analyzed in human (HEK293) and guinea pig cells (GPC16). Generally, transfection of 104C1 cells (guinea pig) resulted in higher transfection efficiencies and better production of iVLPs and VLPs than in GPC16 cells. However, for the interferon reporter assays GPC16 cells were used instead of 104C1 cells, since 104C1 showed only a weak induction of the interferon response upon induction with the interferon hybrid. The cells were transfected with a reporter plasmid encoding *Firefly* luciferase under the control of the Mx1 promoter, a pGL 4.73 encoding *Renilla* luciferase reporter construct under the control of a SV40 promoter, and either VP40 or $VP40_{D184N}$. The cells transfected with an empty pCAGGS vector instead of VP40 encoding plasmids, served as negative and positive controls and displayed the reporter gene activity with or without induction with interferon.

The IFN response was induced by incubation of the cell with 500 U/mL of an IFN-α/β B/D hybrid which had a broad species reactivity (Horisberger & de Staritzky, 1987).

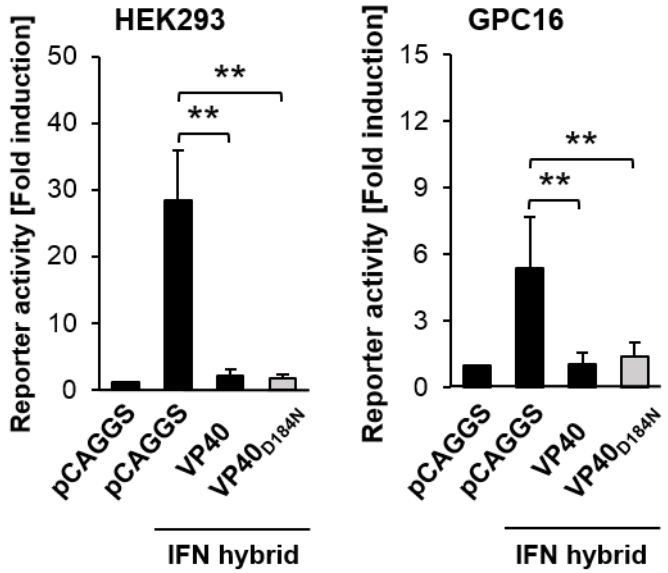

Figure 9: Characterization of the interferon antagonistic function of $VP40_{D184N}$ in human and guinea pig cells

Human (HEK293) and guinea pig (GPC-16) cells were co-transfected with reporter plasmids expressing *Firefly* luciferase under the control of the Mx1 promoter, plasmids encoding VP40 or $VP40_{D184N}$ or an empty vector. Treatment of the cells with IFN hybrid (500 U/ml) was performed 24 h post transfection (p.t.) Cells were incubated with IFN-hybrid for 24 h. At 48 h p.t., cells were harvested and the *Renilla*; reflecting minigenome reporter activity and *Firefly* luciferase signal, to normalize for transfection efficiency, was measured. The relative reporter gene activity was determined by normalization of the *Firefly* luciferase (Mx1) to the *Renilla* luciferase signal (cellular transcription and transfection efficiency). The means and standard deviations displayed are from three independent experiments and shown above, statistical analysis was performed using Student's t-test. ** $P < 0.01$.

Treatment with IFN-α/β B/D hybrid in human cells increased the reporter gene activity by 28.3-fold. Expression of VP40 and $VP40_{D184N}$ significantly suppressed the IFN response, the reporter gene activity was only 2.1- and 1.7-fold over the reporter gene activity in untreated cells (Fig. 9, left graph).

Guinea pig cells were less responsive to the treatment with IFN-α/β B/D and resulted in a 5.4-fold induction of the reporter gene activity. Presence of VP40 or $VP40_{D184N}$ suppressed the IFN response (Fig. 9, right graph). To sum this up, the D184N mutation does not alter VP40s IFN antagonistic function in human and guinea pig cells.

‘

3.1.2 Characterization of the intracellular distribution of $VP40_{D184N}$

VP40 is a peripheral membrane protein that starts to associate with membranes shortly after synthesis. Immunofluorescence analysis of VP40-expressing human cells showed that VP40 is distributed diffusely in the cytoplasm and sometimes in the nuclei. In addition, VP40 accumulates at the plasma membrane in form of very bright VP40-enriched clusters (Kolesnikova *et al.*, 2004a; Kolesnikova *et al.*, 2002). To analyze whether the D184N mutation influenced the intracellular distribution of VP40, either human (Huh-7) or guinea pig (104C1) cells were transfected with plasmids encoding wildtype VP40 or $VP40_{D184N}$. At 24 h p.t., cells were fixed and processed for IFA. Both proteins, VP40 and $VP40_{D184N}$ displayed a similar intracellular distribution in human and guinea pig cells. In addition to a diffuse distribution in the cytoplasm VP40 and $VP40_{D184N}$ were detectable in small amounts in the nuclei (arrowhead). The majority of the two proteins was located in the VP40-enriched clusters at the plasma membrane (arrows) (Fig. 10). These data suggest that the D184N mutation in VP40 does not influence the synthesis and transport of $VP40_{D184N}$ in human and guinea pig cells.

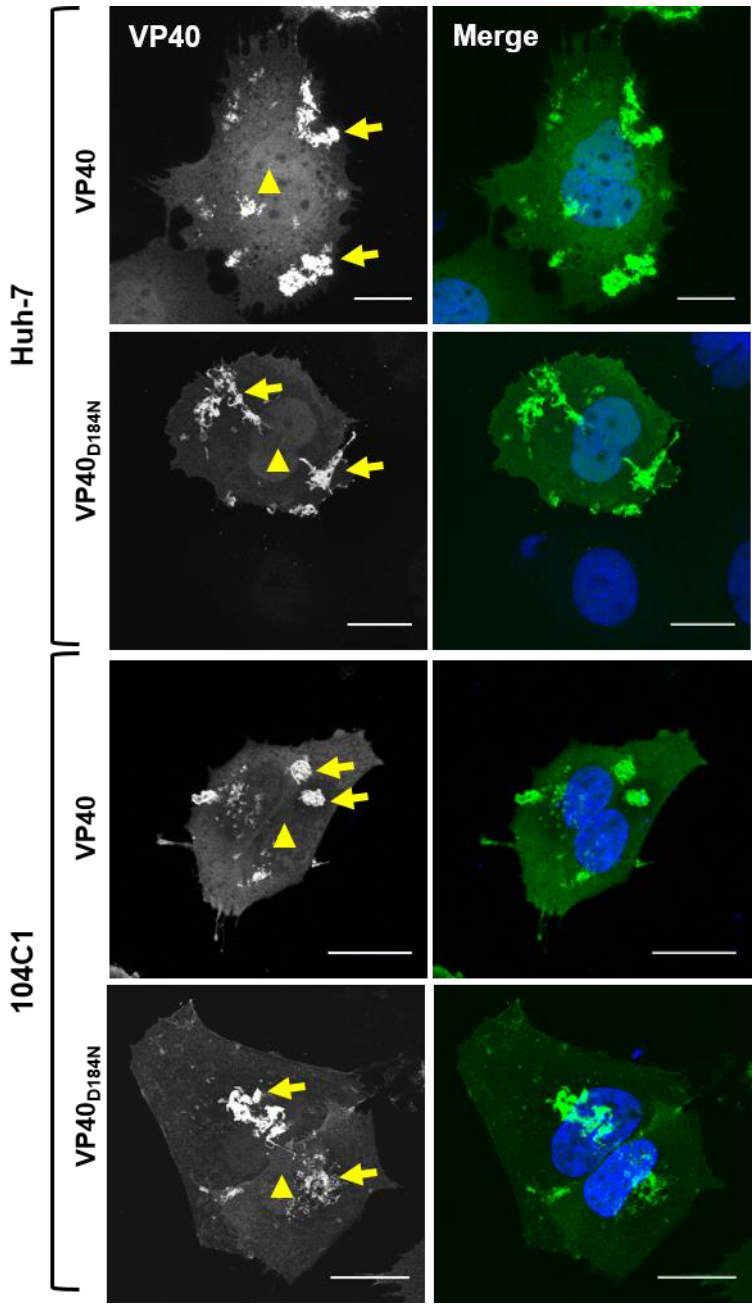

Figure 10: Cellular localization of VP40 and $VP40_{D184N}$ in human and guinea pig cells Human (Huh-7) or guinea pig (104C1) cells were transfected with plasmids encoding VP40 or $VP40_{D184N}$ and fixed 24 h p.t.. Cells were stained with a VP40-specific antibody (green) and DAPI (blue). Arrowheads show VP40 in the nuclei, arrows show VP40 in plasma membrane clusters. Bars represent 20 µM.

3.1.3 Accumulation of VP40 in cholesterol enriched clusters

Sites of filovirus budding have been shown to associate with cholesterol-enriched clusters (Bavari *et al.*, 2002). Since VP40 is the driving force of virus budding, we wanted to test whether single ectopic expression of VP40 or $VP40_{D184N}$ is accompanied by recruitment of cholesterol into the VP40-enriched clusters in cells from different species. Human or guinea pig cells expressing either wildtype VP40 or $VP40_{D184N}$ were fixed and stained with a VP40-specific antibody and 50 µg/ml of freshly prepared filipin III as marker for cholesterol (Fig. 11) (Börnig & Geyer, 1974; Du *et al.*, 2011).

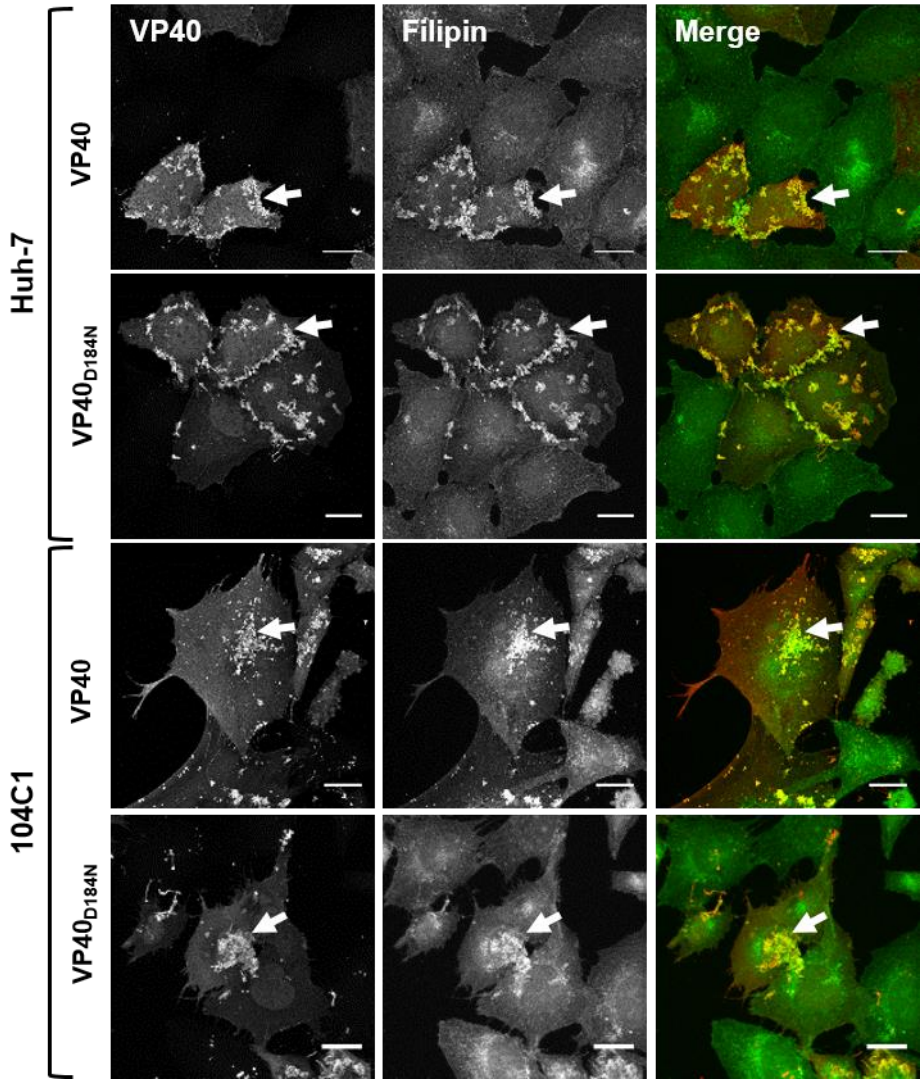

Figure 11: Recruitment of cholesterol into VP40-enriched clusters

Human (Huh-7) or guinea pig (104C1) cells were transfected with plasmids encoding VP40 or $VP40_{D184N}$ and fixed 24 h p.t.. Cells were stained with a VP40-specific antibody (red) and filipin III (green) to detect cholesterol. VP40 induced clusters are indicated by arrows. Bars represent 20 µM.

In both cell lines the VP40- and $VP40_{D184N}$-enriched clusters displayed accumulation of cholesterol (arrows). The VP40-positive clusters were located predominantly at the dorsal site of guinea pig cells, while in human cells these clusters were at the cells' periphery (Fig. 11, indicated by arrows). In spite of this slight difference, the intensity of the filipin staining in the wildtype VP40- and $VP40_{D184N}$- enriched clusters were similar indicating that $VP40_{D184N}$ maintained the ability to recruit cholesterol with the same efficiency as wildtype VP40, and that this ability is conserved in human and guinea pig cells (Fig. 11).

3.1.4 Membrane binding capability of $VP40_{D184N}$

As mentioned previously, VP40 is synthesized as a cytosolic protein and starts to associate with membranes quickly after synthesis (Kolesnikova *et al.*, 2004b; Kolesnikova *et al.*, 2002). It has been shown that binding of VP40 to membranes is dependent on the oligomeric state of VP40 (Oda *et al.*, 2015). The D184N mutation in VP40 is located at the beginning of the C-terminal domain which has no influence on oligomerization of VP40, but is important for membrane binding (Bornholdt *et al.*, 2013; Oda *et al.*, 2015). To analyze the influence of the D184N mutation on the membrane binding capabilities of VP40, human and guinea pig cells expressing either VP40 or $VP40_{D184N}$ were subjected to flotation assays (Fig. 12). The membrane-associated portion of wildtype VP40 was 47%, when it was expressed in human cells, and 46%, when it was expressed in guinea pig cells. This observation demonstrated that the intrinsic association of VP40 with membranes was not disrupted in guinea pig cells. The membrane-associated portion of $VP40_{D184N}$ was higher, in human cells it comprised 61% and reached 62% in guinea pig cells. However, this effect was not statistically significant. Altogether, the D184N mutation in VP40 resulted in an increased membrane binding of VP40 in human and guinea pig cells.

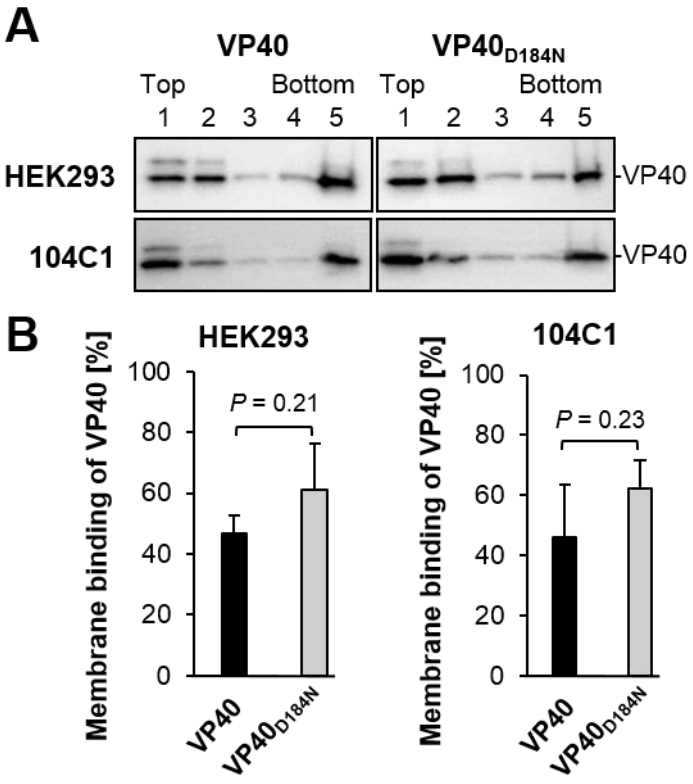

Figure 12: Membrane association of VP40$_{D184N}$ in human and guinea pig cells

The membrane binding capabilities of VP40 and VP40$_{D184N}$ were determined by flotation analysis in human (HEK293) and guinea pig (104C1) cells. The cells were transfected with either plasmids encoding VP40 or VP40$_{D184N}$ and cell lysates were harvested 24 h p.t.. Membrane-associated proteins and proteins from the cytosolic phase were separated by flotation assay analysis. Presence of VP40 was determined by SDS-PAGE and Western blot analysis via staining with a VP40-specific antibody (A). Fraction 1-2 (top) reflect membrane-associated VP40 and Fraction 5 (bottom) cytosolic VP40. (B) The percentage of membrane-associated VP40 (black) and VP40$_{D184N}$ (gray) in human and guinea pig cells is shown. The means and the standard deviations are shown from three independent experiments, statistical analysis was performed using the Student's t-test.

3.1.5 Characterization of membrane-associated NP upon co-expression with VP40$_{D184N}$

One of VP40's assembly functions is the attraction of nucleocapsids to the plasma membrane (Dolnik *et al.*, 2008). Although the mechanism of interaction between MARV VP40 and the nucleocapsid proteins remains obscure, it has been shown that the membrane binding capability of NP is increased upon co-expression with VP40 (Dolnik *et al.*, 2010).

It was of interest to determine whether the D184N mutation in VP40 influences the recruitment of NP to membranes upon co-expression and thereby might modulate the assembly function. To address this question, flotation analysis was performed on human and guinea pig cells expressing NP only or co-expressing NP and either VP40 or VP40$_{D184N}$. Single expression of NP resulted in 12-15% of membrane-associated NP in human and guinea pig cells (Fig. 13). The highest amount of membrane-associated NP, 34%, was detected when it was co-expressed with VP40$_{D184N}$ in human cells, whereas co-expression with wildtype VP40 resulted in only 19% of membrane-associated NP (Fig. 13). In contrary to previously published data, instead of a 2-fold difference we observed only a 1.5-fold increase of membrane associated NP upon presence of VP40 (Dolnik *et al.*, 2010). However, Dolnik *et al.* have used Huh-7 cells whereas in this experiment HEK293 cells have been used, might explaining the difference. In guinea pig cells a similar phenotype was observed, upon single expression 15% of NP was associated with membranes (Fig. 13). Co-expression of NP with VP40$_{D184N}$ resulted in 24% of membrane-associated NP compared to 18% in presence of VP40 (Fig. 13). These results indicate that the enhanced membrane binding properties of VP40$_{D184N}$ might recruit an enhanced amount of NP to the membranes in both human and guinea pig cells. Although this effect is not statistically significant it might result in a slight improvement in the attraction of nucleocapsid proteins to the site of budding in human and guinea pig cells.

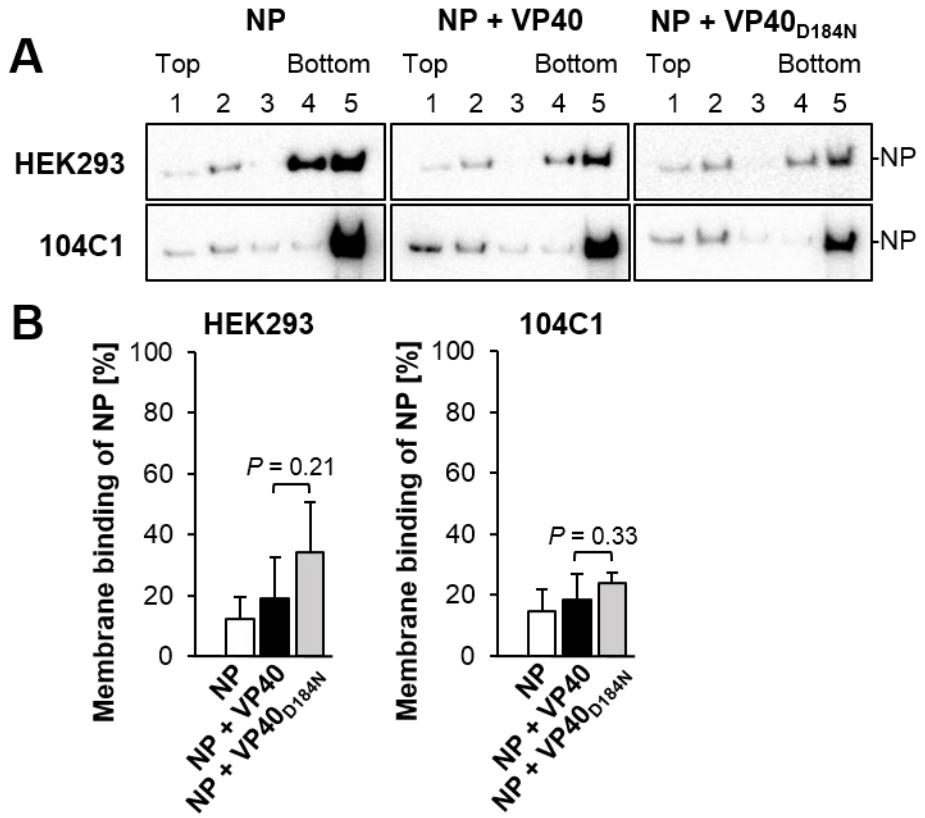

Figure 13: Flotation analysis of VP40$_{D184N}$ co-expressed with NP in human and guinea pig cells. To determine the membrane binding capabilities of NP upon co-expression with either VP40 or VP40$_{D184N}$ we used flotation analysis for human (HEK293) and guinea pig (104C1) cells. Cells were transfected with plasmids encoding only NP or NP and either VP40 or VP40$_{D184N}$, the cell lysates were harvested 24h p.t. and subjected to the flotation assay. The presence of NP was determined by SDS-PAGE and Western blot analysis by staining with a NP-specific antibody (Fig. 13A). Fraction 1-2 (top) reflects membrane-associated NP and fraction 5 (bottom) cytosolic NP. (B) Shows the percentage of membrane-associated NP in human and guinea pig cells. The means and the standard deviations are shown from three independent experiments, statistical analysis was performed using the Student's t-test.

3.1.6 Analysis of the budding capacity of wildtype VP40 and $VP40_{D184N}$

Single expression of VP40 results in formation and budding of VP40-enriched VLPs (Kolesnikova *et al.*, 2004b; Swenson *et al.*, 2004). Released VP40-induced VLPs possess the filamentous form of authentic virions but do not contain nucleocapsids. The production of VP40-induced VLPs can be used as an indicator of the budding function of VP40 (Kolesnikova *et al.*, 2004b; Swenson *et al.*, 2004). To investigate whether the D184N mutation in VP40 has an influence on the budding capacity of VP40, we transfected human or guinea pig cells with either VP40 or $VP40_{D184N}$. VLPs were purified from the supernatants of transfected cells 72 h p.t. by centrifugation through a sucrose cushion. Presence of VP40 in cell lysates and the amount of VP40 in VLPs were quantified by Western blot analysis (Fig. 14A). The relative VLP release was calculated as ratio of the intensity of VP40 signals in VLPs and cell lysates. The relative VLP release in cells expressing wildtype VP40 was set to 1. In human cells, the relative VLP release was not affected by the D184N mutation in VP40 (Fig. 14B, left graph). In contrast, the D184N mutation resulted in a 1.5-fold enhanced release of VLPs in guinea pig cells. These data demonstrated that the D184N mutation positively influenced the budding function of VP40 in a species-specific manner (Fig. 14B, right graph).

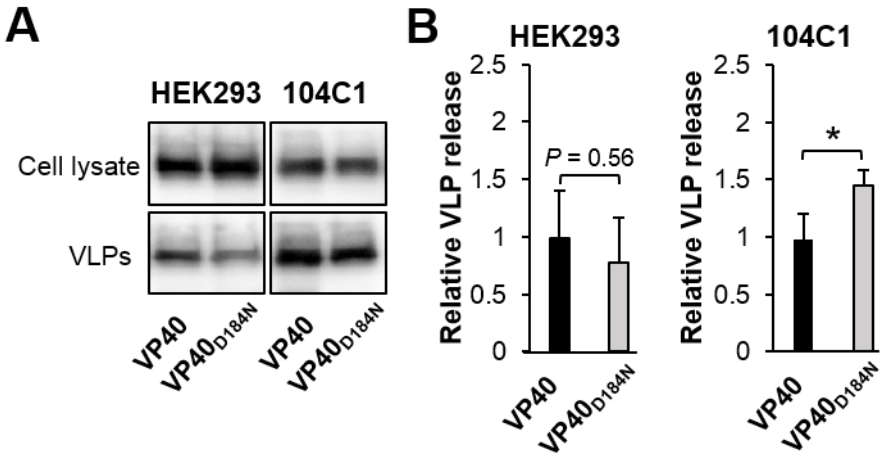

Figure 14: Analysis of the budding capacity of VP40$_{D184N}$ in human and guinea pig cells VLPs were purified from the supernatants of VP40 or VP40$_{D184N}$ expressing human (HEK293) and guinea pig (104C1) cells at 72 h p.t. through a sucrose cushion. SDS-PAGE and Western blot analysis was performed from equal amounts of cell lysates and VLPs (A). The mean intensity of the VP40-specific bands were measured with the Image Lab software and the relative VLP release was calculated (amount of VP40 in VLPs divided by the amount of VP40 in cell lysates). The graphics (B) represent the relative VLP release in either human or guinea pig cells expressing VP40 or VP40$_{D184N}$ from three independent experiments, statistical analysis was performed using the Student's t-test. * $P < 0.01$.

3.1.7 Characterization of the VP40$_{D184N}$-mediated suppression of replication and transcription

It has been shown that VP40 of EBOV and MARV suppresses the transcription and replication activity in the minigenome system (Hoenen *et al.*, 2010). To assess the influence of the D184N mutation on the VP40-mediated suppression of replication and transcription in human and guinea pig cells, we performed following experiments. Human and guinea pig cells were transfected with the plasmids necessary for the minigenome assay and with increasing amounts (100 ng, 200 ng and 400 ng) of plasmids encoding either wildtype VP40 (pCAGGS-VP40) or VP40$_{D184N}$ (pCAGGS-VP40 $_{D184N}$). Cells were lysed at 24 h p.t. and the reporter gene activity was measured.

Increasing amounts of wildtype VP40 resulted in a significant dose-dependent decrease of the reporter gene activity in both human and guinea pig cells. Both VP40 and VP40$_{D184N}$ decreased the reporter gene activity to comparable levels in human (Fig. 15). In guinea pig cells, the transfection of 100 ng DNA encoding wildtype VP40, reduced the reporter gene activity to 43%, whereas transfection of 100 ng pCAGGS-VP40$_{D184N}$ did not lead to any reduction of the reporter gene activity. In fact, the reporter gene activity in VP40$_{D184N}$-transfected guinea pig cells was 2.5-fold higher than in pCAGGS-VP40 transfected cells (Fig. 15A, right panel). Nevertheless, VP40$_{D184N}$ preserved its inhibitory capabilities in guinea pig cells, which were observed at DNA concentrations of 200 ng and 400 ng. The reporter gene activity was reduced to 61% at 200 ng pCAGGS-VP40$_{D184N}$ and to 27% at 200 ng pCAGGS-VP40 (Fig. 15). A distinct difference in wildtype VP40- and VP40$_{D184N}$-induced suppression of minigenome transcription and replication activity was observed only in guinea pig cells (Fig. 15). These data demonstrates that the D184N mutation in VP40 relieved the effect of VP40 on viral replication and transcription in guinea pig, but not in human cells.

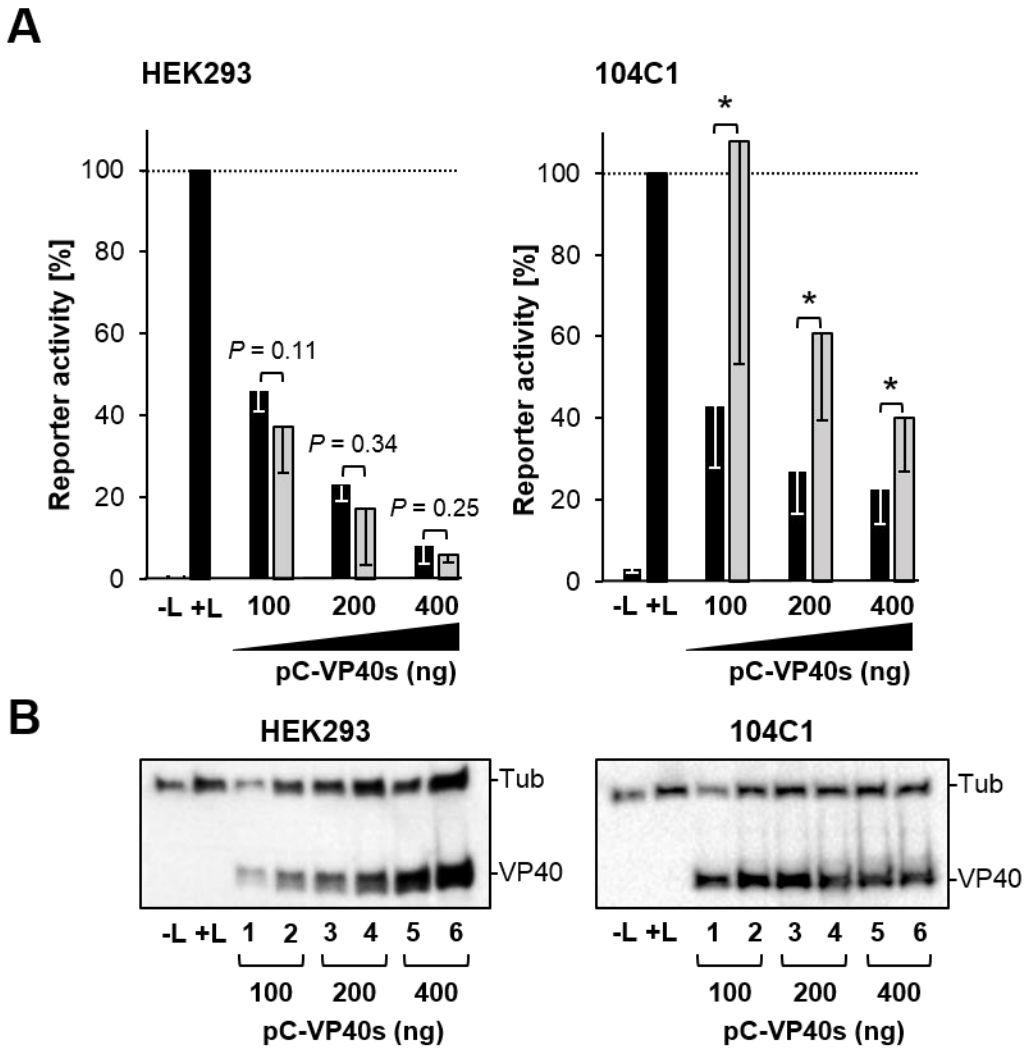

Figure 15: Characterization of the VP40$_{D184N}$ mediated suppression of minigenome replication and transcription in human and guinea pig cells

(A) All plasmids required for the minigenome system including L (positive control, +L) or without L (negative control, -L) were transfected together with increasing amounts of either wildtype VP40 (black column) or VP40$_{D184N}$ (gray columns) coding plasmids (pC-VP40s) into human (HEK293) or guinea pig (104C1) cells. Cells were lysed 24 h p.t., and the reporter gene activity was measured. The normalized reporter gene activity was set to 100% (positive control). The means and standard deviations are shown from the results of triplicates of three independent experiments, statistical analysis was performed using the Student's t-test. *, $P < 0.05$. (B) The protein levels of VP40 and tubulin in cell lysates of human (HEK293) and guinea pig (104C1) cells were determined by SDS-PAGE and Western blotting using alpha-tubulin (Tub)- and VP40-specific antibodies. Lane 1, 3 and 5 show VP40 and lanes 2, 4, and 6, VP40$_{D184N}$.

3.1.8 The effect of the D184N mutation in VP40 on replication and transcription in an iVLP assay

To verify the species-specific effect of the D184N mutation on the VP40-mediated regulation of transcription and replication in presence of not only VP40, but also VP24 and GP, we used the iVLP assay in human or guinea pig cells (chapter 1.8.2). Producer (p0) cells were transfected with plasmids encoding all seven viral proteins, T7-pol and a *Renilla* luciferase-encoding minigenome. Expression of all viral proteins resulted in assembly of minigenome-containing nucleocapsid-like complexes which were transported to the cell surface, coated with a lipid enveloped enriched with VP40 and GP and released in form of iVLPs into the supernatant. The iVLPs were used for infection of indicator (p1) cells.

The p1 cells were pre-transfected with plasmids encoding NP, VP30, VP35 this allowed to support the replication and transcription activity of incoming nucleocapsids (p1 tr cells). Alternatively, the p1 cells were not pre-transfected with plasmids encoding the nucleocapsid proteins (p1 naïve cells). In this case, the reporter gene activity reflected the ability of incoming nucleocapsids to mediate primary transcription.

Expression of $VP40_{D184N}$ in human p0 cells (HEK293) resulted in a slight reduction of reporter gene activity compared to wildtype VP40 expressing cells (Fig. 16 A, left panel). In contrast, expression of $VP40_{D184N}$ in guinea pig p0 cells did not suppress the reporter gene as efficiently as wildtype VP40 (Fig. 16 B, left panel). These results confirm that the D184N mutation in VP40 allows higher levels of replication and transcription in the presence of all viral proteins in p0 guinea pig cells.

Supernatants of p0 cells were then used to purify iVLPs and equal amounts of iVLPs, quantified by Western blot analysis, were used to infect either p1 tr or p1 naïve cells. In p1 tr cells, infection with iVLPs from $VP40_{D184N}$-expressing human cells resulted in a lower reporter gene activity compared to infection with iVLPs produced upon expression of wildtype VP40 (Fig. 16 middle panel). In contrast, when guinea pig cells were infected with iVLPs from $VP40_{D184N}$-expressing cells

the reporter gene activity was increased by 240% in p1 tr and by 150% in p1 naïve cells (104C1) (Fig. 16, middle and right panel).

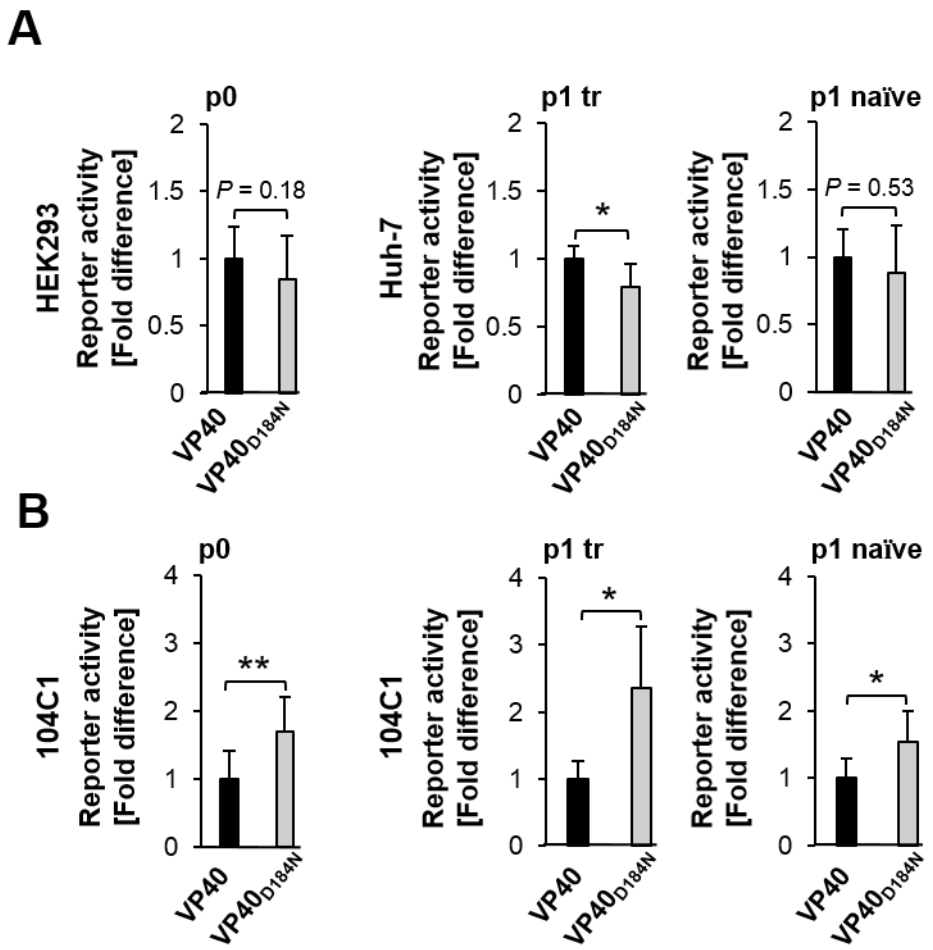

Figure 16: Importance of the D184N mutation in VP40 on replication and transcription in the iVLP assay

(A) Human cells (p0 = HEK293, p1 = Huh-7) were transfected with plasmids required for the iVLP assay. Either VP40 or $VP40_{D184N}$ were transfected. 72 h p.t. p0 cell lysates were harvested and the *Renilla* and *Firefly* activity was measured (left panel). The reporter gene activity was determined by normalizing the *Renilla* reporter signal to the measured *Firefly* activity. Equal amounts of iVLPs were used to infect either pre-transfected p1 (p1 tr, middle panel) or naïve p1 (p1 naïve, right panel). p1 tr were pre-transfected with the plasmids necessary to support replication and transcription of the minigenome, NP, VP30, VP35 and L, transfection was done 24 h in advance to the infection with iVLPs. To monitor the ability of the iVLPs to induce reporter gene activity upon infection, both p1 tr and p1 naïve cells were lysed 24 h p.i. and the relative reporter gene activity was determined as indicated above. (B) Guinea pig (104C1) cells were treated as described in (A). Shown are the means and standard deviations from three independent experiments performed in triplicates, statistical analysis was performed using the Student's t-test. * $P< 0.05$; **, $P<0.01$.

We suggest that the higher levels of the reporter gene activity in guinea pig p1 naïve and p1 tr cells cannot be explained by the influence of the D184N mutation in VP40 on transcription and replication in indicator cells, because in these cells VP40 is provided only from incoming iVLPs and present in rather low amounts. We consider that the observed higher levels of transcription and replication in guinea pig cells was induced by the higher infectivity of iVLPs which were produced in guinea pig p0 cells and contained $VP40_{D184N}$.

3.1.9 Composition of the iVLPs in presence of $VP40_{D184N}$

To address the importance of the D184N mutation in VP40 on iVLP composition we quantified the amount of GP, NP and VP40 in iVLP preparations. The iVLPs were purified from the supernatant of human and guinea pig p0 cells at 72 h p.t. as described above and the amount of VP40, NP and GP was determined by Western blot. The ratio of NP or GP to VP40 was calculated (Fig. 17). In addition, we quantified the amounts of iVLP-associated minigenomes via RT-qPCR (Fig. 17). The ratio of NP or GP to wildtype VP40 was set to 1. The GP to $VP40_{D184N}$ ratio in iVLPs produced by both human and guinea pig p0 cells was not altered. The ratio of NP to $VP40_{D184N}$ in iVLPs produced in human p0 cells was not affected as well (Fig. 17A). However, the ratio of NP to $VP40_{D184N}$ in iVLPs produced in guinea pig p0 cells showed a 1.3-fold increase (Fig. 17B). Although not statistically significant, the number of minigenomes in the $VP40_{D184N}$-induced iVLPs was higher both for human and guinea pig p0 cells (Fig. 17A-B). These results suggest that the D184N mutation in VP40 enhances the incorporation of nucleocapsid-like structures into iVLPs in a species-specific manner. This result could explain the higher reporter gene activity $VP40_{D184N}$-induced iVLPs produced in guinea pig p1 cells (Fig.16 A-B)

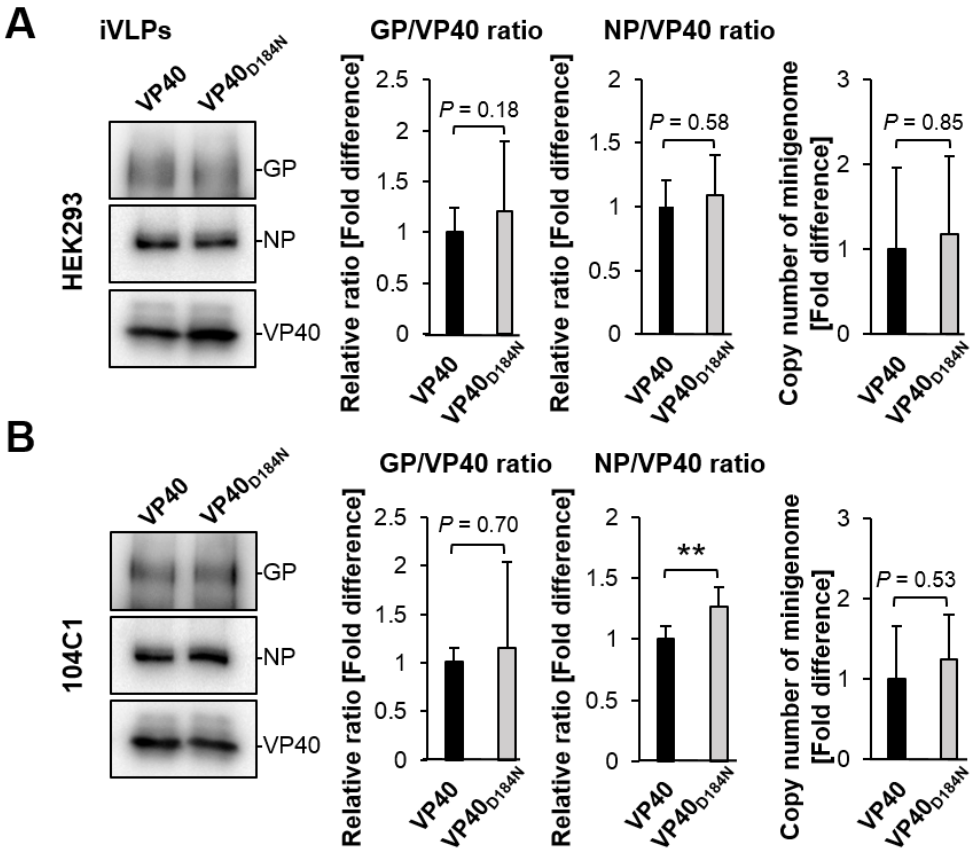

Figure 17: Impact of the D184N mutation on the particle composition of iVLPs produced in human and guinea pig cells

iVLPs from either wildtype VP40- or $VP40_{D184N}$-expressing human (A) or guinea pig (B) cells were analyzed by SDS-PAGE and Western blot analysis. The viral proteins VP40, NP and GP were detected by either VP40-, NP- or GP-specific antibodies (left panel). The signal intensity of VP40, NP and GP bands was measured by the Image Lab software and the relative ratio of either GP to VP40 or NP to VP40 was determined. The relative ratio of either GP (left middle panel) or NP (right middle panel) to wildtype VP40 was set to one. The amount of minigenomes incorporated into iVLP minigenomes was measured by qRT-PCR (right panel). Shown are the means and standard deviations from three independent experiments performed in triplicates, statistical analysis was performed using the Student's t-test. **, $P<0.01$.

3.2 Analysis of the impact of the D184N mutation in VP40 on the viral fitness of recombinant MARV in guinea pig and human cells

This chapter aims to determine the species-specific viral fitness of a recombinant wildtype MARV and a recombinant MARV containing only the D184N mutation in VP40 in human and guinea pig cells.

3.2.1 Characterization of a recombinant Marburg virus (rMARV) containing a single point mutation D184N in VP40 (rMARV$_{VP40(D184N)}$)

To evaluate the importance of the D184N mutation in the viral context, a recombinant virus containing only the D184N mutation in VP40 was used. As mentioned in the methods section, a full-length plasmid encoding the genomic sequence of a recombinant virus containing only the D184N single point mutation in VP40 was cloned by Ulla Welzel, and the rescue of this recombinant virus (rMARV$_{VP40(D184N)}$) was performed by Gordian Schudt. A recombinant MARV Musoke with the wildtype genome (rMARV$_{WT}$) was rescued by Olga Dolnik (Dolnik *et al.*, 2014).

To determine the virion morphology of rMARV$_{WT}$ and rMARV$_{VP40(D184N)}$, VeroE6 cells were infected at an MOI of 1 and incubated for three days. Virus was purified from supernatants of infected cells by centrifugation through a sucrose cushion. EM analysis and immunogold staining with a goat polyclonal anti-GP antibody were performed by Larissa Kolesnikova. A comparative EM analysis determined that preparations of rMARV$_{WT}$ and rMARV$_{VP40(D184N)}$ were indistinguishable from each other (Fig. 18A). To compare the amount of the glycoprotein GP incorporated into viral particles of rMARV$_{WT}$ and rMARV$_{VP40(D184N)}$, the number of immunogold particles associated with virions were quantified in at least 13 particles for each preparation. When the amount of GP present on rMARV$_{WT}$ was set to 100%, the amount of GP in rMARV$_{VP40(D184N)}$ particles comprised 99.2% (Fig. 18C).

To determine changes in the protein composition of $rMARV_{WT}$ and $rMARV_{VP40(D184N)}$, purified virus stocks were subjected to SDS-PAGE and silver stained. The protein composition of $rMARV_{WT}$ and $rMARV_{VP40(D184N)}$ was similar (Fig. 18B).

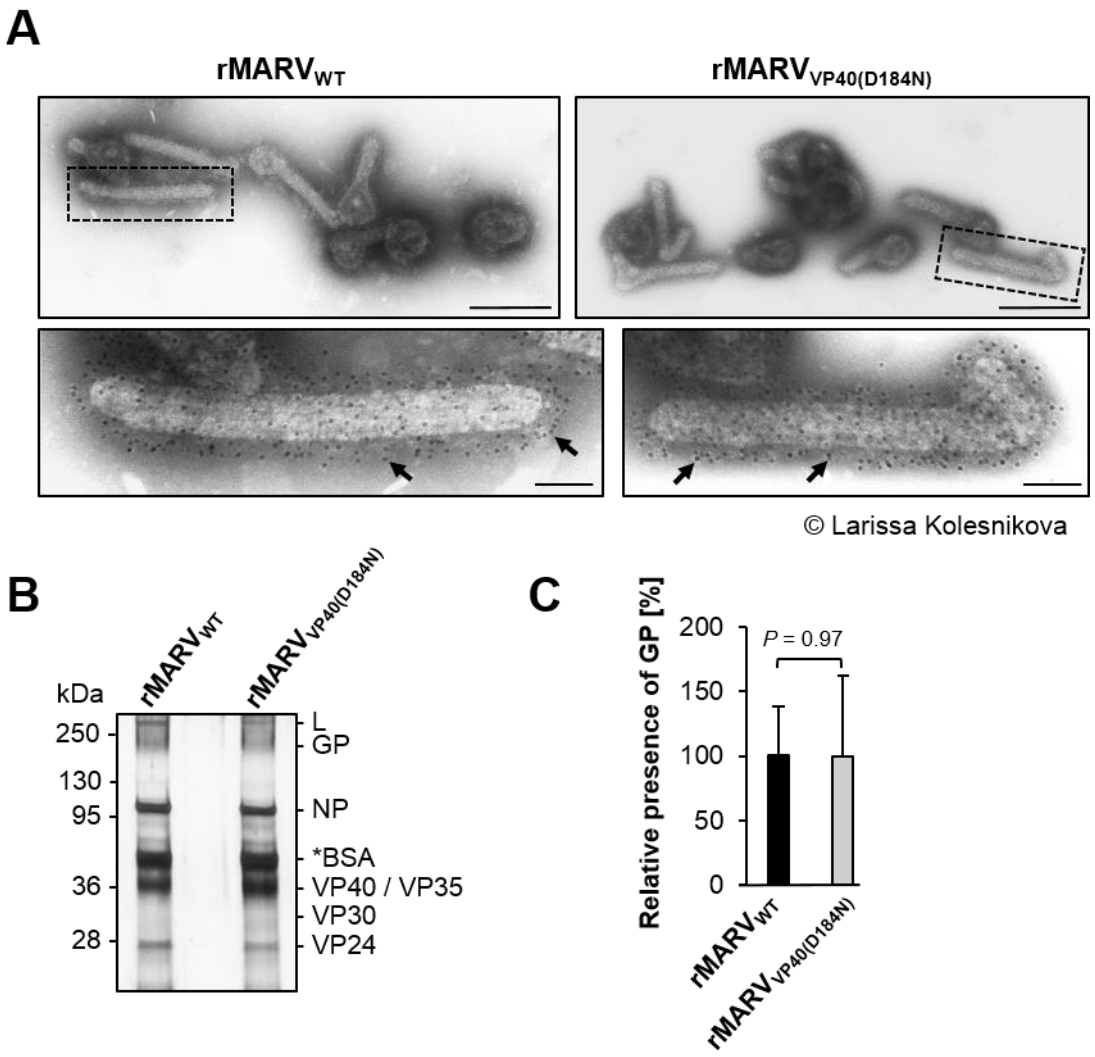

Figure 18: Characterization of $rMARV_{WT}$ and $rMARV_{VP40(D184N)}$

(A) Electron microscopic analysis of $rMARV_{WT}$ and $rMARV_{VP40(D184N)}$. The virus preparations were fixed in 4% PFA in DMEM and immunogold labelled with anti-GP specific antibody, 12 nm gold particles. Negative staining was performed using 2% phosphotungstic acid. An overview of each preparation is shown in the upper panel. The black box indicates the single particle shown at a higher magnification in the lower panel, 12 nm gold particles are indicated by arrows. The bar indicates 500 nm in the upper panel and 100 nm in the lower panel. (B) SDS-PAGE and subsequent silver staining of $rMARV_{WT}$ and $rMARV_{VP40(D184N)}$ preparations. (C) Relative incorporation of GP into virus particles in $rMARV_{WT}$ and $rMARV_{VP40(D184N)}$ preparations. Shown are the means and standard deviations from at least thirteen particles, statistical analysis was performed using the Student's t-test.

3.2.2 Comparison of viral growth of rMARV$_{VP40(D184N)}$ and rMARV$_{WT}$ in human and guinea pig cells

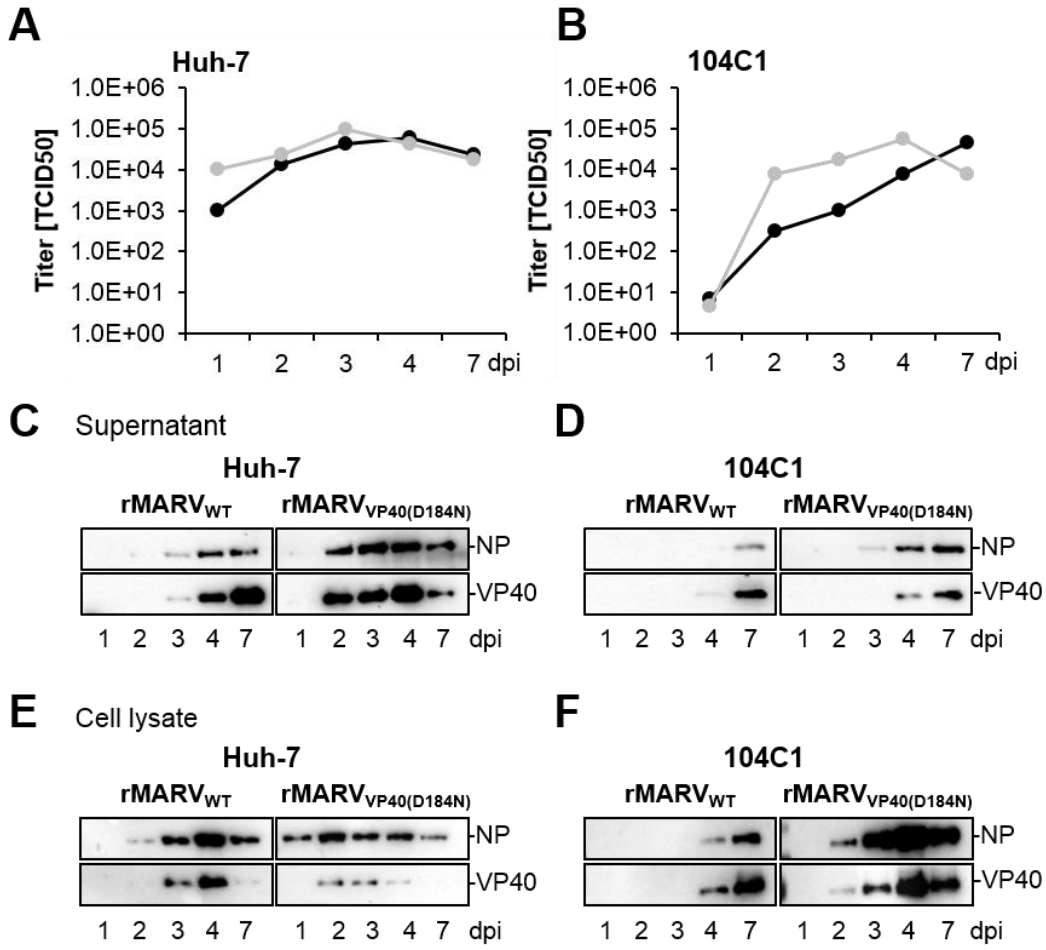

Figure 19: Comparative growth curve analysis of rMARV$_{VP40(D184N)}$ and rMARV$_{WT}$ in human and guinea pig cells.

(A-B) Growth kinetics of rMARV$_{WT}$ (black circles) and rMARV$_{VP40(D184N)}$ (gray circles) in (A) Huh-7 and (B) 104C1 cells infected with either virus at an MOI of 0.01. (C-F) Western blot analysis of viral protein levels, in culture supernatants (C-D) or cell lysates (E-F) of Huh-7 or 104C1 cells infected at different days after infection. Supernatants and cell lysates were collected at the indicated time points and analyzed by SDS-PAGE and Western blotting using NP- and VP40-specific antibodies. dpi, Days p.i.

To determine the effect of the D184N mutation on the viral production kinetics in human and guinea pig cells, growth curve analysis of rMARV$_{WT}$ and rMARV$_{VP40(D184N)}$ was performed by Astrid Herwig. Either human (Huh-7) or guinea pig (104C1) cells were infected with rMARV$_{WT}$ or rMARV$_{VP40(D184N)}$ at an MOI of 0.01. Supernatants and cell lysates were harvested on day one to four and at day seven p.i. and used for Western blot analysis. Viral titers in the supernatants were quantified by TCID50.

The titers of both recombinant viruses in human Huh-7 cells one day p.i. were

two to three logarithmic magnitudes higher than those in guinea pig 104C1 cells, indicating a major difference in the intrinsic susceptibility of these cell lines to MARV infection. Comparison of growth kinetics of both recombinant viruses showed that in human cells, the titer of $rMARV_{VP40(D184N)}$ at day one p.i. ($1x10^4$) was one order of magnitude higher than the titer of $rMARV_{WT}$ ($1x10^3$) (Fig. 19A). After two days of infection the titers of $rMARV_{WT}$ and $rMARV_{VP40(D184N)}$ were comparable in human cells (Fig. 19A). A different picture emerged in guinea pig cells. At day two and three p.i, the titers of $rMARV_{VP40(D184N)}$ were more than one logarithmic magnitude higher compared to $rMARV_{WT}$ (Fig. 19B). A difference in titers was not detectable after day four p.i., possibly due to cell death. In general, $rMARV_{VP40(D184N)}$ showed improved growth compared to $rMARV_{WT}$ in guinea pig cells.

Western blot analysis showed that infection with $rMARV_{VP40(D184N)}$ resulted in earlier detection of the viral proteins, VP40 and NP, compared to $rMARV_{WT}$ in both, human and guinea pig cells (Fig. 19 C-F). In the supernatant of $rMARV_{VP40(D184N)}$ infected cells, viral proteins were detectable at day two (supernatant of human cells) or day three (supernatant of guinea pig cells). In the supernatant of $rMARV_{WT}$ infected cells, viral proteins were detectable at day three (human cells) and at day four (guinea pig cells) (Fig. 19C and 18D). The viral proteins of the $rMARV_{VP40(D184N)}$ were detectable at day one p.i. in cell lysates from human cells and at day two p.i. in guinea pig cells. In fact, viral proteins of $rMARV_{VP40(D184N)}$ were detectable in cell lysates one day earlier in human cells and two days earlier in guinea pig cells compared to $rMARV_{WT}$-infected cells (Fig. 19E and Fig. 19F). In summary, infection with $rMARV_{VP40(D184N)}$ resulted in earlier detection of viral proteins in the supernatant and cell lysates of human and guinea pig cells.

The amount of NP in released virions was significantly higher in $rMARV_{VP40(D184N)}$ resulting in an increased ratio of NP over VP40. The increased ratio of NP to VP40 suggests an enhanced incorporation of nucleocapsid-like structures, which in turn would result in more infectious virions (Fig. 19C and Fig. 19D, day seven). Altogether, $rMARV_{VP40(D184N)}$ replicated better in guinea pig cells compared to $rMARV_{WT}$. This is reflected by higher viral titers and earlier detection of viral proteins in the supernatant and cell lysates of $rMARV_{VP40(D184N)}$-infected guinea pig cells.

3.2.3 Quantification of viral genomes in the supernatant and cells infected with rMARV$_{VP40(D184N)}$ or rMARV$_{WT}$

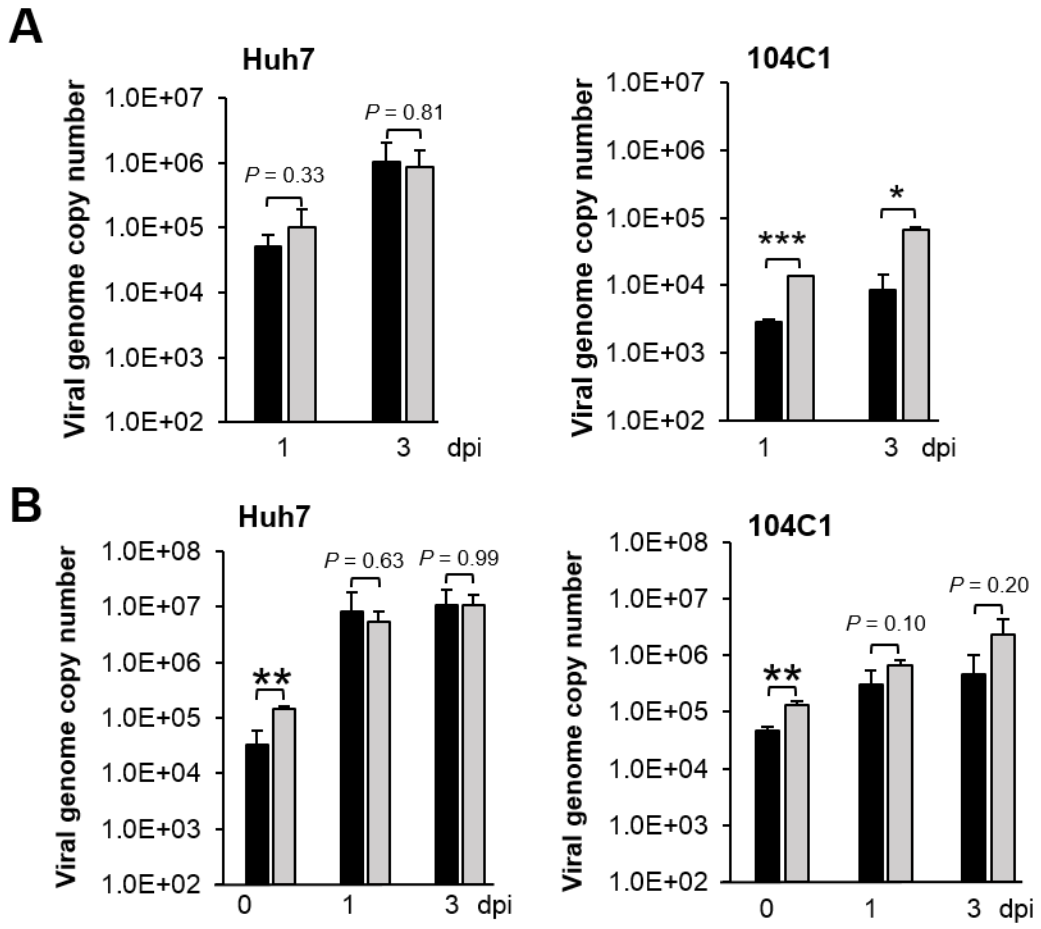

Figure 20: Comparative quantification of viral genomes of either rMARV$_{WT}$ or rMARV$_{VP40(D184N)}$ infected human and guinea pig cells

(A-B) Viral genomes copies present in the supernatants (A) or cells(B) infected with rMARV$_{WT}$ or rMARV$_{VP40(D184N)}$ at an MOI of 3 were determined by RT-qPCR. Cellular RNAs were harvested at 0, 1 and 3 days p.i.. Supernatants were collected at day 1 and 3 p.i.. rMARV$_{WT}$ (black columns) and rMARV$_{VP40(D184N)}$ (gray columns). Shown are the means and standard deviations from two independent experiments performed in duplicates, statistical analysis was performed using the Student's t-test. *,P<0.05; **,P<0.01, ***,P<0.001.

To determine the number of viral genomes in the supernatant of either rMARV$_{WT}$- or rMARV$_{VP40(D184N)}$-infected human or guinea pig cells RT-qPCR was performed. For this purpose either Huh-7 or 104C1 cells were infected with either rMARV$_{WT}$- or rMARV$_{VP40(D184N)}$ at an MOI of 3. The used qPCR probe targets a highly conserved region of the viral polymerase. In order to quantify the genome copy numbers a standard curve of serially diluted MARV-specific in vitro transcripts was amplified in parallel to samples of viral RNA. Total cellular RNA and RNA

from cell culture supernatants was isolated at day one and three p.i. In addition, cellular RNA was isolated from cells harvested immediately after 1 h of incubation with virus (0 dpi). The amount of viral genome copies present in the supernatant of human cells infected with $rMARV_{VP40(D184N)}$ or $rMARV_{WT}$ did not differ (Fig. 20A). However, infection with $rMARV_{VP40(D184N)}$ resulted in the detection of significant more viral genome copies in the supernatant of guinea pig cells compared to those infected with $rMARV_{WT}$ (Fig. 20A). Namely, the number of viral genomes in the supernatant of $rMARV_{VP40(D184N)}$ infected guinea pig cells was 4.7-fold higher at day one p.i. and 7.8-fold higher at day three p.i. compared to $rMARV_{WT}$ (Fig. 20A).

The amount of viral genomes detected in the total RNA of $rMARV_{VP40(D184N)}$-infected human cells showed an increase of 4.4-fold 1 h p.i. (0 dpi) compared to $rMARV_{WT}$. At day one and three p.i. the number of viral genomes detected in the total RNA was similar between $rMARV_{WT}$- and $rMARV_{VP40(D184N)}$-infected human cells (Fig. 20B). The number of viral genomes in the total RNA of $rMARV_{VP40(D184N)}$-infected guinea pig cells were increased compared to $rMARV_{WT}$-infected cells at all tested time points, although these differences were not statistically significant. Briefly, the increase of viral genome copies in $rMARV_{VP40(D184N)}$-infected guinea pig cells 1 h p.i., one day and three days after infection was 3-fold, 2.2-fold and 5.1-fold higher than those of $rMARV_{WT}$-infected guinea pig cells (Fig. 20B). These findings underline that $rMARV_{VP40(D184N)}$ replicates more efficiently only in guinea pig cells but not in human Huh-7 cells.

3.2.4 Comparison of the infectivity of rMARV$_{WT}$ and rMARV$_{VP40(D184N)}$

Our data on growth kinetics of rMARV$_{WT}$ and rMARV$_{VP40(D184N)}$ in human and guinea pig cells suggested that rMARV$_{VP40(D184N)}$ might display higher infectivity compared to rMARV$_{WT}$ specifically in guinea pig cells. To determine the infectivity of MARV$_{WT}$ or rMARV$_{VP40(D184N)}$ in cells from different species, human (Huh-7), guinea pig (104C1) and monkey (VeroE6) cells were infected with either rMARV$_{WT}$ or rMARV$_{VP40(D184N)}$ at an MOI of 1. The cells were fixed after a single cycle growth curve, 19 h p.i.. Cells were stained with DAPI and antibodies against NP. The number of infected cells was quantified by immunofluorescence analysis. Cells displaying NP-positive inclusion bodies were considered as infected. The number of cells infected with rMARV$_{WT}$ was set to one and the relative fold change was calculated for rMARV$_{VP40(D184N)}$-infected cells.

VeroE6 cells were used as control for the inoculum, since preparation and titration of both viral stocks was carried out in this cell line. Infection of VeroE6 cells with equal TCID50 units of both recombinant viruses was expected to result in similar numbers of infected cells. Indeed, infection of VeroE6 cells displayed comparable infectivity of rMARV$_{WT}$ and rMARV$_{VP40(D184N)}$ (35.7% and 40.6% cells, Fig. 21A bottom panel and Fig. 21B, right graph). Infection of human Huh-7 cells with rMARV$_{VP40(D184N)}$ resulted in 2.2-fold higher number of infected cells (76.8%) compared to rMARV$_{WT}$-infected cells (34.8%) (Fig. 21A, top panel and Fig. 21B, left graph). Guinea pig 104C1 cells were less susceptible to infection, the number of rMARV$_{VP40(D184N)}$-infected cells comprised 13.1%, but this number was 5.5-fold higher than the number of guinea pig cells infected with rMARV$_{WT}$ (2.4%) (Fig. 21A middle panel and Fig. 21B, middle graph). In summary, rMARV$_{VP40(D184N)}$ displayed a higher infectivity than rMARV$_{WT}$ both in human and guinea pig cells, but the effect was more pronounced in guinea pig cells. This data supported the results of the growth kinetics analysis shown in Fig. 19 A-B.

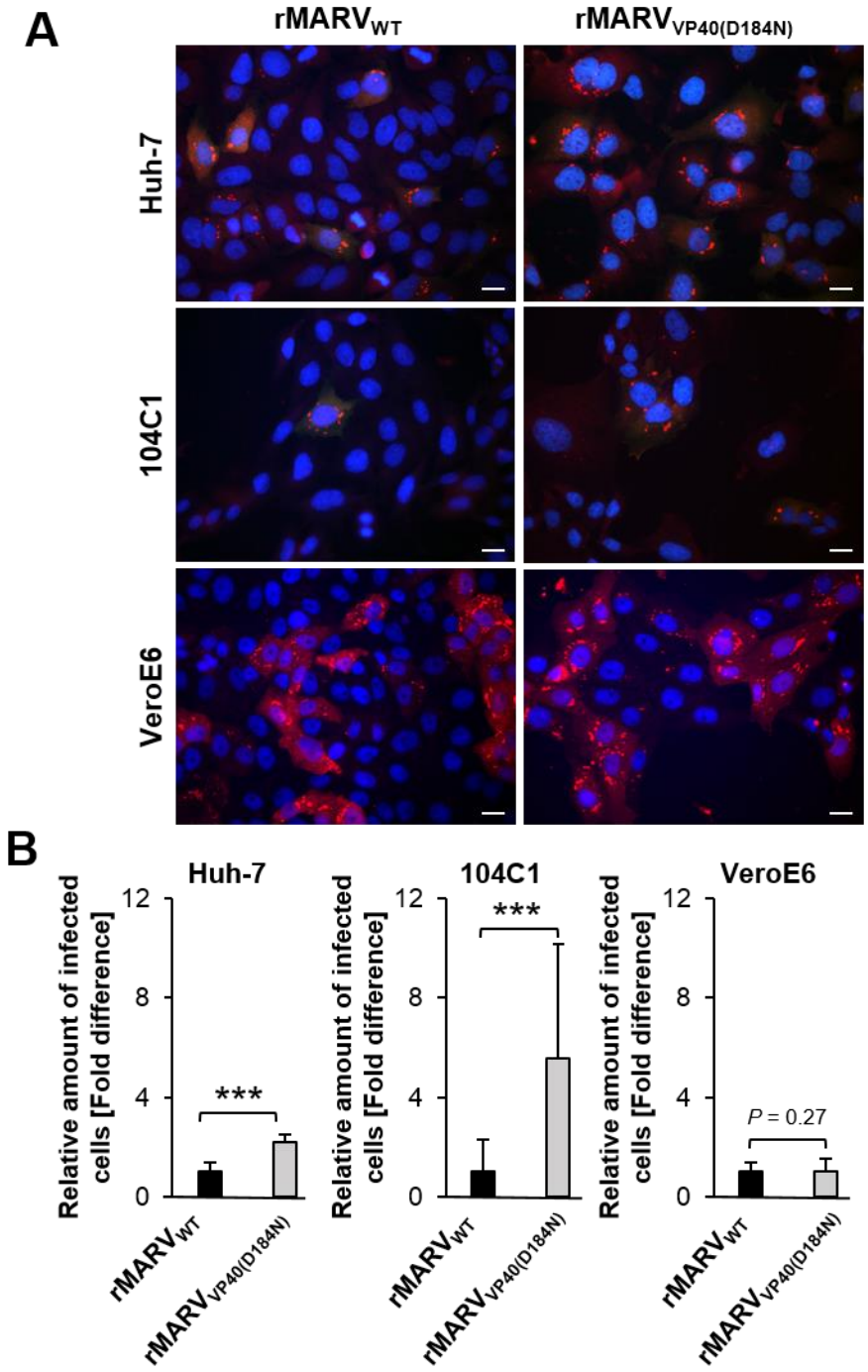

Figure 21: Analysis of the intrinsic infectivity of rMARV$_{VP40(D184N)}$ and rMARV$_{WT}$ in human and guinea pig cells

(A) Huh-7, 104C1 and VeroE6 cells were grown on coverslips and infected at an MOI of 1. The cells were fixed with 4% PFA in DMEM at 19 h p.i. and stained with DAPI (nuclei) and a NP-specific antibody (shown in red). Bars indicate 20 µm. (B) Graphics show the relative amount of infected cells based on the percentage of infected cells, this number was set to 1 for cells infected with rMARV$_{WT}$ in all tested cell lines. Means values and standard deviations of the results from three independent experiments are shown. For each experiment infection was quantified for 10 random fields. The results reflect data from three independent experiments, statistical analysis was performed using the Student's t-test. ***,P< 0.001.

3.2.5 Characterization of the inclusion body formation in rMARV$_{WT}$ and rMARV$_{VP40(D184N)}$ infected cells

Perinuclear inclusion bodies containing viral nucleocapsid proteins are a hallmark of filovirus-infected cells. The NP-positive inclusion bodies can be detected at 10-12 h p.i., and are considered as site of viral replication and transcription (Dolnik *et al.*, 2015). To assess the influence of the D184N mutation on inclusion body formation, human or guinea pig cells were infected with either rMARV$_{WT}$ or rMARV$_{VP40(D184N)}$ with at an MOI of 1.

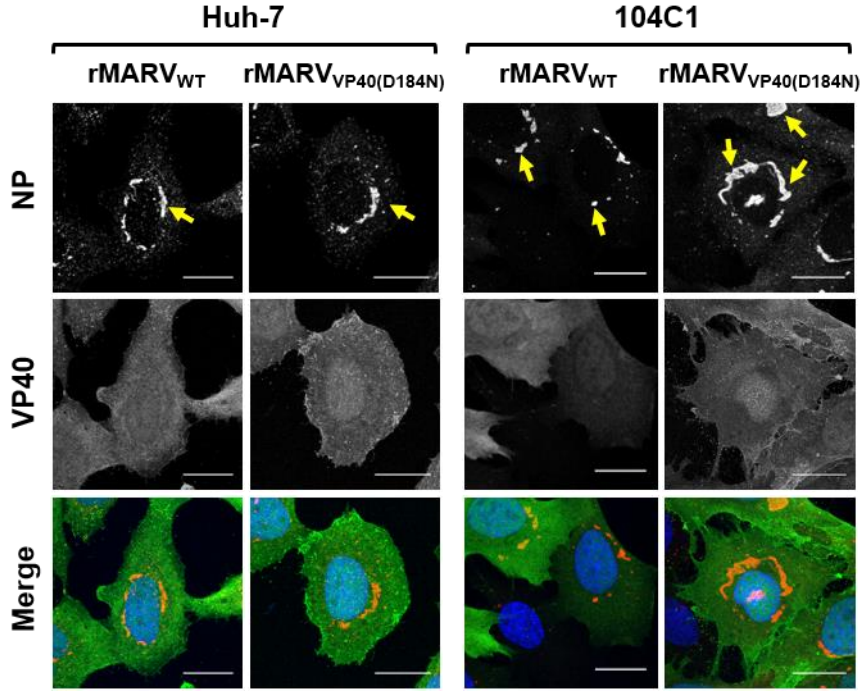

Figure 22: Inclusion body formation upon infection of human and guinea pig cells with rMARV$_{WT}$ and rMARV$_{VP40(D184N)}$

Huh-7 or 104C1 cells were infected with either rMARV$_{WT}$ or rMARV$_{VP40(D184N)}$ at an MOI of one. The cells were fixed at 19 h p.i. with 4% PFA in DMEM and stained with MARV NP- (red) and MARV VP40- specific (green) antibodies as well as the nuclei with DAPI (blue). Shown images are maximum intensity projections of infected cells. Yellow arrows indicate viral inclusions. Bars represent 20 µm.

Inclusion bodies were detected in the perinuclear region of rMARV$_{WT}$- and rMARV$_{VP40(D184N)}$-infected cells, the shape of the inclusion bodies did not differ between human and guinea pig cells, however the size of inclusion bodies in rMARV$_{VP40(D184N)}$-infected guinea pig cells was larger than those in rMARV$_{WT}$-infected guinea pig cells (Fig. 22). This observation was further analyzed by quantifying the cross-sectional area of the maximal size of a single inclusion body, the total area of inclusions per cell, and the average area of a single

inclusion body within an infected cell. No differences were found in all tested parameters in human cells infected with either $rMARV_{WT}$ or $rMARV_{VP40(D184N)}$. Thus, the single inclusion size in human cells infected with $rMARV_{WT}$ was 19.2 μm^2 compared to 17.7 μm^2 in $rMARV_{VP40(D184N)}$-infected cells. The total area of inclusion bodies in human cells comprised 46.1 μm^2 in $rMARV_{WT}$-infected cells compared to 47.2 μm^2 in $rMARV_{VP40(D184N)}$-infected cells. Finally, the maximal inclusion body size in human cells was 46.4 μm^2 in $rMARV_{WT}$-infected cells compared to 43.2 μm^2 in cells infected with $rMARV_{VP40(D184N)}$. These findings demonstrated that both viruses $rMARV_{WT}$ and $rMARV_{VP40(D184N)}$ form inclusions of equal size in human cells (Fig. 23, upper panel).

In contrast, infection of guinea pig cells with $rMARV_{VP40(D184N)}$ led to formation of significantly larger inclusions (Fig. 23, lower panel). The cross-sectional area of a single viral inclusion was 21.7μm^2 in $rMARV_{WT}$-infected guinea pig cells and reached 36.9 μM^2 in cells infected with $rMARV_{VP40(D184N)}$, thus the difference was 1.7-fold. The total area of inclusion in $rMARV_{VP40(D184N)}$ infected guinea pig cells was 84.9 μm^2 and 54.9 μm^2 in cells infected with $rMARV_{WT}$ infection resulting in a 1.5-fold difference. The maximum inclusion body size displayed the strongest change (by 2.0-fold) and comprised 93.5 μm^2 in cells infected with $rMARV_{VP40(D184N)}$ and 47.5 μm^2 in guinea pig cells infected with $rMARV_{WT}$ (Fig. 23, lower panel).

To assess whether the observed difference in the inclusion body size in guinea pig and human cells is associated with morphologic changes within the inclusion bodies, a comparative electron microscopic analysis of either $rMARV_{WT}$ or $rMARV_{VP40(D184N)}$ infected human or guinea pig cells was performed. In human cells, the morphology of viral inclusions, as well as the number of mature nucleocapsids, were similar in cells infected with either $rMARV_{WT}$ or $rMARV_{VP40(D184N)}$ (Fig. 24, left panel). In contrast, guinea pig cells infected with $rMARV_{VP40(D184N)}$ showed significant larger viral inclusions and a significantly increased amount of mature nucleocapsids (Fig. 24, right panel). Altogether, these data suggests that the insertion of the D184N mutation into MARV VP40 provides MARV more efficient replication and improves the virus assembly, specifically in guinea pig cells.

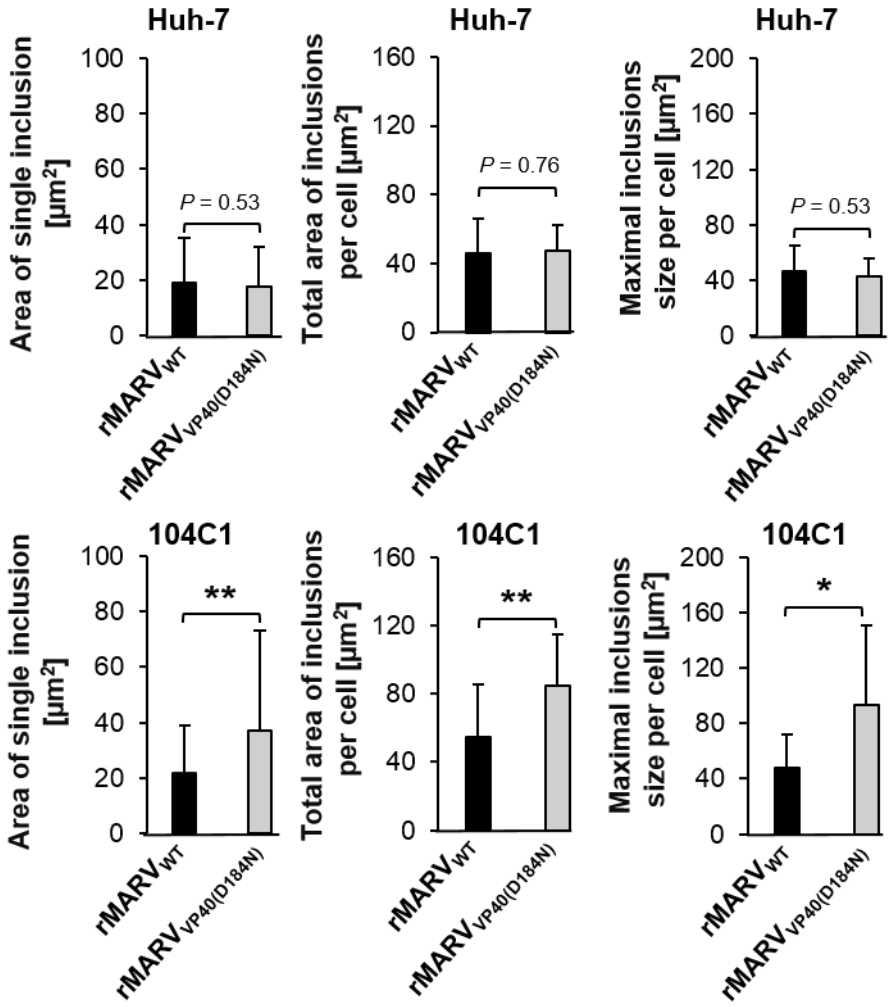

Figure 23: Comparative quantification of viral inclusions in human and guinea pig cells

The graphs indicate the size of the viral inclusion bodies in human (Huh-7) or guinea pig (104C1) cells infected with either $rMARV_{WT}$ (black) or $rMARV_{VP40(D184N)}$ (gray) at an MOI of 1. The pictures were acquired as described in Figure 21. The Leica Application Suite X software was used for analysis of the inclusion body size. The cross-sectional area of a single inclusion body (left panel), the total area of inclusions (middle panel) and the maximal size of a single inclusion body (right panel) were measured in at least ten cells. Shown are the means and standard deviations, statistical analysis was performed using the Student's t-test. *, P<0.05; **,P<0.01.

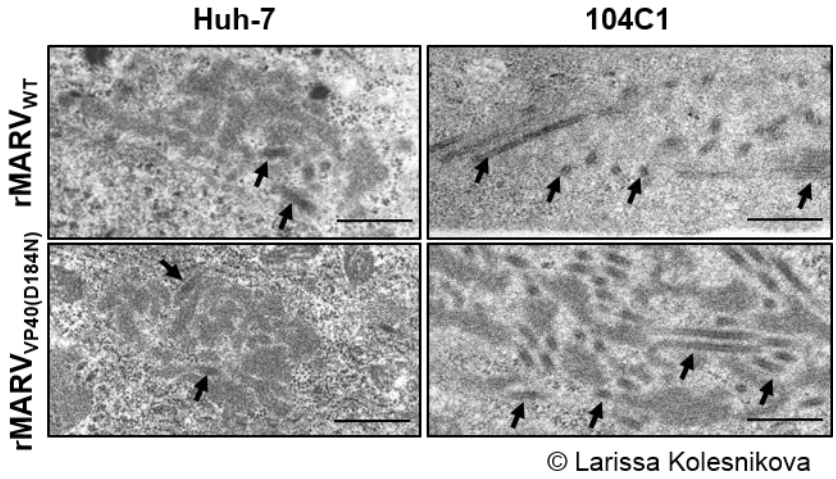

Figure 24: Electron microscopic analysis of rMARV$_{WT}$ and rMARV$_{VP40(D184N)}$-infected human and guinea pig cells

Cells were infected with viruses at an MOI of 1 fixed with 4% PFA in DMEM 24 h p.i. and embedded in an epoxy resin. Ultrathin sections of infected cells were contrasted with uranyl acetate and lead citrate. Tubular-like structures with electron dense wall represent mature nucleocapsids and indicated by arrows. Bars indicate 500 nm.

3.3 Influence of the mutations S741C, D758A, A759D in L on its functions in guinea pig and human cells

This part aims to shed light on the species-specific importance of the S741C, D758A and A759D mutations on the L protein function in guinea pig and human cells. Due to the lack of detection tools, a plasmid encoding a mCherry-tagged L protein was created and characterized. This plasmid (pCAGGS-mCherry-L) containing the tagged L variant was used to generate L mutants containing the different combinations of the mutations observed in the guinea pig-lethal MARV. The mutations were characterized regarding their function and species-specific effects in human and guinea pig cells.

3.3.1 Characterization of mCherry-tagged L

The L protein of MARV is the largest MARV protein with a size of 220 kDA. It carries out several functions such as replication, transcription, capping and methylation of mRNAs. L has six conserved domains, CR I - VI (Fig. 25). Functional studies on the MARV L protein are complicated, due to the lack of tools for proper detection of the L protein. To assess the importance of the three mutations present in a guinea pig-lethal MARV we created a mCherry-tagged MARV L construct allowing to perform such studies.

For tagging of the MARV L protein with mCherry we used an approach developed for the closely related EBOV L (Hoenen *et al.*, 2012). The mCherry-tag was introduced to a variable hinge region between the amino acids 1704 and 1705 (Fig. 25). The recently published crystal structure of the closely related VSV polymerase allowed to assume that the mCherry-tag places between the connector- and the methyltransferase domain of the polymerase (Liang *et al.*, 2015). MARV-L containing a mCherry-tag (L) preserved 60% of its reporter gene activity in a minigenome assay compared to wildtype L (L_{WT}) (Fig. 25). A previous study on a flag-tagged MARV L showed that co-expression of the L protein with NP and VP35 resulted in localization of the L protein in NP-derived inclusion

bodies through interactions with VP35, while solely expressed L protein was diffusely distributed in the cytoplasm (Becker *et al.*, 1998).

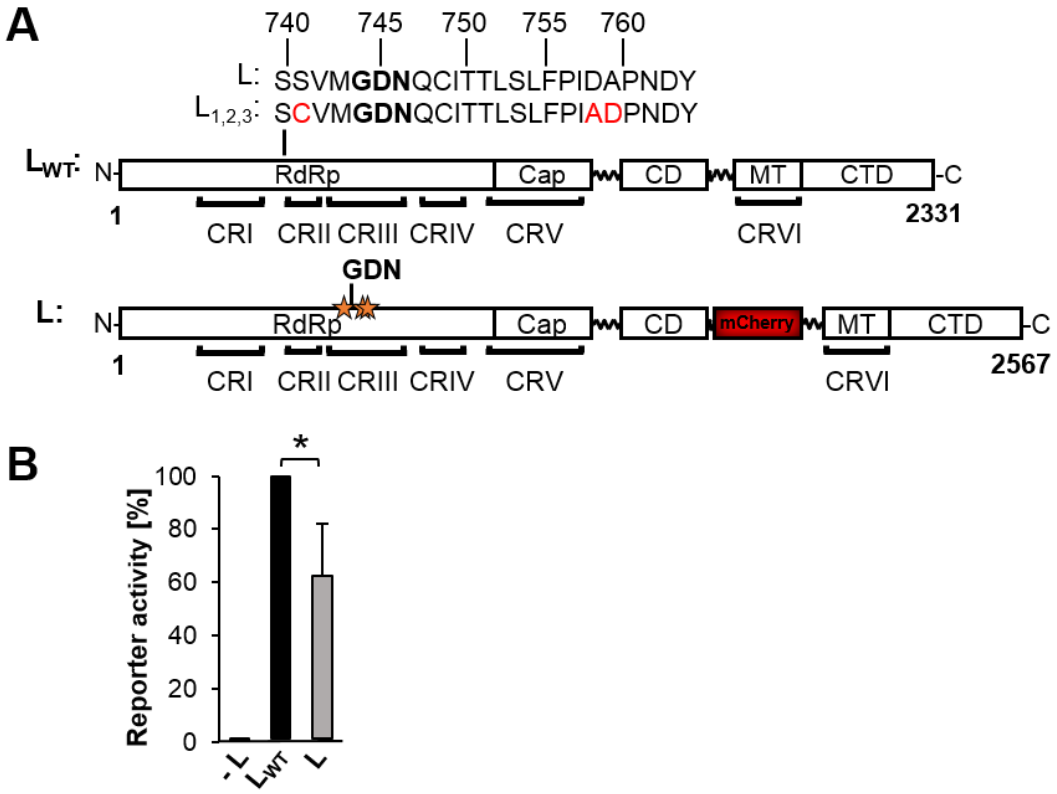

Figure 25: Characterization of a mCherry-tagged L (L)

(A) Schematic domain architecture of wildtype L (L_{WT}) and mCherry-tagged L (L). Amino acid region from 740 to 763 including the highly conserved GDN active site motif (bold) and the positions of the amino acid substitutions of the guinea pig-lethal MARV L ($L_{1,2,3,}$) (upper scheme red, lower scheme asterisks) are shown. Below each scheme a schematic presentation of the non-segmented negative strand viruses conserved regions (CR I to CR VI). The location of the mCherry-tag is shown in red. RdRp: polymerase domain Cap: capping domain, CD: connector domain, MT: methyltransferase domain, and CTD: C-terminal domain (B) Comparison of the polymerase activity of L_{WT} and L in HEK293 cells. Cells were transfected required for to the minigenome assay and either L_{WT} or L encoding plasmid was used. Cells were lysed 48 h post transfection and the reporter gene activity was determined. The L_{WT} activity was set to 100%. Shown are the means and standard deviations from three independent experiments performed in triplicates in a logarithmic scale, statistical analysis was performed using the Student's t-test. * $P < 0.05$.

To analyze whether MARV L containing a mCherry-tag (L) preserved the capability to relocate into inclusion bodies, we performed IFA of cells transfected either with only pCAGGS-mCherry-L or together with the plasmids necessary for the minigenome assay (pCAGGS-NP, VP30, VP35, 3M5M, T7-pol). In agreement with previous observations, single expression of L led to diffuse expression in the cytoplasm (Fig. 26, i), whereas co-expression with the viral nucleocapsid complex and the minigenome resulted in localization of L into NP-induced inclusion bodies where a clear colocalization with VP35 and NP was observed (Fig. 26, ii-v)

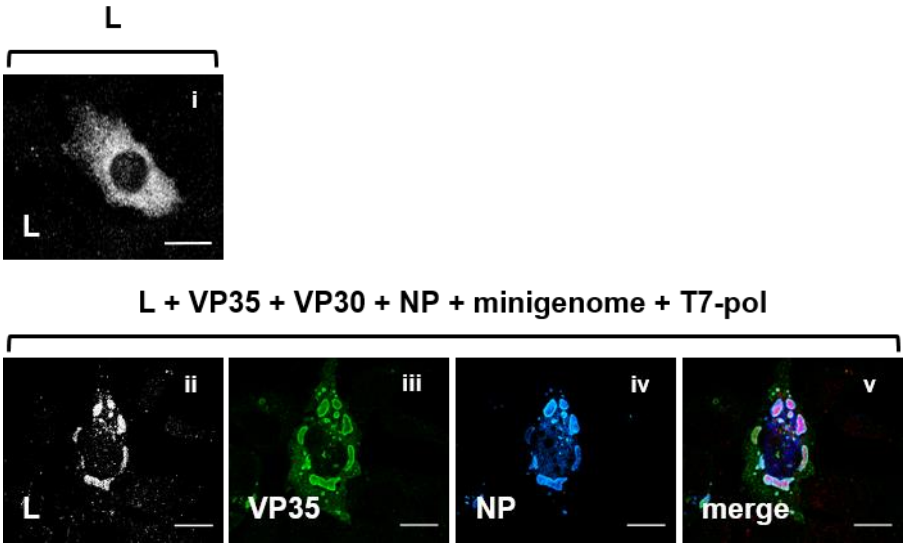

Figure 26: Cellular distribution of a mCherry-tagged L (L)

(i) Localization of singly expressed mCherry-tagged L (L). (ii-v) Expression of L in the context of the minigenome assay. Huh-7 cells were transfected only with L gene or L was co-expressed with proteins required for the minigenome assay. Cells were fixed 48 h p.t. and stained with anti-VP35 (green) and anti-NP (blue) specific antibodies. The auto fluorescence of mCherry was detected (i, ii, black and white). Bars indicate 20 µm.

3.3.2 Intracellular localization of the mCherry-L mutants

Efficient interactions of L with the nucleocapsid proteins are mandatory to fulfill efficient replication and transcription (Becker *et al.*, 1998; Mühlberger *et al.*, 1998). It was unclear whether the three mutations of the guinea pig-lethal MARV L affect the interactions of the viral polymerase with other proteins of the viral polymerase complex. Efficient replication and transcription requires interaction of the L protein with the polymerase co-factor VP35 leading to recruitment of L into NP-derived inclusion bodies (Becker *et al.*, 1998; Mühlberger *et al.*, 1998). To analyze whether the mutations in L affect the interactions with nucleocapsid proteins, we constructed L mutants. Recombinant L proteins containing only a single amino acid substitution L_1 (S741C), L_2 (D758A), L_3 (A759D), all possible double amino acid substitutions $L_{1,2}$ (S741C, D758A), $L_{1,3}$ (S741C, A759D), $L_{2,3}$ (D758A, A759D) and a mutant containing all three amino acid substitutions $L_{1,2,3}$ (S741C, D758A, A759D) were constructed (Fig. 27).

To determine whether the L mutants are efficiently recruited into NP-induced inclusion bodies plasmids required for the minigenome assay and one of the plasmids encoding the mCherry-tagged L mutants were transfected into human and guinea pig cells. The cells were fixed 48 h post transfection and stained with Phalloidin-FITC (green). The cellular localization of the wildtype mCherry-L protein and of the mCherry-L protein mutants (red) was assessed by IFA. All tested mCherry-L proteins were located in perinuclear inclusion bodies, in both human and guinea pig cells (Fig. 27). None of the mutants displayed a diffuse cytoplasmic distribution, indicating that the mutations in the active site of viral polymerase did not alter the interactions with the nucleocapsid proteins. In addition, the size and shape of the inclusion bodies was not affected by the polymerase mutations and no significant changes were observed in the intensity of mCherry fluorescence between all mutants.

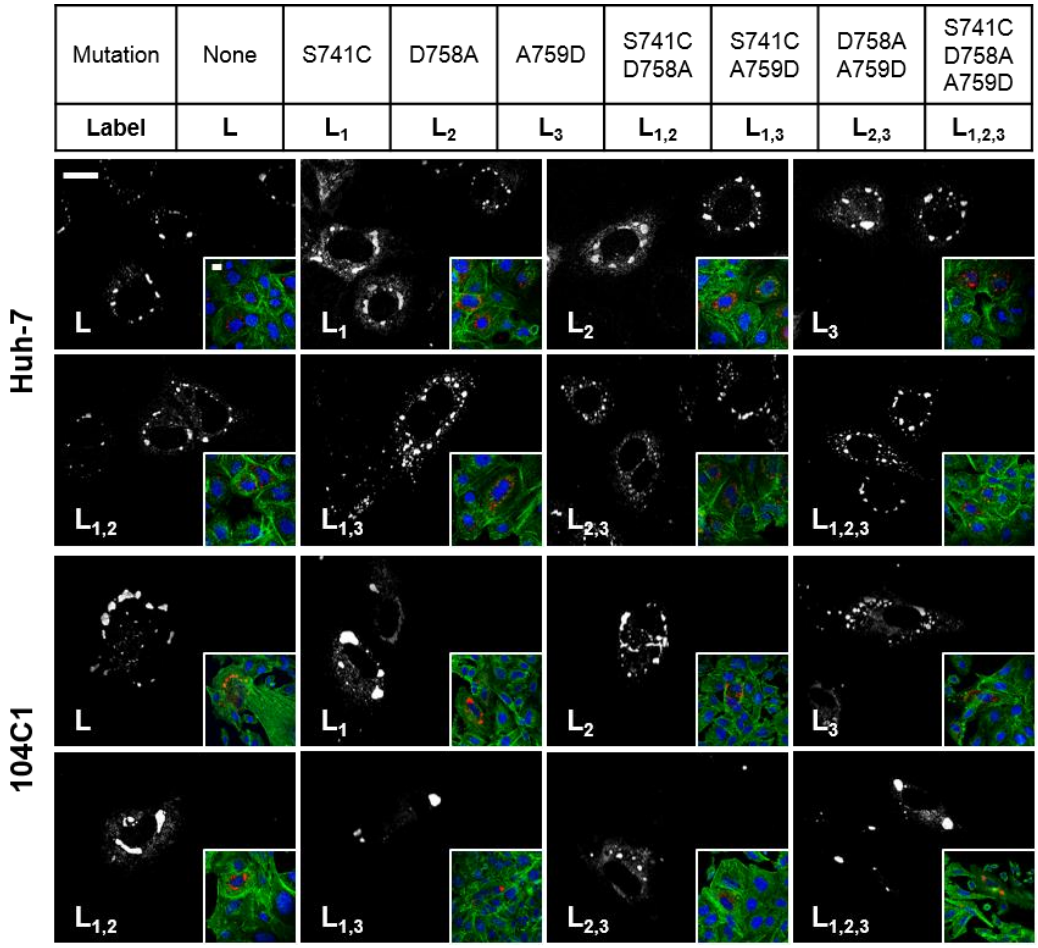

Figure 27: Localization of L mutant constructs in human and guinea pig cells

Indicated in the table are the construct names and the corresponding amino acid substitutions. Human (Huh-7) or guinea pig (104C1) cells were transfected with plasmids required for the minigenome assay. Cells were fixed with 4% PFA in DMEM 48 h p.t. The localization of the L protein was determined by auto fluorescence of mCherry (black and white images). The smaller colored images in the lower right corner show cells at lower magnification. L auto fluorescence (red), actin filaments stained with FITC-phalloidin (green) and nuclei (blue, DAPI staining). All images were acquired with Leica SP5 confocal laser scanning microscope. Bars indicate 20 µM.

3.3.3 Characterization of the impact of the mutations in L on the polymerase function

All mutations in the guinea pig-lethal MARV L are located in the conserved region III, the active site domain. The appearance of the adaptive mutations in the active site domain suggests a direct effect on the replication and transcription capacities of the polymerase complex. Whether this is the case, the polymerase activity of the L mutants was analyzed by the minigenome assay. Human and guinea pig cells were transfected with plasmids required for the minigenome assay, a plasmid encoding either wildtype L or one of the L mutants were used (Nomenclature of the mutants is indicated in Fig. 27). Cell lysates were harvested 48 h post transfection and the reporter gene activity was determined using the dual luciferase assay. The reporter gene activity of the L protein was set to 100%. Mutants displaying less than 5% of reporter gene activity were considered as non-functional.

Western blot analysis verified proper expression of all constructs. The amino acid substitution S741C (L_1) significantly increased the reporter gene activity by 2.6-fold in human- and 4.6-fold in guinea pig cells (Fig. 28A-C). Surprisingly, the mutations D758A and A759D in L_2, L_3, $L_{1,3}$, $L_{2,3}$, and $L_{1,2,3}$ abrogated the polymerase function (reporter gene activity was 1.4% or less) (Fig. 28A-C). The observed effect of these mutations was consistent in human and guinea pig cells. Polymerase activity of $L_{1,2}$ was inhibited in human cells, the reporter gene activity was lower than 2.5%. However, in guinea pig cells expression of $L_{1,2}$ resulted in 12.1% reporter gene activity, indicating a possible species-specific effect of these mutations (Fig. 28A). Interestingly, even highly expressed L_3, $L_{2,3}$ or $L_{1,2,3}$ proteins were not able to induce reporter gene activity (Fig. 28A). These data indicate, that the mutations D758A and A759D strongly inhibit the polymerase function without any effects on expression and localization.

The body core temperature is one of the many physiological differences between humans and guinea pigs. Guinea pigs have a higher body temperature than humans, whereas the body temperature of guinea pigs is 39.5°C, the body temperature of humans is at 37°C (Terril, 1998). It was of interest to determine whether the change in temperature could restore the polymerase activity of the L

mutants. To address this question human and guinea pig cells were transfected as described above (Fig.27A) and then incubated at 39.5°C (Fig. 28B). During incubation of cells at 39.5°C, expression of L_1 resulted in a 3.5- / 5.2-fold increase in reporter gene activity in human /guinea pig cells. Expression of $L_{1,2}$ resulted in reporter gene activity levels of 2.1% in human and 6.8% in guinea pig cells. The mutations D758A and A759D in the L_2, L_3, $L_{1,3}$, $L_{2,3}$, and $L_{1,2,3}$ mutants abrogated the replication and transcription activity in both human and guinea pig cells, the reporter gene activity level was 0.8% or less. Altogether these data indicate that the impairment of the polymerase function of the L_2, L_3, $L_{1,3}$, $L_{2,3}$, and $L_{1,2,3}$ mutants is temperature-independent (Fig. 28B).

To exclude an effect of the mCherry-tag on the active site of the polymerase, we constructed the polymerase mutants without mCherry-tag. Removal of the mCherry-tag did not alter the activity of the polymerase constructs (Fig. 28C). The S741C mutation in L_1 enhanced the minigenome based replication and transcription activity by 2.5-fold in human- and 3.1-fold in guinea pig cells. Expression of $L_{1,2}$ without mCherry-tag resulted in a slight increase in polymerase activity: 17,7% activity in human cells and 29.8% activity in guinea pig cells. Despite the slight increase in activity of the $L_{1,2}$ mutant, the polymerase activity of the mutants L_2, L_3, $L_{1,3}$, $L_{2,3}$, and $L_{1,2,3}$ was not rescued in constructs without the mCherry-tag (Fig. 28C). These results indicate that the mCherry-tag is not involved in the strong inhibitory effect of the D758A and A759D mutations on the transcription and replication activities of the L protein.

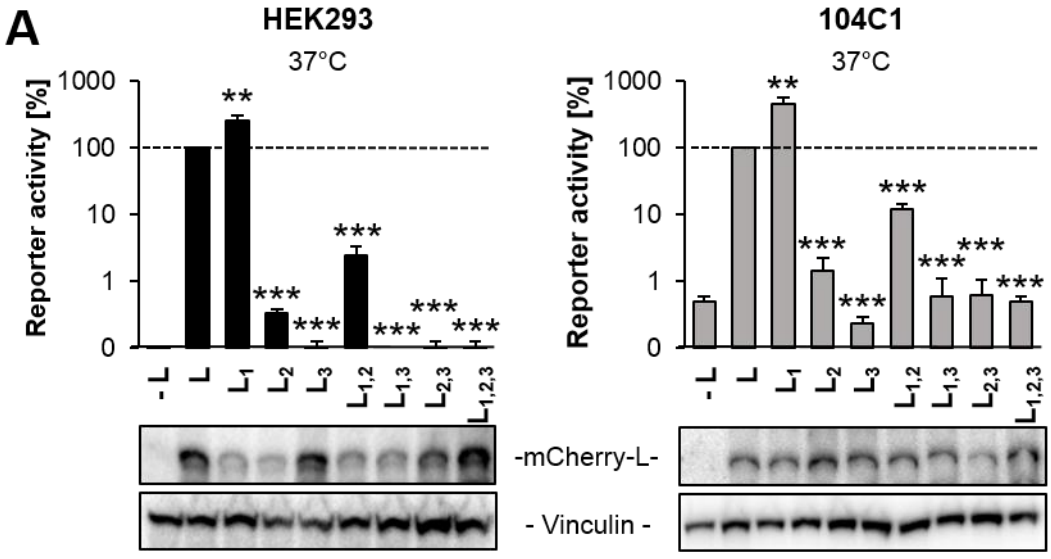

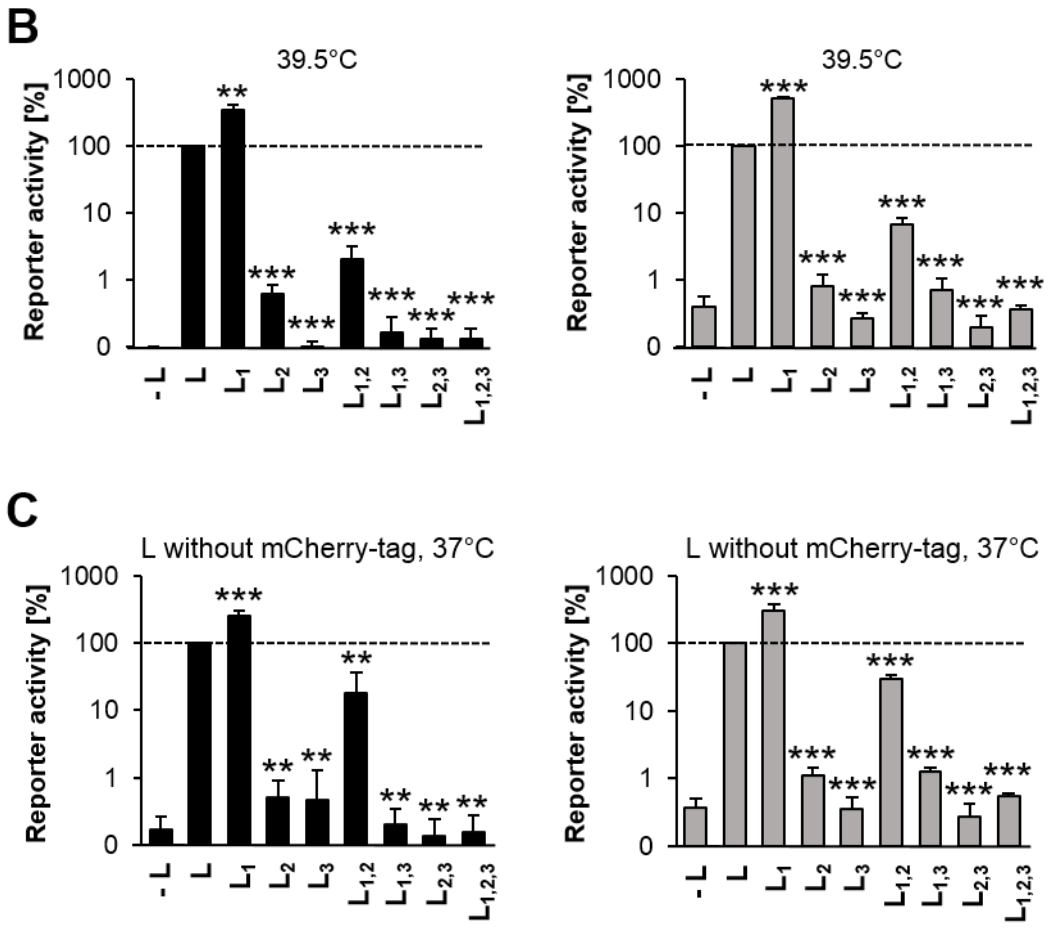

Figure 28: Characterization of the polymerase mutants in human and guinea pig cells Human (HEK293, shown in black) and guinea pig (104C1, shown in gray) cells were transfected with the plasmids required for the minigenome assay and plasmids encoding either wildtype L or one of the L mutants (the name of the mutants is indicated in Fig. 26). 48h p.t. cells were lysed and the reporter gene activity was determined. (A) Incubation of the cells at 37°C. The lower panel shows the Western blot data on the expression of the L protein constructs and vinculin. Detection of the proteins was performed by SDS-PAGE and Western blot analysis using mCherry- and vinculin-specific primary antibodies. (B) Cells were transfected and processed as described above and incubated at 39.5°C. (C) Cells were transfected and processed as described in above, but the polymerase constructs without mCherry-tag were used instead of the mCherry-tagged constructs. L expression was set to 100%. The negative control was without expression of L (-L) and displayed the background of the assay. Shown are the means and standard deviations of three independent experiments in a logarithmic scale, statistical analysis was performed using the Student's t-test. **P<0.01, ***P<0.001.

3.3.4 Characterization of the polymerase mutants in an iVLP assay

To exclude that unknown interactions of the polymerase with other viral proteins such as VP24, VP40 or GP contribute to the reconstruction of the polymerase function, the polymerase activities of L_1, $L_{1,2}$ and $L_{1,2,3}$ were analyzed using the iVLP assay. In addition, it was of interest to determine the capacity of the different polymerase constructs to induce primary transcription, using infection of naïve cells with iVLPs.

The reporter gene activity of the L_1 mutant increased by 3.6-fold in human p0 cells and by 2.7-fold in guinea pig p0 cells (Fig. 29A-B). As expected, the reporter gene activity of the $L_{1,2,3}$ mutant was strongly inhibited in human and guinea pig cells (less than 5% reporter gene activity). This finding indicates that the expression of the other viral proteins does not recover the polymerase function of the L construct carrying all three mutations (Fig. 29A-B). The polymerase activity of $L_{1,2}$ was reduced to 26.3% in guinea pig cells and almost undetectable in human cells (Fig. 29A-B).

The reporter gene activity in pre-transfected (p1 tr) indicator cells infected with iVLPs reflects the capacities of the incoming nucleocapsid complex to transcribe and replicate the minigenome with the support of the ectopically expressed nucleocapsid proteins. To compare the reporter gene activity of different L mutants, the p1 tr human and guinea pig cells were infected with iVLPs, containing different L mutants. The reporter gene activity in p1 tr cells infected with $L_{1,2,3}$-containing iVLPs was extremely low (less than 5% of reporter gene activity) in human and guinea pig cells (Fig. 29A-B). The reporter gene activity in p1 tr cells infected with L_1-containing iVLPs was strongly enhanced upon infection, by 7.4-fold in human and 13.5-fold in guinea pig cells (Fig. 29A-B). Interestingly, while $L_{1,2}$-containing iVLPs did not induce reporter gene activity in human p1 tr indicator cells, these iVLPs induced 28% of reporter gene activity of L-containing iVLPs in p1 tr guinea pig cells. The different reporter gene activity of $L_{1,2}$ in human and guinea pig cells supports the conclusion that this combination of mutations might provide a species-specific advantage.

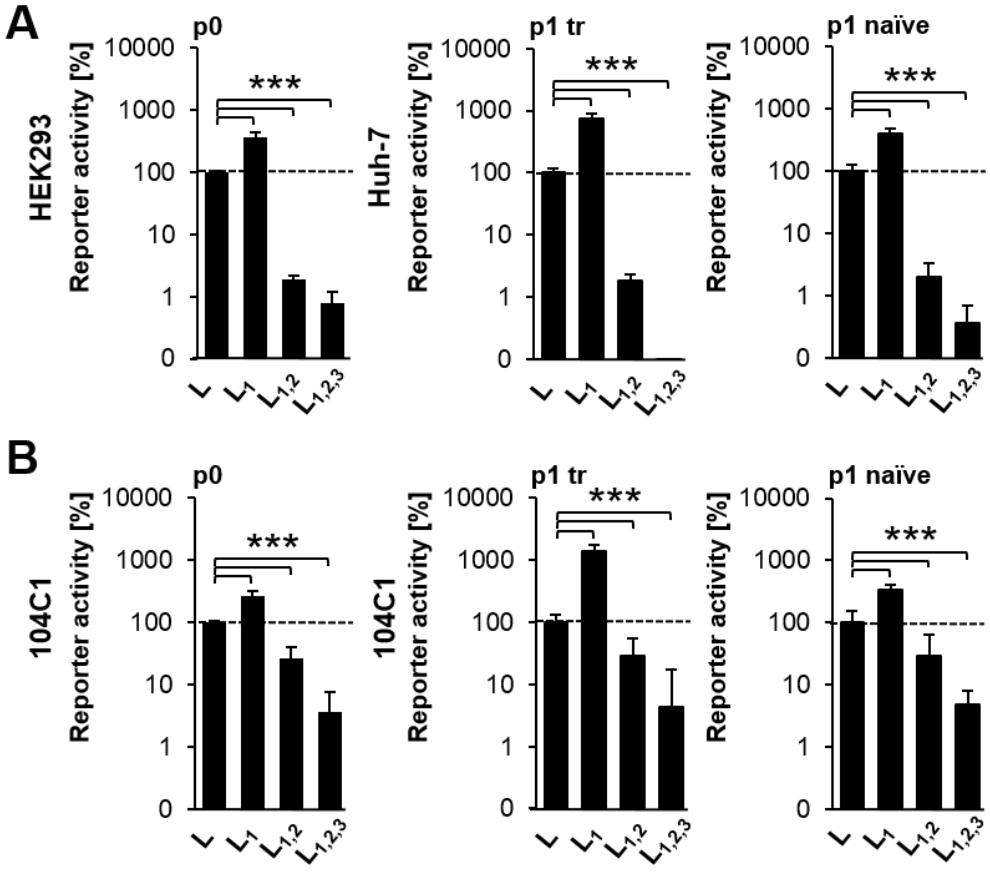

Figure 29: Characterization of the polymerase mutations in the iVLP assay (A) Human (p0, HEK293, p1, Huh-7) or (B) guinea pig (p0, 104C1, p1, 104C1) cells were transfected with plasmids required for the iVLP assay. Cells were harvested 72h p.t. and the reporter gene activity was measured (left panel). Either human or guinea pig p1 tr (middle panel) or p1 naïve (right panel) cells were infected with iVLPs containing different L variants. Cells were lysed 24h p.t. and the reporter gene activity was determined. The reporter gene activity of L was set to 100%. Results are shown in a logarithmic scale as well as the means and standard deviations from triplicates from three independent experiments, statistical analysis was performed using the Student's t-test., ****P*<0.001.

However, it must be noted that $L_{1,2}$ is significantly impaired in its function compared to L.

Infection of naïve indicator cells with iVLPs reflects the incoming nucleocapsid complex to perform primary transcription of the minigenome in the absence of de novo viral protein synthesis. Infection of p1 naïve cells with L_1 containing iVLPs enhanced primary transcription by 4.1-fold in human- and 3.4-fold in guinea pig cells. Reporter gene activity was below 5% in human and guinea pig cells infected with iVLPs containing $L_{1,2,3}$, reflecting only background activity (Fig. 29A-B). In agreement with data obtained with p1 tr cells, the reporter gene activity in human p1 naïve cells infected with iVLPs containing $L_{1,2}$ was extremely low, but retained

29% of activity in guinea pig cells (Fig. 29A-B). Altogether, these data confirm that the S741C substitution led to a gain of function of the polymerase complex, whereas the substitutions on position 758 and 759 abrogate the polymerase function.

3.4 Characterization of the synergistic effect of the D184N mutation in VP40 and the S741C mutation in L on replication and transcription

In the present study we have found that the D184N mutation in VP40 relieves the suppressive effect of VP40 on replication and transcription of the minigenome specifically in guinea pig cells (Fig. 15). All three analyzed mutations in the polymerase L influenced the polymerase activity. While the S741C mutation induced higher polymerase activity, the D758A and A759D mutations dramatically inhibited the polymerase function both in human and guinea pig cells. In the following experiment we wanted to analyze whether the D184N mutation in VP40 and the S741C mutation in L have species-specific synergistic effects on replication and transcription.

To address this question, human or guinea pig cells were transfected with all plasmids required for the minigenome assay. Plasmids encoding wildtype L or L_1 were used as indicated. In addition, plasmids encoding either wildtype VP40 or $VP40_{D184N}$ were transfected. Cells were lysed 24 h post transfection and the reporter gene activity was measured. The reporter gene activity of L wildtype without co-expression of VP40 and $VP40_{D184N}$ was set to 100% in human and guinea pig cells.

As expected, expression of VP40 significantly reduced the reporter gene activity in human and guinea pig cells, independent of the tested L variant (Fig. 30A-B). In human cells, the replication activity of L was inhibited by 6.3-fold upon co-expression of $VP40_{D184N}$ and by 4.8-fold in presence of wildtype VP40 (Fig. 30A). In guinea pig cells, the replication activity of L was inhibited by 2.1-fold upon co-expression of $VP40_{D184N}$, and to 3.2-fold in presence of wildtype VP40.

In human cells, the polymerase activity of L_1 was decreased upon co-expression of $VP40_{D184N}$ by 10.2-fold, whereas in presence of wildtype VP40 the polymerase activity was suppressed by 4-fold. In guinea pig cells, the polymerase activity of L_1 was decreased upon co-expression of $VP40_{D184N}$ by 2.8-fold, whereas in presence of wildtype VP40 the polymerase activity was suppressed by 6.1-fold. Thus, in guinea pig cells, the inhibitory effect of $VP40_{D184N}$ on reporter gene activity of both L and L_1 was consistently lower than the inhibitory effect of wildtype VP40 on the polymerase activity of L and L_1 (Fig. 30B). Remarkably, the polymerase activity of L_1 remained high in the presence of both wildtype VP40 and $VP40_{D184N}$ and comprised 125% and 280%, correspondingly (Fig. 30B). Expression controls showed that all transfected constructs were expressed (Fig. 30C-D). It is important to note that the polymerase activity of L_1 in presence of $VP40_{D184N}$ in human cells comprised 35%, while in guinea pig cells the polymerase activity of L_1 in presence of $VP40_{D184N}$ reached 280%, showing an 8.0-fold species-specific increase in reporter gene activity. These data suggests a synergistic effect of L_1 and $VP40_{D184N}$ on replication and transcription in guinea pig cells.

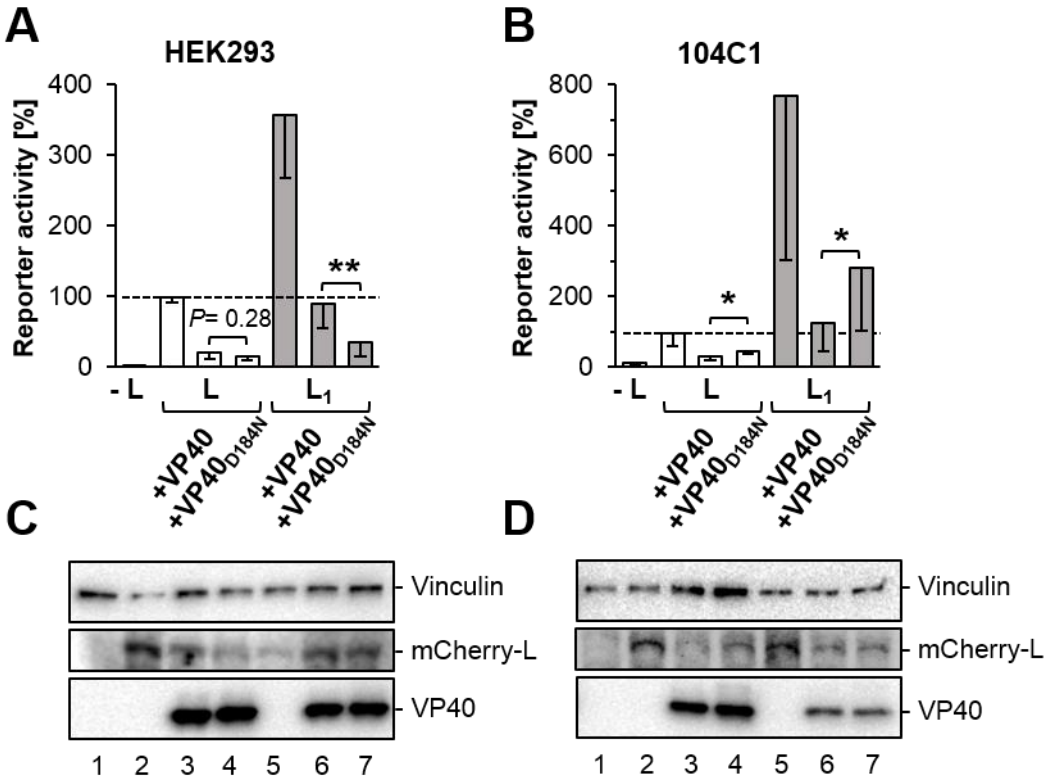

Figure 30: Characterization of synergistic effects between $VP40_{D184N}$ and L_1

(A, C) Human (HEK293) or (B, D) guinea pig (104C1) cells were transfected according to the minigenome assay and either VP40 or $VP40_{D184N}$ encoding plasmids were added. Either L (white columns) or L_1 (gray columns) was transfected. 24 h p.t. cells were lysed and the reporter gene activity was determined. The means and standard deviations of three independent experiments are shown, statistical analysis was performed using the Student's t-test. **P*<0.05, ***P*<0.01. (C-D) Expression control of the samples from A, B. Western blot analysis of proteins was carried out using vinculin-, VP40- and mCherry-specific antibodies. Lane 1 shows the negative control lacking L. Lanes 2, 5 are the positive controls expressing either L (Lane 2) or L_1 (Lane 5) Lanes 3 and 6 show VP40 expression and lanes 4, 7 $VP40_{D184N}$ expression.

4 Discussion

The rodent model for filoviruses provides a unique possibility for the analysis of the molecular mechanisms modulating filoviral pathogenicity. The uniqueness of rodent animal models for filoviruses is that variations in the filoviral pathogenicity are only observed in rodents, while for NHPs filoviral infections are always highly pathogenic (Banadyga *et al.*, 2016). The increase in filoviral pathogenicity in rodents is accompanied by mutations in the viral genome leading to the hypothesis that the mutations are responsible for the enhanced pathogenicity. The analysis of how these mutations affect the functions of the viral proteins and the ability of the virus to grow within cells of a new host can help to understand the molecular mechanisms of filovirus virulence.

Our study was based on the analysis of four mutations detected in a guinea pig-lethal MARV, three amino acids substitutions, S741C, D758A, A759D, were located in the active site of the L protein, and a D184N mutation in the C-terminal domain of VP40. (Lofts *et al.*, 2007). The goal of our study was to analyze how these individual mutations changed the function of the MARV proteins L and VP40 in guinea pig cells compared to human cells.

4.1 The guinea pig-adaptive mutation D184N in VP40

Using a reverse genetics approach we have shown that the D184N mutation in VP40 provided a recombinant MARV ($rMARV_{VP40(D184N)}$) with a replicative advantage in guinea pig cells. Our studies indicated that this replicative advantage of $rMARV_{VP40(D184N)}$ was based on the improved assembly and budding functions of $VP40_{D184N}$, as well as an relieve of its inhibitory effect on transcription and replication in guinea pig cells. The ability of $VP40_{D184N}$ to suppress the IFN signaling in guinea pig cells was not affected.

Mutations in viral matrix proteins, upon adaptation to a new host, have been rarely been observed in lenti- and paramyxoviruses. For example, a E89K mutation in the matrix protein of a cotton rat-adapted measles virus (MeV) has been suggested to have an influence on the viral fitness in a new host (Dong *et al.*, 2009). A single amino acid substitution in the matrix protein of simian immunodeficiency virus (SIV) obtained in course of passages in human lymphoid tissue resulted in increased viral replication in new host cells, however the mechanism explaining the impact of this mutation on the increased viral fitness remained unclear (Bibollet-Ruche *et al.*, 2012).

MARV VP40 is known as an important interferon antagonist (Valmas *et al.*, 2010). It was therefore tempting to presume that the single amino acid mutation D184N in VP40 influenced the interferon antagonistic function of VP40 in guinea pig cells. However, previous studies on MARV adaptive mutations in VP40 demonstrated that the D184N mutation did not alter the interferon antagonism in mouse cells while three other mutations in VP40 of MA-MARV were responsible for the inhibition of the innate immune response (Feagins & Basler, 2014; 2015; Valmas & Basler, 2011). Supporting this data, our results suggested that the D184N mutation alters another than the IFN-antagonistic function of VP40 (Fig. 8-9). A similar observation was made for other filoviral proteins with IFN antagonistic function. Three mutations in VP24 of MA-EBOV, did not alter the interferon antagonistic function of EBOV VP24 in guinea pig cells, however, these mutations were sufficient to induce a lethal disease in guinea pigs (Mateo *et al.*, 2011; Reid *et al.*, 2006).

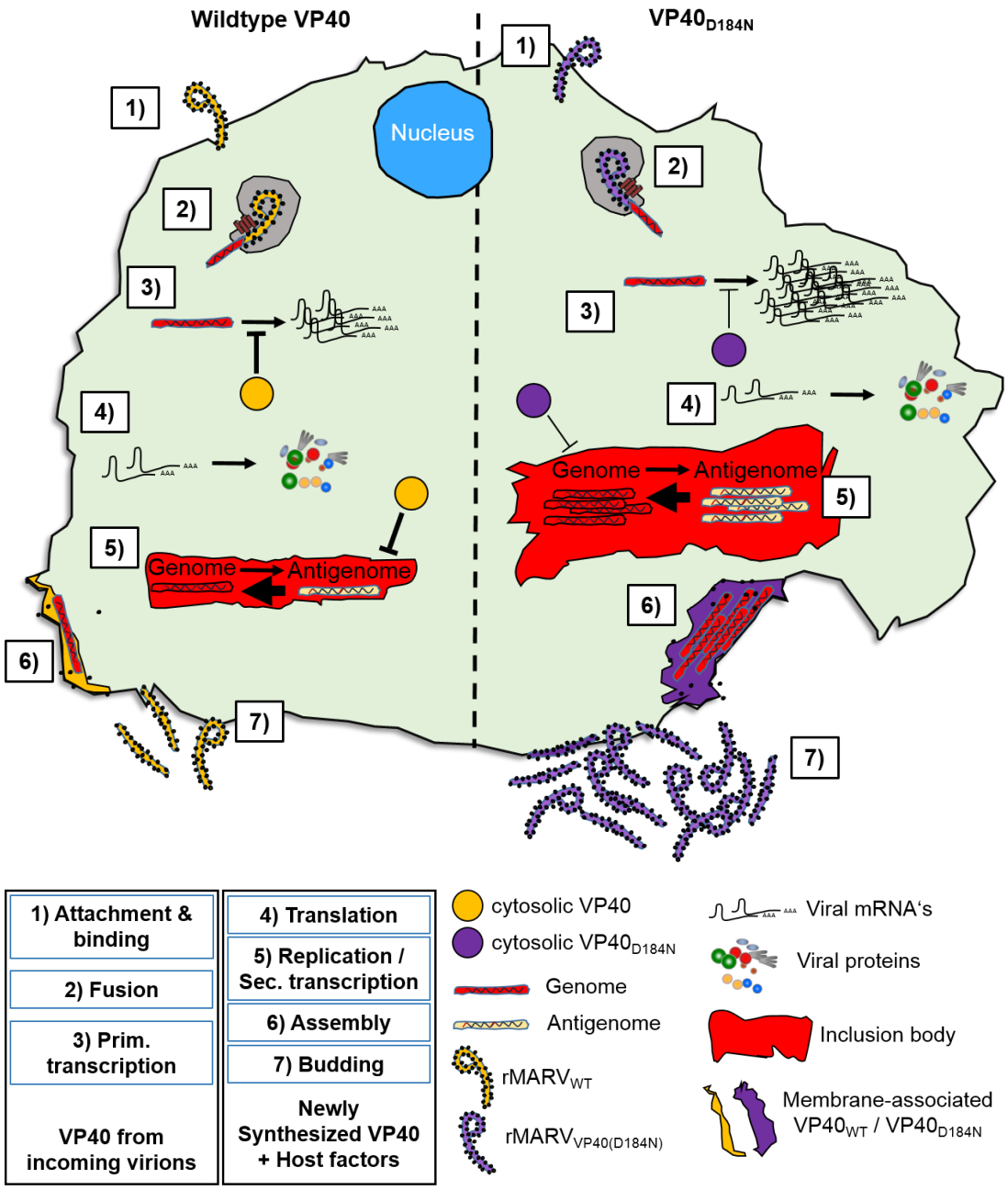

Figure 31: Effects of D184N on the viral life cycle in an rMARV$_{VP40(D184N)}$ infected guinea pig cell
Schematic representation of the viral life cycle upon MARV infection in either rMARV$_{WT}$ (left, indicated by yellow) and rMARV$_{VP40(D184N)}$ (right, indicated by purple) in a guinea pig cell. Attachment and binding of MARV particles to the cell surface via one or more receptors, such as TIM-1 or DC-SIGN (Step 1). Followed by fusion via the endosomal receptor NPC1 and release of the nucleocapsid, containing the viral genome, into the cytoplasm (Step 2). Afterwards primary transcription is initiated, a process which can be inhibited by VP40 from incoming virions (orange/purple spheres, Step 3). The cellular machinery translates the viral mRNAs into the according viral proteins (Step 4). Translation of the viral proteins is followed by replication and secondary transcription within inclusion bodies, replication is inhibited by presence of VP40 (orange/purple spheres, Step 5). Nucleocapsids are transported to the plasma membrane and interact with membrane-associated VP40 leading to the assembly and release of virions (Step 6). Finally, budding of mature virions from the infected cells is facilitated by VP40 (Step 7)

Mutations in the viral matrix proteins may result in changes in the transmission efficiency mediated by morphological changes of virus particles, as it was recently shown for the swine influenza A virus containing a single mutation in the matrix protein (Campbell *et al.*, 2014; Ward, 1995). However, our comparative EM analysis of $rMARV_{WT}$ and $rMARV_{VP40(D184N)}$ showed that the morphology of the viral particles was indistinguishable. These data demonstrated that the virus particle morphology was not altered by the D184N substitution in VP40.

Mutations in viral matrix proteins can modulate the viral infectivity, by increasing or decreasing the incorporation of the viral glycoprotein into viral particles, as it has been shown for mutations in the matrix protein (MA) of SIV (Manrique *et al.*, 2003). We observed an increase in the infectivity of $rMARV_{VP40(D184N)}$ in human and guinea pig cells, and wanted to analyze whether this increase depends on the incorporation of GP. We followed three different approaches which consistently showed that the D184N mutation in VP40 did not alter the incorporation of GP into virus particles. First, equal amounts of GP were detected in iVLP preparations produced either upon expression of VP40 or $VP40_{D184N}$. Second, equal amounts of GP were detected by a silver stained gel of $rMARV_{WT}$ or $rMARV_{VP40(D184N)}$ virus particles. And, third, comparable amounts of immunogold-labeled GP spikes were detected in $rMARV_{WT}$ or $rMARV_{VP40(D184N)}$ particles. Thus our data indicated that the D184N mutation in VP40 did not affect the infectivity of $rMARV_{VP40(D184N)}$ by altering the incorporation of GP into viral particles.

Another factor that might have influenced the infectivity of $rMARV_{VP40(D184N)}$ was the efficiency of incorporation of nucleocapsid complexes into viral particles. MARV VP40 has been shown to be important for the attraction of nucleocapsid proteins into infectious virus-like particles (Dolnik *et al.*, 2008; Urata *et al.*, 2007). Although the mechanism of the interactions between VP40 and NP remains unknown, it could not be excluded that the D184N mutation in VP40 altered the assembly function of VP40. The comparison of the composition of $rMARV_{WT}$ or $rMARV_{VP40(D184N)}$ particles assembled in guinea pig cells indeed showed an increase in the ratio of NP to VP40 in $rMARV_{VP40(D184N)}$ virions. An increased ratio of NP to VP40 was also detected in $VP40_{D184N}$-induced iVLPs formed in guinea

pig cells (Fig. 31, step 6). Hence the D184N mutation in VP40 improved the attraction of NP (or nucleocapsids) into iVLPs and virions in a species-specific manner.

MARV VP40 is the driving force of virus budding, evidenced by the ability of VP40 to form VLPs upon single ectopic expression (Kolesnikova *et al.*, 2004b; Swenson *et al.*, 2004). It has been suggested that the endosomal sorting complex required for transport (ESCRT) machinery is involved in mediating budding of MARV VP40-induced VLPs (Urata *et al.*, 2007). The interactions of MARV VP40 with the ESCRT machinery are mediated by a PPPY motif at the amino acid residues 16 to 19 (Urata *et al.*, 2007). Since the D184N mutation is rather far away from the PPPY motif, it seems unlikely that the D184N substitution affects the interaction of VP40 with the ESCRT machinery. The observed 1.5-fold increase in the relative amount of released VLPs specifically in guinea pig cells might be the result of an altered interaction of $VP40_{D184N}$ with so far unknown guinea pig host factors (Fig. 31, step 7). Among others, tetherin might be a host-specific candidate factor interacting with VP40. It has been shown that VP40 of a MA-Marburg virus Ravn (RAVV) interacts with murine tetherin, but not with human tetherin. However, analysis of mutations in VP40 of MA-RAVV showed that the improved VLP budding in mouse cells was mediated via interactions of tetherin with VP40 containing adaptive mutations at residues 57 and 165 but not via the D184N mutation (Feagins & Basler, 2014).

Filoviral budding does not depend entirely on the ESCRT machinery and was previously shown to be negatively affected by overexpression of dominant negative Sar1, a marker for COPII vesicles (Kolesnikova *et al.*, 2009; Urata *et al.*, 2006; Yamayoshi *et al.*, 2008). Thus, Sar1 might be another host factor possibly interacting with $VP40_{D184N}$ in guinea pig cells, which was responsible for the enhanced release of VLPs.

The matrix proteins of NNS viruses, for example, the matrix proteins of the Lassa virus, rabies virus and VSV are known to play a regulatory role in viral replication and transcription (Carroll & Wagner, 1979; Finke *et al.*, 2003; Hass *et al.*, 2004). The same phenomenon was observed for VP40 of MARV and EBOV (Hoenen *et*

al., 2010; Watanabe *et al.*, 1996). However, it was unknown whether mutations in matrix proteins can specifically affect the regulation of transcription and replication. Our data showed that the D184N mutation in VP40 relieved the suppressive effect of the matrix protein on minigenome replication and transcription specifically in guinea pig cells. This effect likely contributes to the enhanced virus production of $rMARV_{VP40(D184N)}$ in guinea pig cells (Fig. 31, step 3,5). The identification of host cell factors mediating the species-specific increase of replication and transcription in presence of $VP40_{D184N}$ requires further studies.

4.2 The effect of the mutations S741C, D758A, A759D on the replication capacities of MARV L

The functional analysis of L mutants showed that the polymerase function was strongly enhanced by an amino acid substitution at position 741 (S741C), and robustly inhibited by the other two amino substitutions (D758A and A759D) in a non-species-specific manner.

To date there is no specific antibody recognizing MARV L, therefore it was necessary to construct tagged MARV L mutants to confirm proper expression. Our study demonstrated that addition of a fluorescence tag in a highly variable region of the MARV L polymerase neither destroyed the polymerase activity nor affected its interactions with other proteins of the polymerase complex. An insertion of mCherry into the closely related EBOV L resulted in a loss of activity of approx. 90% (Hoenen *et al.*, 2012). The decrease in activity of MARV L with the mCherry-tag (L) was not as dramatic as in the case of EBOV L and showed only 38% reduction of reporter gene activity. This suggests that MARV L tolerates the insertion of mCherry better than EBOV L.

Most of the mutations observed in viral polymerases of NNS viruses during adaptation to a new host were detected in CR V or CR VI (Ackermann et al., 2007; Brown et al., 2011; Dortmans et al., 2011; Ebihara et al., 2006; Fujii et al., 2002; Heiden et al., 2014; Kim et al., 2014b). The CR V of the viral polymerase mediates capping of viral mRNAs, and CR IV represents the methyltransferase function (Liang et al., 2015). CR V and CR VI of NNS virus polymerases are not

highly conserved and considered as domains interacting with unique host cell transacting transcriptional cofactors (Dortmans et al., 2011; Poch et al., 1990; Sidhu et al., 1993).

The position of the mutations, S741C, D758A and A759D, detected in the guinea pig-lethal MARV L is uncommon for adaptive mutations in L proteins, because they locate into the CR III close to the highly conserved GDN motif (residues 744-746). The CR III represents the active site of the viral polymerase function, and mutations located in or close to the GDN motif in the polymerase of NNS has been shown to destroy the processivity of viral RdRps (Carroll *et al.*, 2015; Dietzel *et al.*, 2016; Malur *et al.*, 2002; Schnell & Conzelmann, 1995; Sleat & Banerjee, 1993; Smallwood *et al.*, 2002). Adaptive mutations were only rarely observed in CR III, for example, a T820A substitution has been detected in a guinea pig-adapted EBOV polymerase L (Mateo *et al.*, 2011). However, it is hard to estimate the influence of the T820A mutation in EBOV L on the polymerase activity in a new host, because the recombinant EBOV containing the T820A mutation in L and an additional mutation in NP (F648L) did not induce a lethal disease in the infected guinea pigs, and the polymerase activity of the L mutant was not analyzed by the minigenome assay in guinea pig cells (Mateo *et al.*, 2011). Another example, and the only positive effect on replication due to an amino acid substitution in the active site was observed when a D759G amino acid substitution in EBOV L appeared during the 2014-2016 EBOV outbreak and resulted in an increased polymerase activity in minigenome-based reporter assays (Dietzel *et al.*, 2016).

We have found that the mutation S741C in the active site of MARV L improved the polymerase function. The increased polymerase activity of the L_1 mutant both in human and guinea pig cells suggested that the S741C mutation enhanced the polymerase activity in a species-independent manner (Fig. 27-30). The negative effects of the D758A and A759D mutations on the function of L were astonishing since it was expected that all the selected mutations should contribute to the enhanced replication of the guinea pig-lethal MARV in the new host (Lofts *et al.*, 2007).

It seems reasonable that the amino acid exchange, in the active site of MARV L, at position 741 from serine to cysteine might be beneficial for the polymerase activity. In fact, serines are found regularly in active centers of proteins and can be exchanged with an cysteine fulfilling similar roles in the active center (Betts & Russel, 2007). The lack of polymerase activity in presence of the D758A and A759D substitutions in MARV L is still unclear and needs further investigation. It is possible that the two abrogating mutations represent a minority of the viral quasi-species which had been selected during plaque purification of guinea pig-lethal MARV (Beaucourt *et al.*, 2011). It can only be speculated that these mutations in the active site of the polymerase, destroy either the structure or charge of the active site resulting in a loss of activity. Aspartate is frequently observed in active sites of enzymes to facilitate interactions with positively charged non-protein interactors (Betts & Russel, 2007). Aspartate played a role in both abrogating mutations D758A and A759D. We assume that the exchange of the negatively charged aspartate to the nonpolar alanine might disrupt tightly regulated complex interactions with non-protein interactors such as metal ions necessary for efficient enzymatic activity (Ng *et al.*, 2008).

4.3 The synergistic effect of the S741C mutation in L and the D184N mutation in VP40 on the replication activity in guinea pig cells

The polymerase activity of L carrying the S741C substitution in presence of $VP40_{D184N}$ was eightfold higher in guinea pig than in human cells, suggesting an additive effect of these two mutations on the replication activity in the new host.

Whether only one mutation or a combination of the mutations present in the guinea pig-lethal MARV VP40 and the L protein are necessary to increase the pathogenicity of MARV in guinea pigs remains to be determined by a reverse genetics approach. Based on the finding that the D184N mutation in VP40 appeared at early passages of MARV in mice, but did not result in a lethal disease, it seems reasonable to suggest that additional mutations were necessary to increase MARV virulence in mice (Lofts *et al.*, 2011).

Our study demonstrated that the S741C mutation in the L protein and the D184N mutation in VP40 might have an additive effect on replication and transcription. Rescue of recombinant viruses containing either the D184N mutation in VP40, or the S741C mutation in L or both mutations in combination with challenge studies in guinea pigs will shed light on the role of these mutations as molecular determinants of MARV pathogenicity in guinea pigs.

4.4 Future plans

The several species-specific effects of the D184N mutation in VP40 on many functions of the viral protein in guinea pig cells suggest that the D184N mutation mediates the interaction of VP40 with guinea pig-specific cellular factors. It is of special interest to determine these host factors by co-immunoprecipitation studies. We expect that the detection of guinea pig factors specifically interacting with $VP40_{D184N}$ using conventional co-immunoprecipitation strategies is problematic, due to the potentially transient character of the interaction. Therefore, we plan to use a so called proximity biotin ligation assay which could identify even weak or transiently interacting proteins (Kim *et al.*, 2014a; Kim *et al.*, 2016).

The additive effects of the D184N mutation in VP40 and the S741C mutation in L on the polymerase activity specifically in guinea pig cells suggests that both mutations are important for the replicative fitness of MARV in guinea pig cells. Therefore, full-length cloning and rescue of recombinant viruses containing different combinations of these mutations are necessary for further studies to elucidate the molecular determinants of MARV pathogenicity in guinea pigs. The recombinant viruses will be used to investigate the effects of the mutation in primary guinea pig cells, and finally in the guinea pig model.

5 Summary

5.1 Summary (english)

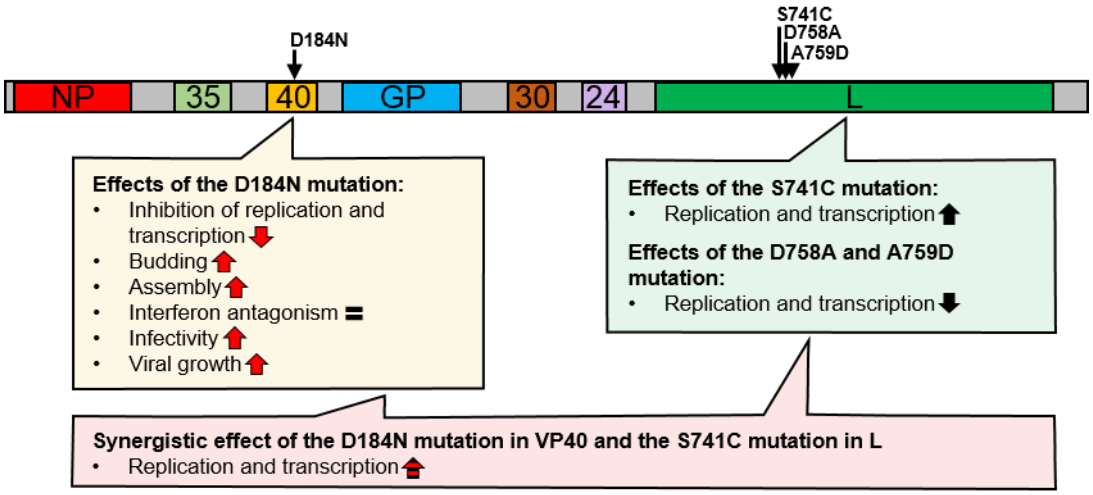

Figure 32: Schematic presentation of the results

Mutations present in viral proteins of the guinea pig-lethal MARV (Lofts *et al.* 2007) are indicated by arrows above the schematic viral genome. The boxes show the effect of the mutations on the viral protein function of either VP40 (yellow), L (green) and synergistic effect of mutations in both proteins (pink). The bold arrows indicate whether the mutation increased, arrow up, or decreased, arrow down, the specific function. Red bold arrows represent species-specific effects observed only in guinea pig cells, black arrows represent non-species-specific effects. The red and black striped arrow indicates that the effect was present in both human and guinea pig cells but more pronounced in guinea pig cells.

Marburg virus (MARV) is a highly pathogenic virus that causes severe, often lethal diseases specifically in humans and non-human primates. In rodents MARV is non-pathogenic. However, sequential passaging of MARV in rodents results in selection of a rodent-lethal virus. Lofts *et al.* established a guinea pig-lethal MARV containing only four non-silent amino acid changes in viral genome (Lofts *et al.*, 2007). One amino acid substitution (D184N) was detected in the viral matrix protein VP40 and three amino acid substitutions were detected in the RNA-dependent RNA polymerase L (S741C, D758A and A759D). We analyzed the effects of the guinea pig-adaptive mutations on the functions of VP40 and L in a comparative study including human and guinea pig cells. Functional analyses were performed with ectopically expressed $VP40_{D184N}$ and L mutants by using different assays. The influence of the D184N mutation in VP40 on the replicative capacities of MARV in guinea pig cells was analyzed by infection of cells with recombinant MARV containing the D184N mutation in VP40.

The first part of the study demonstrated that a recombinant rMARV containing only the

D184N amino acid substitution in VP40 displayed a higher level of viral fitness specifically in guinea pig, but not in human cells. The mutant virus showed higher replicative capacities, enlarged inclusion bodies and enhanced infectivity only in guinea pig cells. Detailed comparative analysis of VP40 functions, in human and guinea pig cells, indicated that the membrane binding capabilities and the interferon antagonistic function were not altered by the D184N amino acid substitution. However, presence of the D184N mutation in VP40 enhanced the production of VP40-induced virus-like particles (VLPs) specifically in guinea pig cells. In addition, the amount of NP in infectious virus-like particles (iVLPs) and virus preparations was enhanced in presence of the D184N mutation in VP40 specifically in guinea pig cells. These data might partially explain the higher infectivity of $VP40_{D184N}$ containing iVLPs compared to wildtype VP40 containing iVLPs. Most importantly, the inhibitory capacity of VP40 on replication and transcription was species-specifically lowered by the D184N mutation in VP40, allowing significantly higher levels of replication and transcription in guinea pig cells.

The second part of the study focused on the importance of the mutations in the L protein observed in the guinea pig-lethal MARV. Interestingly, only the S714C substitution increased replication in both species while the other mutations, D758A and A759D severely impaired the polymerase function. All L mutant proteins displayed proper expression and were able to localize into inclusion bodies which represent the sites of viral transcription/replication.

Finally, co-expression of plasmids encoding L with the S741C amino acid substitution and $VP40_{D184N}$ in guinea pig cells resulted in eight fold higher levels of replication and transcription in comparison to human cells. This suggested that the D184N mutation in VP40 and the S741C mutation in L together significantly improve replication of MARV in guinea pig cells. Altogether these data suggests that the D184N substitution in VP40 and the S714C substitution in L can contribute to the increased pathogenicity of guinea pig-lethal MARV.

5.2 Zusammenfassung (deutsch)

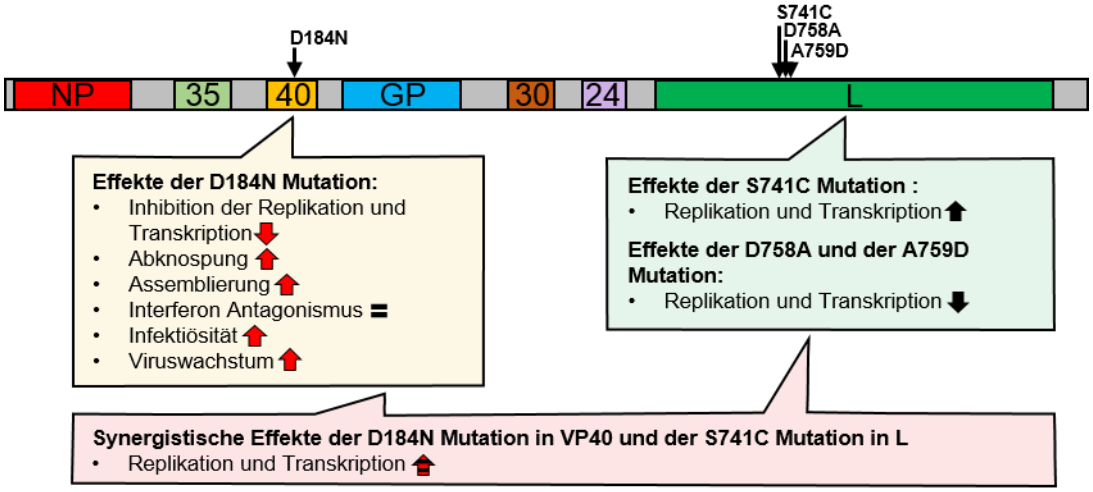

Figure 33: Schematische Darstellung der Ergebnisse

Als Übersicht dargestellt die Effekte der D184N Mutation in VP40 und der S741C, D758A und A759D Mutationen in L des Meerschweinchen-letalen MARV (Lofts *et al.* 2007). Die Mutationen werden dargestellt durch die Pfeile oberhalb des schematischen viralen Genoms. Die Boxen stellen die beobachteten Effekte der Mutationen auf die jeweiligen Proteinfunktionen für VP40 (gelbe Box) und L (grüne Box) und der Kombinationen beider dargestellten Mutationen in VP40 und L (pinke Box) dar. Die Pfeile innerhalb der Boxen zeigen in welcher Form die jeweilige Proteinfunktion beeinflusst worden ist (nach oben, Funktionssteigerung, nach unten, Funktionsverlust). Rote Pfeile zeigen nur in Meerschweinchenzellen auftretende spezies-spezifische Unterschiede an, die schwarzen nicht-spezies-abhängige Effekte. Der rot-schwarz gestreifte Pfeil zeigt Unterschiede welche in beiden Spezies beobachtet wurden, jedoch deutlich ausgeprägter in Meerschweinchenzellen waren.

Das Marburg Virus (MARV) ist hochpathogen und verursacht häufig schwere oft tödlich verlaufende Infektionen in Primaten. In Nagetieren hingegen verursacht das MARV jedoch keine Erkrankung. Sequentielles Passagieren des MARV in Nagetieren führt jedoch zur Selektion von Virusvarianten die eine tödliche Erkrankung in Nagetieren hervorrufen. Lofts *et al.* konnten durch sequentielles Passagieren ein Meerschweinchen adaptiertes MARV etablieren, das sich vom wildtypischen MARV lediglich durch vier ausgetauschte Aminosäuren unterschied, für die Tiere aber tödlich war (Lofts *et al.*, 2007). Eine, Mutation, D184N, befindet sich in VP40 dem viralen Matrix Protein und drei weitere Mutationen, S741C, D758A, A759D, befinden sich in der viralen RNA-abhängigen RNA Polymerase, dem L Protein. Die molekularen Mechanismen, die durch diese Mutation beeinflusst wurden blieben unklar. Ziel dieser Arbeit war es zu analysieren ob diese adaptiven Mutationen im Meerschweinchen-letalen MARV die Funktionen der Proteine VP40 und L in Meerschweinchenzellen im Vergleich zu menschlichen Zellen beeinflussen. Dazu untersuchten wir durch verschiedene Assays mit Hilfe von ektopischer

Überexpression der rekombinanten Proteine VP40 mit der D184N Mutation und für verschiedene L Protein Varianten die jeweiligen Proteinfunktionen.
Zusätzlich wurde der Einfluss der D184N Mutation in VP40 auf die replikative Fitness eines rekombinanten MARV bestimmt, welches lediglich die D184N Mutation in VP40 trägt ($rMARV_{VP40(D184N)}$).

Im ersten Teil dieser Arbeit wurde gezeigt das $rMARV_{VP40(D184N)}$ spezifisch in Meerschweinchenzellen eine gesteigerte Fitness besitzt. Die viralen Transkription/Replikation war verstärkt, es fanden sich vergrößerten viralen Einschlusskörperchen in den infizierten Zellen und die Infektiösität von $rMARV_{VP40(D184N)}$ war spezifisch für Meerschweinchenzellen erhöht. VP40 ist ein multifunktionelles Protein, welches bei der Abwehr der Interferonantwort der Zelle sowie beim Zusammenbau und Abknospen der Viren und bei der Regulation von Transkription/Replikation beteiligt ist. Vergleiche der einzelnen VP40 Funktionen in humanen und Meerschweinchenzellen zeigten, dass die D184N Mutation den VP40-mediierten Interferon Antagonismus sowie die Assoziation von VP40 mit Zellmembranen nicht beeinflussten. Jedoch führte die D184N Mutation in VP40 zu einer Zunahme der Abknospung von VP40-induzierten virus-ähnlichen Partikeln (VLPs) in Meerschweinchenzellen. Zudem führte die D184N Mutation in VP40 zu einer Erhöhung der Menge an Nukleoprotein (NP) in infektiösen virus-ähnlichen Partikeln (iVLPs) lediglich in Meerschweinchenzellen. Diese Daten zeigen, dass viele der Funktionen des VP40 durch die D184N Mutation exklusiv in Meerschweinchenzellen beeinflusst werden und erklären zumindest teilweise die gesteigerte Infektiösität von $VP40_{D184N}$ enthaltenden iVLPs in Meerschweinchenzellen. Der bedeutendste spezies-spezifische Unterschied durch die D184N Mutation in VP40 betraf jedoch die VP40-vermittelten Inhibition der viralen Replikation und Transkription. Diese führte zu einer signifikanten Steigerung der viralen Replikation und Transkription in Meerschweinchenzellen was die Geschwindigkeit des Viruswachstums deutlich beeinflusste.

Der zweite Teil dieser Arbeit untersuchte die Bedeutung der deri Mutationen im L Protein des Meerschweinchen-letalen MARV. Interessanterweise führte die S741C Mutation im L Protein zu einer deutlichen, spezies-unabhängigen, Steigerung der viralen Replikation und Transkription. Die Mutationen D758A und A759D hingegen

hatten einen massiven Verlust der Polymerase Funktion des L Proteins zur Folge.

Abschließend wurde durch Ko-expression der L Variante mit der S741C Mutation und $VP40_{D184N}$ gezeigt dass die Kombination dieser beiden Mutationen zu einer achtfachen Steigerung der viralen Replikation und Transkription in Meerschweinchenzellen gegenüber humanen Zellen führte. Die Daten dieser Arbeit, lassen vermuten, dass die D184N Mutation in VP40 und die S741C Mutation in L zu der hohen Letalität des Meerschweinchen-adaptierten MARV beitragen.

6 References

Acharya, M. (2014). Ebola viral disease outbreak-2014: implications and pitfalls. *Front Public Health* **2**, 263.

Ackermann, A., Staeheli, P. & Schneider, U. (2007). Adaptation of Borna disease virus to new host species attributed to altered regulation of viral polymerase activity. *J Virol* **81**, 7933-7940.

Albariño, C. G., Shoemaker, T., Khristova, M. L., Wamala, J. F., Muyembe, J. J., Balinandi, S., Tumusiime, A., Campbell, S., Cannon, D., Gibbons, A., Bergeron, E., Bird, B., Dodd, K., Spiropoulou, C., Erickson, B. R., Guerrero, L., Knust, B., Nichol, S. T., Rollin, P. E. & Ströher, U. (2013a). Genomic analysis of filoviruses associated with four viral hemorrhagic fever outbreaks in Uganda and the Democratic Republic of the Congo in 2012. *Virology* **442**, 97-100.

Albariño, C. G., Uebelhoer, L. S., Vincent, J. P., Khristova, M. L., Chakrabarti, A. K., McElroy, A., Nichol, S. T. & Towner, J. S. (2013b). Development of a reverse genetics system to generate recombinant Marburg virus derived from a bat isolate. *Virology* **446**, 230-237.

Albariño, C. G., Wiggleton Guerrero, L., Spengler, J. R., Uebelhoer, L. S., Chakrabarti, A. K., Nichol, S. T. & Towner, J. S. (2015). Recombinant Marburg viruses containing mutations in the IID region of VP35 prevent inhibition of Host immune responses. *Virology* **476**, 85-91.

Aleksandrowicz, P., Marzi, A., Biedenkopf, N., Beimforde, N., Becker, S., Hoenen, T., Feldmann, H. & Schnittler, H. J. (2011). Ebola virus enters host cells by macropinocytosis and clathrin-mediated endocytosis. *J Infect Dis* **204 Suppl 3**, S957-967.

Amman, B. R., Nyakarahuka, L., McElroy, A. K., Dodd, K. A., Sealy, T. K., Schuh, A. J., Shoemaker, T. R., Balinandi, S., Atimnedi, P., Kaboyo, W., Nichol, S. T. & Towner, J. S. (2014). Marburgvirus resurgence in Kitaka Mine bat population after extermination attempts, Uganda. *Emerg Infect Dis* **20**, 1761-1764.

Bale, S., Julien, J. P., Bornholdt, Z. A., Kimberlin, C. R., Halfmann, P., Zandonatti, M. A., Kunert, J., Kroon, G. J., Kawaoka, Y., MacRae, I. J., Wilson, I. A. & Saphire, E. O. (2012). Marburg virus VP35 can both fully coat the backbone and cap the ends of dsRNA for interferon antagonism. *PLoS Pathog* **8**, e1002916.

Bamberg, S., Kolesnikova, L., Moller, P., Klenk, H. D. & Becker, S. (2005). VP24 of Marburg virus influences formation of infectious particles. *J Virol* **79**, 13421-13433.

Banadyga, L., Dolan, M. A. & Ebihara, H. (2016). Rodent-Adapted Filoviruses and the Molecular Basis of Pathogenesis. *J Mol Biol*.

Bartsch, S. M., Gorham, K. & Lee, B. Y. (2015). The cost of an Ebola case. *Pathog Glob Health* **109**, 4-9.

Baseler, L., Chertow, D. S., Johnson, K. M., Feldmann, H. & Morens, D. M. (2016). The Pathogenesis of Ebola Virus Disease. *Annu Rev Pathol*.

Bausch, D. G., Nichol, S. T., Muyembe-Tamfum, J. J., Borchert, M., Rollin, P. E., Sleurs, H., Campbell, P., Tshioko, F. K., Roth, C., Colebunders, R., Pirard, P., Mardel, S., Olinda, L. A., Zeller, H., Tshomba, A., Kulidri, A., Libande, M. L., Mulangu, S., Formenty, P., Grein, T., Leirs, H., Braack, L., Ksiazek, T., Zaki, S., Bowen, M. D., Smit, S. B., Leman, P. A., Burt, F. J., Kemp, A., Swanepoel, R. & Congo, I. S. a. T. C. f. M. H. F. C. i. t. D. R. o. t. (2006). Marburg hemorrhagic fever associated with multiple genetic lineages of virus. *N Engl J Med* **355**, 909-919.

Bavari, S., Bosio, C. M., Wiegand, E., Ruthel, G., Will, A. B., Geisbert, T. W., Hevey, M., Schmaljohn, C., Schmaljohn, A. & Aman, M. J. (2002). Lipid raft microdomains: a gateway for compartmentalized trafficking of Ebola and Marburg viruses. *J Exp Med* **195**, 593-602.

Beaucourt, S., Bordería, A. V., Coffey, L. L., Gnädig, N. F., Sanz-Ramos, M., Beeharry, Y. & Vignuzzi, M. (2011). Isolation of fidelity variants of RNA viruses and characterization of virus mutation frequency. *J Vis Exp*.

Becker, S., Klenk, H. D. & Mühlberger, E. (1996). Intracellular transport and processing of the Marburg virus surface protein in vertebrate and insect cells. *Virology* **225**, 145-155.

Becker, S., Rinne, C., Hofsass, U., Klenk, H. D. & Mühlberger, E. (1998). Interactions of Marburg virus nucleocapsid proteins. *Virology* **249**, 406-417.

Becker, S., Spiess, M. & Klenk, H. D. (1995). The asialoglycoprotein receptor is a potential liver-specific receptor for Marburg virus. *J Gen Virol* **76**, 393-399.

Beeching, N. J., Fenech, M. & Houlihan, C. F. (2014). Ebola virus disease. *BMJ* **349**, g7348.

Bente, D., Gren, J., Strong, J. E. & Feldmann, H. (2009). Disease modeling for Ebola and Marburg viruses. *Dis Model Mech* **2**, 12-17.

Betts & Russel (2007). *Bioinformatics for Geneticists: A Bioinformatics Primer for the Analysis of Genetic Data*.

Bharat, T. A., Riches, J. D., Kolesnikova, L., Welsch, S., Krähling, V., Davey, N., Parsy, M. L., Becker, S. & Briggs, J. A. (2011). Cryo-electron tomography of Marburg virus particles and their morphogenesis within infected cells. *PLoS Biol* **9**, e1001196.

Bhattacharyya, S., Hope, T. J. & Young, J. A. (2011). Differential requirements for clathrin endocytic pathway components in cellular entry by Ebola and Marburg glycoprotein pseudovirions. *Virology* **419**, 1-9.

Bibollet-Ruche, F., Heigele, A., Keele, B. F., Easlick, J. L., Decker, J. M., Takehisa, J., Learn, G., Sharp, P. M., Hahn, B. H. & Kirchhoff, F. (2012). Efficient SIVcpz replication in human lymphoid tissue requires viral matrix protein adaptation. *J Clin Invest* **122**, 1644-1652.

Bornholdt, Z. A., Noda, T., Abelson, D. M., Halfmann, P., Wood, M. R., Kawaoka, Y. & Saphire, E. O. (2013). Structural rearrangement of ebola virus VP40 begets multiple functions in the virus life cycle. *Cell* **154**, 763-774.

Bowen, E. T., Lloyd, G., Harris, W. J., Platt, G. S., Baskerville, A. & Vella, E. E. (1977). Viral haemorrhagic fever in southern Sudan and northern Zaire. Preliminary studies on the aetiological agent. *Lancet* **1**, 571-573.

Brauburger, K., Hume, A. J., Mühlberger, E. & Olejnik, J. (2012). Forty-five years of Marburg virus research. *Viruses* **4**, 1878-1927.

Brindley, M. A., Hunt, C. L., Kondratowicz, A. S., Bowman, J., Sinn, P. L., McCray, P. B., Quinn, K., Weller, M. L., Chiorini, J. A. & Maury, W. (2011). Tyrosine kinase receptor Axl enhances entry of Zaire ebolavirus without direct interactions with the viral glycoprotein. *Virology* **415**, 83-94.

Brown, P. A., Lupini, C., Catelli, E., Clubbe, J., Ricchizzi, E. & Naylor, C. J. (2011). A single polymerase (L) mutation in avian metapneumovirus increased virulence and partially maintained virus viability at an elevated temperature. *J Gen Virol* **92**, 346-354.

Bukreyev, A. A., Chandran, K., Dolnik, O., Dye, J. M., Ebihara, H., Leroy, E. M., Mühlberger, E., Netesov, S. V., Patterson, J. L., Paweska, J. T., Saphire, E. O., Smither, S. J., Takada, A., Towner, J. S., Volchkov, V. E., Warren, T. K. & Kuhn, J. H. (2014). Discussions and decisions of the 2012–2014 International Committee on Taxonomy of Viruses (ICTV) Filoviridae Study Group, January 2012–June 2013. *Arch Virol* **159**, 821-830.

Börnig, H. & Geyer, G. (1974). Staining of cholesterol with the fluorescent antibiotic "filipin". *Acta Histochem* **50**, 110-115.

Campbell, P. J., Kyriakis, C. S., Marshall, N., Suppiah, S., Seladi-Schulman, J., Danzy, S., Lowen, A. C. & Steel, J. (2014). Residue 41 of the Eurasian avian-like swine influenza a virus matrix protein modulates virion filament length and efficiency of contact transmission. *J Virol* **88**, 7569-7577.

Carette, J. E., Raaben, M., Wong, A. C., Herbert, A. S., Obernosterer, G., Mulherkar, N., Kuehne, A. I., Kranzusch, P. J., Griffin, A. M., Ruthel, G., Dal Cin, P., Dye, J. M., Whelan, S. P., Chandran, K. & Brummelkamp, T. R. (2011). Ebola virus entry requires the cholesterol transporter Niemann-Pick C1. *Nature* **477**, 340-343.

Carroll, A. R. & Wagner, R. R. (1979). Role of the membrane (M) protein in endogenous inhibition of in vitro transcription by vesicular stomatitis virus. *J Virol* **29**, 134-142.

Carroll, M. W., Matthews, D. A., Hiscox, J. A., Elmore, M. J., Pollakis, G., Rambaut, A., Hewson, R., García-Dorival, I., Bore, J. A., Koundouno, R., Abdellati, S., Afrough, B., Aiyepada, J., Akhilomen, P., Asogun, D., Atkinson, B., Badusche, M., Bah, A., Bate, S., Baumann, J., Becker, D., Becker-Ziaja, B., Bocquin, A., Borremans, B., Bosworth, A., Boettcher, J. P., Cannas, A.,

Carletti, F., Castilletti, C., Clark, S., Colavita, F., Diederich, S., Donatus, A., Duraffour, S., Ehichioya, D., Ellerbrok, H., Fernandez-Garcia, M. D., Fizet, A., Fleischmann, E., Gryseels, S., Hermelink, A., Hinzmann, J., Hopf-Guevara, U., Ighodalo, Y., Jameson, L., Kelterbaum, A., Kis, Z., Kloth, S., Kohl, C., Korva, M., Kraus, A., Kuisma, E., Kurth, A., Liedigk, B., Logue, C. H., Lüdtke, A., Maes, P., McCowen, J., Mély, S., Mertens, M., Meschi, S., Meyer, B., Michel, J., Molkenthin, P., Muñoz-Fontela, C., Muth, D., Newman, E. N., Ngabo, D., Oestereich, L., Okosun, J., Olokor, T., Omiunu, R., Omomoh, E., Pallasch, E., Pályi, B., Portmann, J., Pottage, T., Pratt, C., Priesnitz, S., Quartu, S., Rappe, J., Repits, J., Richter, M., Rudolf, M., Sachse, A., Schmidt, K. M., Schudt, G., Strecker, T., Thom, R., Thomas, S., Tobin, E., Tolley, H., Trautner, J., Vermoesen, T., Vitoriano, I., Wagner, M., Wolff, S., Yue, C., Capobianchi, M. R., Kretschmer, B., Hall, Y., Kenny, J. G., Rickett, N. Y., Dudas, G., Coltart, C. E., Kerber, R., Steer, D., Wright, C., Senyah, F., Keita, S., Drury, P., Diallo, B., de Clerck, H., Van Herp, M., Sprecher, A., Traore, A., Diakite, M., Konde, M. K., Koivogui, L., Magassouba, N., Avšič-Županc, T., Nitsche, A., Strasser, M., Ippolito, G., Becker, S., Stoecker, K., Gabriel, M., Raoul, H., Di Caro, A., Wölfel, R., Formenty, P. & Günther, S. (2015). Temporal and spatial analysis of the 2014-2015 Ebola virus outbreak in West Africa. *Nature* **524**, 97-101.

CDC, C. f. D. C. a. P. (2009). Imported case of Marburg hemorrhagic fever - Colorado, 2008. *MMWR Morb Mortal Wkly Rep* **58**, 1377-1381.

Chandran, K., Sullivan, N. J., Felbor, U., Whelan, S. P. & Cunningham, J. M. (2005). Endosomal proteolysis of the Ebola virus glycoprotein is necessary for infection. *Science* **308**, 1643-1645.

Christie, A., Davies-Wayne, G. J., Cordier-Lassalle, T., Cordier-Lasalle, T., Blackley, D. J., Laney, A. S., Williams, D. E., Shinde, S. A., Badio, M., Lo, T., Mate, S. E., Ladner, J. T., Wiley, M. R., Kugelman, J. R., Palacios, G., Holbrook, M. R., Janosko, K. B., de Wit, E., van Doremalen, N., Munster, V. J., Pettitt, J., Schoepp, R. J., Verhenne, L., Evlampidou, I., Kollie, K. K., Sieh, S. B., Gasasira, A., Bolay, F., Kateh, F. N., Nyenswah, T. G., De Cock, K. M. & (CDC), C. f. D. C. a. P. (2015). Possible sexual transmission of Ebola virus - Liberia, 2015. *MMWR Morb Mortal Wkly Rep* **64**, 479-481.

Cross, R. W., Fenton, K. A., Geisbert, J. B., Ebihara, H., Mire, C. E. & Geisbert, T. W. (2015). Comparison of the Pathogenesis of the Angola and Ravn Strains of Marburg Virus in the Outbred Guinea Pig Model. *J Infect Dis* **212 Suppl 2**, S258-270.

Daddario-DiCaprio, K. M., Geisbert, T. W., Geisbert, J. B., Ströher, U., Hensley, L. E., Grolla, A., Fritz, E. A., Feldmann, F., Feldmann, H. & Jones, S. M. (2006). Cross-protection against Marburg virus strains by using a live, attenuated recombinant vaccine. *J Virol* **80**, 9659-9666.

Deen, G. F., Knust, B., Broutet, N., Sesay, F. R., Formenty, P., Ross, C., Thorson, A. E., Massaquoi, T. A., Marrinan, J. E., Ervin, E., Jambai, A., McDonald, S. L., Bernstein, K., Wurie, A. H., Dumbuya, M. S., Abad, N., Idriss, B., Wi, T., Bennett, S. D., Davies, T., Ebrahim, F. K., Meites, E., Naidoo, D., Smith, S., Banerjee, A., Erickson, B. R., Brault, A., Durski, K. N., Winter, J., Sealy, T., Nichol, S. T., Lamunu, M., Ströher, U., Morgan, O. & Sahr, F. (2015). Ebola RNA Persistence in Semen of Ebola Virus Disease Survivors - Preliminary Report. *N Engl J Med*.

Dietzel, E., Schudt, G., Krähling, V., Matrosovich, M. & Becker, S. (2016). Functional characterization of adaptive mutations during the West African Ebola virus outbreak. *J Virol*.

Dolnik, O., Kolesnikova, L. & Becker, S. (2008). Filoviruses: Interactions with the host cell. *Cell Mol Life Sci* **65**, 756-776.

Dolnik, O., Kolesnikova, L., Stevermann, L. & Becker, S. (2010). Tsg101 is recruited by a late domain of the nucleocapsid protein to support budding of Marburg virus-like particles. *J Virol* **84**, 7847-7856.

Dolnik, O., Kolesnikova, L., Welsch, S., Strecker, T., Schudt, G. & Becker, S. (2014). Interaction with Tsg101 is necessary for the efficient transport and release of nucleocapsids in marburg virus-infected cells. *PLoS Pathog* **10**, e1004463.

Dolnik, O., Stevermann, L., Kolesnikova, L. & Becker, S. (2015). Marburg virus inclusions: A virus-induced microcompartment and interface to multivesicular bodies and the late endosomal compartment. *Eur J Cell Biol* **94**, 323-331.

Dong, J. B., Saito, A., Mine, Y., Sakuraba, Y., Nibe, K., Goto, Y., Komase, K., Nakayama, T., Miyata, H., Iwata, H. & Haga, T. (2009). Adaptation of wild-type measles virus to cotton rat lung cells: E89K mutation in matrix protein contributes to its fitness. *Virus Genes* **39**, 330-334.

Dortmans, J. C., Rottier, P. J., Koch, G. & Peeters, B. P. (2011). Passaging of a Newcastle disease virus pigeon variant in chickens results in selection of viruses with mutations in the polymerase complex enhancing virus replication and virulence. *J Gen Virol* **92**, 336-345.

Drosten, C., Göttig, S., Schilling, S., Asper, M., Panning, M., Schmitz, H. & Günther, S. (2002). Rapid detection and quantification of RNA of Ebola and Marburg viruses, Lassa virus, Crimean-Congo hemorrhagic fever virus, Rift Valley fever virus, dengue virus, and yellow fever virus by real-time reverse transcription-PCR. *J Clin Microbiol* **40**, 2323-2330.

Du, X., Kumar, J., Ferguson, C., Schulz, T. A., Ong, Y. S., Hong, W., Prinz, W. A., Parton, R. G., Brown, A. J. & Yang, H. (2011). A role for oxysterol-binding protein-related protein 5 in endosomal cholesterol trafficking. *J Cell Biol* **192**, 121-135.

Ebihara, H., Takada, A., Kobasa, D., Jones, S., Neumann, G., Theriault, S., Bray, M., Feldmann, H. & Kawaoka, Y. (2006). Molecular determinants of Ebola virus virulence in mice. *PLoS Pathog* **2**, e73.

Enterlein, S., Schmidt, K. M., Schümann, M., Conrad, D., Krähling, V., Olejnik, J. & Mühlberger, E. (2009). The marburg virus 3' noncoding region structurally and functionally differs from that of ebola virus. *J Virol* **83**, 4508-4519.

Enterlein, S., Volchkov, V., Weik, M., Kolesnikova, L., Volchkova, V., Klenk, H. D. & Mühlberger, E. (2006). Rescue of recombinant Marburg virus from cDNA is dependent on nucleocapsid protein VP30. *J Virol* **80**, 1038-1043.

Faix, J. & Rottner, K. (2006). The making of filopodia. *Curr Opin Cell Biol* **18**, 18-25.

Feagins, A. R. & Basler, C. F. (2014). The VP40 protein of Marburg virus exhibits impaired budding and increased sensitivity to human tetherin following mouse adaptation. *J Virol* **88**, 14440-14450.

Feagins, A. R. & Basler, C. F. (2015). Amino Acid Residue at Position 79 of Marburg Virus VP40 Confers Interferon Antagonism in Mouse Cells. *J Infect Dis* **212 Suppl 2**, S219-225.

Feldmann, H., Klenk, H. D. & Sanchez, A. (1993). Molecular biology and evolution of filoviruses. *Arch Virol Suppl* **7**, 81-100.

Feldmann, H., Muhlberger, E., Randolf, A., Will, C., Kiley, M. P., Sanchez, A. & Klenk, H. D. (1992). Marburg virus, a filovirus: messenger RNAs, gene order, and regulatory elements of the replication cycle. *Virus Res* **24**, 1-19.

Feldmann, H., Will, C., Schikore, M., Slenczka, W. & Klenk, H. D. (1991). Glycosylation and oligomerization of the spike protein of Marburg virus. *Virology* **182**, 353-356.

Finke, S., Mueller-Waldeck, R. & Conzelmann, K. K. (2003). Rabies virus matrix protein regulates the balance of virus transcription and replication. *J Gen Virol* **84**, 1613-1621.

Fowler, T., Bamberg, S., Möller, P., Klenk, H.-D., Meyer, T. F., Becker, S. & Rudel, T. (2005). Inhibition of Marburgvirus Protein Expression and Viral Release by RNA Interference. *J Gen Virol* **86**, 1181-1188.

Fujii, Y., Sakaguchi, T., Kiyotani, K., Huang, C., Fukuhara, N. & Yoshida, T. (2002). Identification of mutations associated with attenuation of virulence of a field Sendai virus isolate by egg passage. *Virus Genes* **25**, 189-193.

Funke, C., Becker, S., Dartsch, H., Klenk, H. D. & Muhlberger, E. (1995). Acylation of the Marburg virus glycoprotein. *Virology* **208**, 289-297.

Geisbert, T. W., Geisbert, J. B., Leung, A., Daddario-DiCaprio, K. M., Hensley, L. E., Grolla, A. & Feldmann, H. (2009). Single-injection vaccine protects nonhuman primates against infection with marburg virus and three species of ebola virus. *J Virol* **83**, 7296-7304.

Geisbert, T. W. & Jahrling, P. B. (1995). Differentiation of filoviruses by electron microscopy. *Virus Res* **39**, 129-150.

Gnirss, K., Kühl, A., Karsten, C., Glowacka, I., Bertram, S., Kaup, F., Hofmann, H. & Pöhlmann, S. (2012). Cathepsins B and L activate Ebola but not Marburg virus glycoproteins for efficient

entry into cell lines and macrophages independent of TMPRSS2 expression. *Virology* **424**, 3-10.

Gramberg, T., Hofmann, H., Möller, P., Lalor, P. F., Marzi, A., Geier, M., Krumbiegel, M., Winkler, T., Kirchhoff, F., Adams, D. H., Becker, S., Münch, J. & Pöhlmann, S. (2005). LSECtin interacts with filovirus glycoproteins and the spike protein of SARS coronavirus. *Virology* **340**, 224-236.

Halfmann, P., Kim, J. H., Ebihara, H., Noda, T., Neumann, G., Feldmann, H. & Kawaoka, Y. (2008). Generation of biologically contained Ebola viruses. *Proc Natl Acad Sci U S A* **105**, 1129-1133.

Han, Z. & Harty, R. N. (2005). Packaging of actin into Ebola virus VLPs. *Virol J* **2**, 92.

Hashiguchi, T., Fusco, M. L., Bornholdt, Z. A., Lee, J. E., Flyak, A. I., Matsuoka, R., Kohda, D., Yanagi, Y., Hammel, M., Crowe, J. E. & Saphire, E. O. (2015). Structural basis for Marburg virus neutralization by a cross-reactive human antibody. *Cell* **160**, 904-912.

Hass, M., Gölnitz, U., Müller, S., Becker-Ziaja, B. & Günther, S. (2004). Replicon system for Lassa virus. *J Virol* **78**, 13793-13803.

Heald, A. E., Charleston, J. S., Iversen, P. L., Warren, T. K., Saoud, J. B., Al-Ibrahim, M., Wells, J., Warfield, K. L., Swenson, D. L., Welch, L. S., Sazani, P., Wong, M., Berry, D., Kaye, E. M. & Bavari, S. (2015). AVI-7288 for Marburg Virus in Nonhuman Primates and Humans. *N Engl J Med* **373**, 339-348.

Heiden, S., Grund, C., Höper, D., Mettenleiter, T. C. & Römer-Oberdörfer, A. (2014). Pigeon paramyxovirus type 1 variants with polybasic F protein cleavage site but strikingly different pathogenicity. *Virus Genes* **49**, 502-506.

Henao-Restrepo, A. M., Camacho, A., Longini, I. M., Watson, C. H., Edmunds, W. J., Egger, M., Carroll, M. W., Dean, N. E., Diatta, I., Doumbia, M., Draguez, B., Duraffour, S., Enwere, G., Grais, R., Gunther, S., Gsell, P. S., Hossmann, S., Watle, S. V., Kondé, M. K., Kéïta, S., Kone, S., Kuisma, E., Levine, M. M., Mandal, S., Mauget, T., Norheim, G., Riveros, X., Soumah, A., Trelle, S., Vicari, A. S., Røttingen, J. A. & Kieny, M. P. (2016). Efficacy and effectiveness of an rVSV-vectored vaccine in preventing Ebola virus disease: final results from the Guinea ring vaccination, open-label, cluster-randomised trial (Ebola Ça Suffit!). *Lancet*.

Hoenen, T., Jung, S., Herwig, A., Groseth, A. & Becker, S. (2010). Both matrix proteins of Ebola virus contribute to the regulation of viral genome replication and transcription. *Virology* **403**, 56-66.

Hoenen, T., Shabman, R. S., Groseth, A., Herwig, A., Weber, M., Schudt, G., Dolnik, O., Basler, C. F., Becker, S. & Feldmann, H. (2012). Inclusion bodies are a site of ebolavirus replication. *J Virol* **86**, 11779-11788.

Horisberger, M. A. & de Staritzky, K. (1987). A recombinant human interferon-alpha B/D hybrid with a broad host-range. *J Gen Virol* **68 (Pt 3)**, 945-948.

Hug, H., Costas, M., Staeheli, P., Aebi, M. & Weissmann, C. (1988). Organization of the murine Mx gene and characterization of its interferon- and virus-inducible promoter. *Mol Cell Biol* **8**, 3065-3079.

Hunt, L. & Knott, V. (2016). Serious and common sequelae after Ebola virus infection. *Lancet Infect Dis* **16**, 270-271.

Ignatyev, G. M., Agafonov, A. P., Streltsova, M. A. & Kashentseva, E. A. (1996). Inactivated Marburg virus elicits a nonprotective immune response in Rhesus monkeys. *J Biotechnol* **44**, 111-118.

Jorns, C., Holzinger, D., Thimme, R., Spangenberg, H. C., Weidmann, M., Rasenack, J., Blum, H. E., Haller, O. & Kochs, G. (2006). Rapid and simple detection of IFN-neutralizing antibodies in chronic hepatitis C non-responsive to IFN-alpha. *J Med Virol* **78**, 74-82.

Kiley, M. P., Cox, N. J., Elliott, L. H., Sanchez, A., DeFries, R., Buchmeier, M. J., Richman, D. D. & McCormick, J. B. (1988). Physicochemical properties of Marburg virus: evidence for three distinct virus strains and their relationship to Ebola virus. *J Gen Virol* **69 (Pt 8)**, 1957-1967.

Kim, D. I., Birendra, K. C., Zhu, W., Motamedchaboki, K., Doye, V. & Roux, K. J. (2014a). Probing nuclear pore complex architecture with proximity-dependent biotinylation. *Proc Natl Acad Sci U S A* **111**, E2453-2461.

Kim, D. I., Jensen, S. C., Noble, K. A., Kc, B., Roux, K. H., Motamedchaboki, K. & Roux, K. J. (2016). An improved smaller biotin ligase for BioID proximity labeling. *Mol Biol Cell* **27**, 1188-1196.

Kim, S. H., Thu, B. J., Skall, H. F., Vendramin, N. & Evensen, O. (2014b). A single amino acid mutation (I1012F) of the RNA polymerase of marine viral hemorrhagic septicemia virus changes in vitro virulence to rainbow trout gill epithelial cells. *J Virol* **88**, 7189-7198.

Koehler, A., Kolesnikova, L. & Becker, S. (2016). An active site mutation increases the polymerase activity of the guinea pig-lethal Marburg virus. *J Gen Virol* **97**, 2494-2500.

Koehler, A., Kolesnikova, L., Welzel, U., Schudt, G., Herwig, A. & Becker, S. (2015). A Single Amino Acid Change in the Marburg Virus Matrix Protein VP40 Provides a Replicative Advantage in a Species-Specific Manner. *J Virol* **90**, 1444-1454.

Koellhoffer, J. F., Malashkevich, V. N., Harrison, J. S., Toro, R., Bhosle, R. C., Chandran, K., Almo, S. C. & Lai, J. R. (2012). Crystal structure of the Marburg virus GP2 core domain in its postfusion conformation. *Biochemistry* **51**, 7665-7675.

Kolesnikova, L., Bamberg, S., Berghöfer, B. & Becker, S. (2004a). The matrix protein of Marburg virus is transported to the plasma membrane along cellular membranes: exploiting the retrograde late endosomal pathway. *J Virol* **78**, 2382-2393.

Kolesnikova, L., Berghöfer, B., Bamberg, S. & Becker, S. (2004b). Multivesicular bodies as a platform for formation of the Marburg virus envelope. *J Virol* **78**, 12277-12287.

Kolesnikova, L., Bohil, A. B., Cheney, R. E. & Becker, S. (2007a). Budding of Marburgvirus is associated with filopodia. *Cell Microbiol* **9**, 939-951.

Kolesnikova, L., Bugany, H., Klenk, H. D. & Becker, S. (2002). VP40, the matrix protein of Marburg virus, is associated with membranes of the late endosomal compartment. *J Virol* **76**, 1825-1838.

Kolesnikova, L., Mittler, E., Schudt, G., Shams-Eldin, H. & Becker, S. (2012). Phosphorylation of Marburg virus matrix protein VP40 triggers assembly of nucleocapsids with the viral envelope at the plasma membrane. *Cell Microbiol* **14**, 182-197.

Kolesnikova, L., Mühlberger, E., Ryabchikova, E. & Becker, S. (2000). Ultrastructural organization of recombinant Marburg virus nucleoprotein: comparison with Marburg virus inclusions. *J Virol* **74**, 3899-3904.

Kolesnikova, L., Ryabchikova, E., Shestopalov, A. & Becker, S. (2007b). Basolateral budding of Marburg virus: VP40 retargets viral glycoprotein GP to the basolateral surface. *J Infect Dis* **196 Suppl 2**, S232-236.

Kolesnikova, L., Strecker, T., Morita, E., Zielecki, F., Mittler, E., Crump, C. & Becker, S. (2009). Vacuolar protein sorting pathway contributes to the release of Marburg virus. *J Virol* **83**, 2327-2337.

Kondratowicz, A. S., Lennemann, N. J., Sinn, P. L., Davey, R. A., Hunt, C. L., Moller-Tank, S., Meyerholz, D. K., Rennert, P., Mullins, R. F., Brindley, M., Sandersfeld, L. M., Quinn, K., Weller, M., McCray, P. B., Chiorini, J. & Maury, W. (2011). T-cell immunoglobulin and mucin domain 1 (TIM-1) is a receptor for Zaire Ebolavirus and Lake Victoria Marburgvirus. *Proc Natl Acad Sci U S A* **108**, 8426-8431.

Krähling, V., Dolnik, O., Kolesnikova, L., Schmidt-Chanasit, J., Jordan, I., Sandig, V., Günther, S. & Becker, S. (2010). Establishment of fruit bat cells (Rousettus aegyptiacus) as a model system for the investigation of filoviral infection. *PLoS Negl Trop Dis* **4**, e802.

Kuhn, J. H., Becker, S., Ebihara, H., Geisbert, T. W., Johnson, K. M., Kawaoka, Y., Lipkin, W. I., Negredo, A. I., Netesov, S. V., Nichol, S. T., Palacios, G., Peters, C. J., Tenorio, A., Volchkov, V. E. & Jahrling, P. B. (2010). Proposal for a revised taxonomy of the family Filoviridae: classification, names of taxa and viruses, and virus abbreviations. *Arch Virol* **155**, 2083-2103.

Lenard, J. (1996). Negative-strand virus M and retrovirus MA proteins: all in a family? *Virology* **216**, 289-298.

Liang, B., Li, Z., Jenni, S., Rahmeh, A. A., Morin, B. M., Grant, T., Grigorieff, N., Harrison, S. C. & Whelan, S. P. (2015). Structure of the L Protein of Vesicular Stomatitis Virus from Electron Cryomicroscopy. *Cell* **162**, 314-327.

Liu, Y., Stone, S. & Harty, R. N. (2011). Characterization of filovirus protein-protein interactions in mammalian cells using bimolecular complementation. *J Infect Dis* **204 Suppl 3**, S817-824.

Lofts, L. L., Ibrahim, M. S., Negley, D. L., Hevey, M. C. & Schmaljohn, A. L. (2007). Genomic differences between guinea pig lethal and nonlethal Marburg virus variants. *J Infect Dis* **196 Suppl 2**, S305-312.

Lofts, L. L., Wells, J. B., Bavari, S. & Warfield, K. L. (2011). Key genomic changes necessary for an in vivo lethal mouse marburgvirus variant selection process. *J Virol* **85**, 3905-3917.

Magoffin, D. E., Halpin, K., Rota, P. A. & Wang, L. F. (2007). Effects of single amino acid substitutions at the E residue in the conserved GDNE motif of the Nipah virus polymerase (L) protein. *Arch Virol* **152**, 827-832.

Malur, A. G., Gupta, N. K., De Bishnu, P. & Banerjee, A. K. (2002). Analysis of the mutations in the active site of the RNA-dependent RNA polymerase of human parainfluenza virus type 3 (HPIV3). *Gene Expr* **10**, 93-100.

Manrique, J. M., Celma, C. C., Hunter, E., Affranchino, J. L. & González, S. A. (2003). Positive and negative modulation of virus infectivity and envelope glycoprotein incorporation into virions by amino acid substitutions at the N terminus of the simian immunodeficiency virus matrix protein. *J Virol* **77**, 10881-10888.

Markosyan, R. M., Miao, C., Zheng, Y. M., Melikyan, G. B., Liu, S. L. & Cohen, F. S. (2016). Induction of Cell-Cell Fusion by Ebola Virus Glycoprotein: Low pH Is Not a Trigger. *PLoS Pathog* **12**, e1005373.

Martini, G. A. & Schmidt, H. A. (1968). [Spermatogenic transmission of the "Marburg virus". (Causes of "Marburg simian disease")]. *Klin Wochenschr* **46**, 398-400.

Martini, G. A. & Siegert, R., (eds) (1971). *Marburg virus disease*. Berlin, Heidelberg, New York: Springer.

Marzi, A., Banadyga, L., Haddock, E., Thomas, T., Shen, K., Horne, E. J., Scott, D. P., Feldmann, H. & Ebihara, H. (2016). A hamster model for Marburg virus infection accurately recapitulates Marburg hemorrhagic fever. *Sci Rep* **6**, 39214.

Marzi, A., Gramberg, T., Simmons, G., Moller, P., Rennekamp, A. J., Krumbiegel, M., Geier, M., Eisemann, J., Turza, N., Saunier, B., Steinkasserer, A., Becker, S., Bates, P., Hofmann, H. & Pohlmann, S. (2004). DC-SIGN and DC-SIGNR Interact with the Glycoprotein of Marburg Virus and the S Protein of Severe Acute Respiratory Syndrome Coronavirus. *J Virol* **78**, 12090-12095.

Mate, S. E., Kugelman, J. R., Nyenswah, T. G., Ladner, J. T., Wiley, M. R., Cordier-Lassalle, T., Christie, A., Schroth, G. P., Gross, S. M., Davies-Wayne, G. J., Shinde, S. A., Murugan, R., Sieh, S. B., Badio, M., Fakoli, L., Taweh, F., de Wit, E., van Doremalen, N., Munster, V. J., Pettitt, J., Prieto, K., Humrighouse, B. W., Ströher, U., DiClaro, J. W., Hensley, L. E., Schoepp, R. J., Safronetz, D., Fair, J., Kuhn, J. H., Blackley, D. J., Laney, A. S., Williams, D. E., Lo, T., Gasasira, A., Nichol, S. T., Formenty, P., Kateh, F. N., De Cock, K. M., Bolay, F., Sanchez-Lockhart, M. & Palacios, G. (2015). Molecular Evidence of Sexual Transmission of Ebola Virus. *N Engl J Med* **373**, 2448-2454.

Mateo, M., Carbonnelle, C., Reynard, O., Kolesnikova, L., Nemirov, K., Page, A., Volchkova, V. A. & Volchkov, V. E. (2011). VP24 is a molecular determinant of Ebola virus virulence in guinea pigs. *J Infect Dis* **204 Suppl 3**, S1011-1020.

Matsuno, K., Kishida, N., Usami, K., Igarashi, M., Yoshida, R., Nakayama, E., Shimojima, M., Feldmann, H., Irimura, T., Kawaoka, Y. & Takada, A. (2010). Different potential of C-type lectin-mediated entry between Marburg virus strains. *J Virol* **84**, 5140-5147.

Mattia, J. G., Vandy, M. J., Chang, J. C., Platt, D. E., Dierberg, K., Bausch, D. G., Brooks, T., Conteh, S., Crozier, I., Fowler, R. A., Kamara, A. P., Kang, C., Mahadevan, S., Mansaray, Y., Marcell, L., McKay, G., O'Dempsey, T., Parris, V., Pinto, R., Rangel, A., Salam, A. P., Shantha, J., Wolfman, V., Yeh, S., Chan, A. K. & Mishra, S. (2016). Early clinical sequelae of Ebola virus disease in Sierra Leone: a cross-sectional study. *Lancet Infect Dis* **16**, 331-338.

McInerney, P., Adams, P. & Hadi, M. Z. (2014). Error Rate Comparison during Polymerase Chain Reaction by DNA Polymerase. *Mol Biol Int* **2014**, 287430.

Mehedi, M., Groseth, A., Feldmann, H. & Ebihara, H. (2011). Clinical aspects of Marburg hemorrhagic fever. *Future Virol* **6**, 1091-1106.

Misasi, J., Chandran, K., Yang, J. Y., Considine, B., Filone, C. M., Côté, M., Sullivan, N., Fabozzi, G., Hensley, L. & Cunningham, J. (2012). Filoviruses require endosomal cysteine proteases for entry but exhibit distinct protease preferences. *J Virol* **86**, 3284-3292.

Mittler, E., Kolesnikova, L., Herwig, A., Dolnik, O. & Becker, S. (2013). Assembly of the Marburg virus envelope. *Cell Microbiol* **15**, 270-284.

Mittler, E., Kolesnikova, L., Strecker, T., Garten, W. & Becker, S. (2007). Role of the transmembrane domain of marburg virus surface protein GP in assembly of the viral envelope. *J Virol* **81**, 3942-3948.

Mulherkar, N., Raaben, M., de la Torre, J. C., Whelan, S. P. & Chandran, K. (2011). The Ebola virus glycoprotein mediates entry via a non-classical dynamin-dependent macropinocytic pathway. *Virology* **419**, 72-83.

Murphy, F. A., van der Groen, G., Whiteflied, S. G. & Lange, J. V. (1978). Ebola and Marburg virus morphology and taxonomy. In *Ebola Virus Haemorrhagic Fever*, pp. 61-84. Edited by P. S. Amsterdam: Elsevier/North Holland.

Mühlberger, E. (2007). Filovirus replication and transcription. *Future Virol* **2**, 205-215.

Mühlberger, E., Lötfering, B., Klenk, H. D. & Becker, S. (1998). Three of the four nucleocapsid proteins of Marburg virus, NP, VP35, and L, are sufficient to mediate replication and transcription of Marburg virus-specific monocistronic minigenomes. *J Virol* **72**, 8756-8764.

Mühlberger, E., Sanchez, A., Randolf, A., Will, C., Kiley, M. P., Klenk, H. D. & Feldmann, H. (1992). The nucleotide sequence of the L gene of Marburg virus, a filovirus: homologies with paramyxoviruses and rhabdoviruses. *Virology* **187**, 534-547.

Mühlberger, E., Trommer, S., Funke, C., Volchkov, V., Klenk, H. D. & Becker, S. (1996). Termini of all mRNA species of Marburg virus: sequence and secondary structure. *Virology* **223**, 376-380.

Mühlberger, E., Weik, M., Volchkov, V. E., Klenk, H. D. & Becker, S. (1999). Comparison of the transcription and replication strategies of marburg virus and Ebola virus by using artificial replication systems. *J Virol* **73**, 2333-2342.

Nakayama, E. & Saijo, M. (2013). Animal models for Ebola and Marburg virus infections. *Front Microbiol* **4**, 267.

Nanbo, A., Imai, M., Watanabe, S., Noda, T., Takahashi, K., Neumann, G., Halfmann, P. & Kawaoka, Y. (2010). Ebolavirus is internalized into host cells via macropinocytosis in a viral glycoprotein-dependent manner. *PLoS Pathog* **6**, e1001121.

Nanbo, A., Watanabe, S., Halfmann, P. & Kawaoka, Y. (2013). The spatio-temporal distribution dynamics of Ebola virus proteins and RNA in infected cells. *Sci Rep* **3**, 1206.

Nanyonga, M., Saidu, J., Ramsay, A., Shindo, N. & Bausch, D. G. (2016). Sequelae of Ebola Virus Disease, Kenema District, Sierra Leone. *Clin Infect Dis* **62**, 125-126.

Negredo, A., Palacios, G., Vázquez-Morón, S., González, F., Dopazo, H., Molero, F., Juste, J., Quetglas, J., Savji, N., de la Cruz Martínez, M., Herrera, J. E., Pizarro, M., Hutchison, S. K., Echevarría, J. E., Lipkin, W. I. & Tenorio, A. (2011). Discovery of an ebolavirus-like filovirus in europe. *PLoS Pathog* **7**, e1002304.

Ng, K. K., Arnold, J. J. & Cameron, C. E. (2008). Structure-function relationships among RNA-dependent RNA polymerases. *Curr Top Microbiol Immunol* **320**, 137-156.

Noda, T., Sagara, H., Suzuki, E., Takada, A., Kida, H. & Kawaoka, Y. (2002). Ebola virus VP40 drives the formation of virus-like filamentous particles along with GP. *J Virol* **76**, 4855-4865.

Noton, S. L., Deflubé, L. R., Tremaglio, C. Z. & Fearns, R. (2012). The respiratory syncytial virus polymerase has multiple RNA synthesis activities at the promoter. *PLoS Pathog* **8**, e1002980.

Oda, S., Noda, T., Wijesinghe, K. J., Halfmann, P., Bornholdt, Z. A., Abelson, D. M., Armbrust, T., Stahelin, R. V., Kawaoka, Y. & Saphire, E. O. (2015). Crystal Structure of Marburg Virus VP40 Reveals a Broad, Basic Patch for Matrix Assembly and a Requirement of the N-Terminal Domain for Immunosuppression. *J Virol* **90**, 1839-1848.

Pattnaik, A. K., Ball, L. A., LeGrone, A. W. & Wertz, G. W. (1992). Infectious defective interfering particles of VSV from transcripts of a cDNA clone. *Cell* **69**, 1011-1020.

Pattnaik, A. K. & Wertz, G. W. (1990). Replication and amplification of defective interfering particle RNAs of vesicular stomatitis virus in cells expressing viral proteins from vectors containing cloned cDNAs. *J Virol* **64**, 2948-2957.

Pattnaik, A. K. & Wertz, G. W. (1991). Cells that express all five proteins of vesicular stomatitis virus from cloned cDNAs support replication, assembly, and budding of defective interfering particles. *Proc Natl Acad Sci U S A* **88**, 1379-1383.

Poch, O., Blumberg, B. M., Bougueleret, L. & Tordo, N. (1990). Sequence comparison of five polymerases (L proteins) of unsegmented negative-strand RNA viruses: theoretical assignment of functional domains. *J Gen Virol* **71 (Pt 5)**, 1153-1162.

Pourrut, X., Souris, M., Towner, J. S., Rollin, P. E., Nichol, S. T., Gonzalez, J. P. & Leroy, E. (2009). Large serological survey showing cocirculation of Ebola and Marburg viruses in Gabonese bat populations, and a high seroprevalence of both viruses in Rousettus aegyptiacus. *BMC Infect Dis* **9**, 159.

Qiu, X., Wong, G., Audet, J., Cutts, T., Niu, Y., Booth, S. & Kobinger, G. P. (2014). Establishment and characterization of a lethal mouse model for the Angola strain of Marburg virus. *J Virol* **88**, 12703-12714.

Ramanan, P., Edwards, M. R., Shabman, R. S., Leung, D. W., Endlich-Frazier, A. C., Borek, D. M., Otwinowski, Z., Liu, G., Huh, J., Basler, C. F. & Amarasinghe, G. K. (2012). Structural basis for Marburg virus VP35-mediated immune evasion mechanisms. *Proc Natl Acad Sci U S A* **109**, 20661-20666.

Reid, S. P., Leung, L. W., Hartman, A. L., Martinez, O., Shaw, M. L., Carbonnelle, C., Volchkov, V. E., Nichol, S. T. & Basler, C. F. (2006). Ebola virus VP24 binds karyopherin alpha1 and blocks STAT1 nuclear accumulation. *J Virol* **80**, 5156-5167.

Rosenke, K., Adjemian, J., Munster, V. J., Marzi, A., Falzarano, D., Onyango, C. O., Ochieng, M., Juma, B., Fischer, R. J., Prescott, J. B., Safronetz, D., Omballa, V., Owuor, C., Hoenen, T., Groseth, A., Martellaro, C., van Doremalen, N., Zemtsova, G., Self, J., Bushmaker, T., McNally, K., Rowe, T., Emery, S. L., Feldmann, F., Williamson, B. N., Best, S. M., Nyenswah, T. G., Grolla, A., Strong, J. E., Kobinger, G., Bolay, F. K., Zoon, K. C., Stassijns, J., Giuliani, R., de Smet, M., Nichol, S. T., Fields, B., Sprecher, A., Massaquoi, M., Feldmann, H. & de Wit, E. (2016). Plasmodium Parasitemia Associated With Increased Survival in Ebola Virus-Infected Patients. *Clin Infect Dis* **63**, 1026-1033.

Saeed, M. F., Kolokoltsov, A. A., Albrecht, T. & Davey, R. A. (2010). Cellular entry of ebola virus involves uptake by a macropinocytosis-like mechanism and subsequent trafficking through early and late endosomes. *PLoS Pathog* **6**, e1001110.

Sanchez, A., Geisbert, T. & Feldmann, H. (2006). *Fields Virology 5th edition, vol. 1*

Marburg and Ebola viruses: Lippincott Williams and Wilkins.

Sanchez, A., Kiley, M. P., Holloway, B. P. & Auperin, D. D. (1993). Sequence analysis of the Ebola virus genome: organization, genetic elements, and comparison with the genome of Marburg virus. *Virus Res* **29**, 215-240.

Schmidt, K. M. & Mühlberger, E. (2016). Marburg Virus Reverse Genetics Systems. *Viruses* **8**.

Schmidt, K. M., Schümann, M., Olejnik, J., Krähling, V. & Mühlberger, E. (2011). Recombinant Marburg virus expressing EGFP allows rapid screening of virus growth and real-time visualization of virus spread. *J Infect Dis* **204 Suppl 3**, S861-870.

Schnell, M. J. & Conzelmann, K. K. (1995). Polymerase activity of in vitro mutated rabies virus L protein. *Virology* **214**, 522-530.

Schnell, M. J., Mebatsion, T. & Conzelmann, K. K. (1994). Infectious rabies viruses from cloned cDNA. *EMBO J* **13**, 4195-4203.

Schudt, G., Kolesnikova, L., Dolnik, O., Sodeik, B. & Becker, S. (2013). Live-cell imaging of Marburg virus-infected cells uncovers actin-dependent transport of nucleocapsids over long distances. *Proc Natl Acad Sci U S A* **110**, 14402-14407.

Shabman, R. S., Hoenen, T., Groseth, A., Jabado, O., Binning, J. M., Amarasinghe, G. K., Feldmann, H. & Basler, C. F. (2013). An upstream open reading frame modulates ebola virus polymerase translation and virus replication. *PLoS Pathog* **9**, e1003147.

Shabman, R. S., Jabado, O. J., Mire, C. E., Stockwell, T. B., Edwards, M., Mahajan, M., Geisbert, T. W. & Basler, C. F. (2014). Deep Sequencing Identifies Noncanonical Editing of Ebola and Marburg Virus RNAs in Infected Cells. *MBio* **5**.

Shimojima, M., Takada, A., Ebihara, H., Neumann, G., Fujioka, K., Irimura, T., Jones, S., Feldmann, H. & Kawaoka, Y. (2006). Tyro3 family-mediated cell entry of Ebola and Marburg viruses. *J Virol* **80**, 10109-10116.

Sidhu, M. S., Menonna, J. P., Cook, S. D., Dowling, P. C. & Udem, S. A. (1993). Canine distemper virus L gene: sequence and comparison with related viruses. *Virology* **193**, 50-65.

Siegert, R., Shu, H.-L., Slenczka, W., Peters, D. & Müller, G. (1967). Zur Aetiologie einer unbekannten, von Affen ausgegangenen menschlichen Infektioskrankheit. *Dtsch Med Wschr* **51**, 2341-2343.

Sinn, P. L., Hickey, M. A., Staber, P. D., Dylla, D. E., Jeffers, S. A., Davidson, B. L., Sanders, D. A. & McCray, P. B. (2003). Lentivirus vectors pseudotyped with filoviral envelope glycoproteins transduce airway epithelia from the apical surface independently of folate receptor alpha. *J Virol* **77**, 5902-5910.

Sleat, D. E. & Banerjee, A. K. (1993). Transcriptional activity and mutational analysis of recombinant vesicular stomatitis virus RNA polymerase. *J Virol* **67**, 1334-1339.

Slenczka, W. & Klenk, H. D. (2007). Forty years of marburg virus. *J Infect Dis* **196 Suppl 2**, S131-135.

Smallwood, S., Hövel, T., Neubert, W. J. & Moyer, S. A. (2002). Different substitutions at conserved amino acids in domains II and III in the Sendai L RNA polymerase protein inactivate viral RNA synthesis. *Virology* **304**, 135-145.

Spearman, C. & Karber, G. (1974). *Virologische ArbeitsmethodenVirologische Arbeitsmethoden*: Fischer Verlag.

Spiegelberg, L., Wahl-Jensen, V., Kolesnikova, L., Feldmann, H., Becker, S. & Hoenen, T. (2011). Genus-specific recruitment of filovirus ribonucleoprotein complexes into budding particles. *J Gen Virol* **92**, 2900-2905.

Swanepoel, R., Smit, S. B., Rollin, P. E., Formenty, P., Leman, P. A., Kemp, A., Burt, F. J., Grobbelaar, A. A., Croft, J., Bausch, D. G., Zeller, H., Leirs, H., Braack, L. E., Libande, M. L., Zaki, S., Nichol, S. T., Ksiazek, T. G., Paweska, J. T. & Congo, I. S. a. T. C. f. M. H. F. C. i. t. D. R. o. (2007). Studies of reservoir hosts for Marburg virus. *Emerg Infect Dis* **13**, 1847-1851.

Swenson, D. L., Warfield, K. L., Kuehl, K., Larsen, T., Hevey, M. C., Schmaljohn, A., Bavari, S. & Aman, M. J. (2004). Generation of Marburg virus-like particles by co-expression of glycoprotein and matrix protein. *FEMS Immunol Med Microbiol* **40**, 27-31.

Swenson, D. L., Warfield, K. L., Larsen, T., Alves, D. A., Coberley, S. S. & Bavari, S. (2008). Monovalent virus-like particle vaccine protects guinea pigs and nonhuman primates against infection with multiple Marburg viruses. *Expert Rev Vaccines* **7**, 417-429.

Swenson, D. L., Warfield, K. L., Negley, D. L., Schmaljohn, A., Aman, M. J. & Bavari, S. (2005). Virus-like particles exhibit potential as a pan-filovirus vaccine for both Ebola and Marburg viral infections. *Vaccine* **23**, 3033-3042.

Sänger, C., Mühlberger, E., Lötfering, B., Klenk, H.-D. & Becker, S. (2002). The Marburg virus surface protein is phosphorylated at its ectodomain. *Virology* **295**, 20-29.

Terril, L. A. a. C., D. J. (1998). The Laboratory Guinea Pig: Boca Raton, Florida: CRC Press.

Thi, E. P., Mire, C. E., Ursic-Bedoya, R., Geisbert, J. B., Lee, A. C., Agans, K. N., Robbins, M., Deer, D. J., Fenton, K. A., MacLachlan, I. & Geisbert, T. W. (2014). Marburg virus infection in nonhuman primates: Therapeutic treatment by lipid-encapsulated siRNA. *Sci Transl Med* **6**, 250ra116.

Towner, J. S., Amman, B. R., Sealy, T. K., Carroll, S. A., Comer, J. A., Kemp, A., Swanepoel, R., Paddock, C. D., Balinandi, S., Khristova, M. L., Formenty, P. B., Albarino, C. G., Miller, D. M., Reed, Z. D., Kayiwa, J. T., Mills, J. N., Cannon, D. L., Greer, P. W., Byaruhanga, E., Farnon, E. C., Atimnedi, P., Okware, S., Katongole-Mbidde, E., Downing, R., Tappero, J. W., Zaki, S. R.,

Ksiazek, T. G., Nichol, S. T. & Rollin, P. E. (2009). Isolation of genetically diverse Marburg viruses from Egyptian fruit bats. *PLoS Pathog* **5**, e1000536.

Towner, J. S., Khristova, M. L., Sealy, T. K., Vincent, M. J., Erickson, B. R., Bawiec, D. A., Hartman, A. L., Comer, J. A., Zaki, S. R., Ströher, U., Gomes da Silva, F., del Castillo, F., Rollin, P. E., Ksiazek, T. G. & Nichol, S. T. (2006). Marburgvirus genomics and association with a large hemorrhagic fever outbreak in Angola. *J Virol* **80**, 6497-6516.

Towner, J. S., Pourrut, X., Albariño, C. G., Nkogue, C. N., Bird, B. H., Grard, G., Ksiazek, T. G., Gonzalez, J. P., Nichol, S. T. & Leroy, E. M. (2007). Marburg virus infection detected in a common African bat. *PLoS One* **2**, e764.

Urata, S., Noda, T., Kawaoka, Y., Morikawa, S., Yokosawa, H. & Yasuda, J. (2007). Interaction of Tsg101 with Marburg Virus VP40 Depends on the PPPY Motif, but Not the PT/SAP Motif as in the Case of Ebola Virus, and Tsg101 Plays a Critical Role in the Budding of Marburg Virus-Like Particles Induced by VP40, NP, and GP. *J Virol* **81**, 4895-4899.

Urata, S., Noda, T., Kawaoka, Y., Yokosawa, H. & Yasuda, J. (2006). Cellular factors required for Lassa virus budding. *J Virol* **80**, 4191-4195.

Ursic-Bedoya, R., Mire, C. E., Robbins, M., Geisbert, J. B., Judge, A., MacLachlan, I. & Geisbert, T. W. (2014). Protection against lethal Marburg virus infection mediated by lipid encapsulated small interfering RNA. *J Infect Dis* **209**, 562-570.

Valmas, C. & Basler, C. F. (2011). Marburg virus VP40 antagonizes interferon signaling in a species-specific manner. *J Virol* **85**, 4309-4317.

Valmas, C., Grosch, M. N., Schümann, M., Olejnik, J., Martinez, O., Best, S. M., Krähling, V., Basler, C. F. & Mühlberger, E. (2010). Marburg virus evades interferon responses by a mechanism distinct from ebola virus. *PLoS Pathog* **6**, e1000721.

Varkey, J. B., Shantha, J. G., Crozier, I., Kraft, C. S., Lyon, G. M., Mehta, A. K., Kumar, G., Smith, J. R., Kainulainen, M. H., Whitmer, S., Ströher, U., Uyeki, T. M., Ribner, B. S. & Yeh, S. (2015). Persistence of Ebola Virus in Ocular Fluid during Convalescence. *N Engl J Med* **372**, 2423-2427.

Volchkov, V. E., Chepurnov, A. A., Volchkova, V. A., Ternovoj, V. A. & Klenk, H. D. (2000a). Molecular characterization of guinea pig-adapted variants of Ebola virus. *Virology* **277**, 147-155.

Volchkov, V. E., Volchkova, V. A., Stroher, U., Becker, S., Dolnik, O., Cieplik, M., Garten, W., Klenk, H. D. & Feldmann, H. (2000b). Proteolytic processing of Marburg virus glycoprotein. *Virology* **268**, 1-6.

Wang, D., Hevey, M., Juompan, L. Y., Trubey, C. M., Raja, N. U., Deitz, S. B., Worarattanadharm, J., Luo, M., Yu, H., Swain, B. M., Moore, K. M. & Dong, J. Y. (2006). Complex adenovirus-vectored vaccine protects guinea pigs from three strains of Marburg virus challenges. *Virology* **353**, 324-332.

Ward, A. C. (1995). Specific changes in the M1 protein during adaptation of influenza virus to mouse. *Arch Virol* **140**, 383-389.

Warfield, K. L., Alves, D. A., Bradfute, S. B., Reed, D. K., VanTongeren, S., Kalina, W. V., Olinger, G. G. & Bavari, S. (2007). Development of a model for marburgvirus based on severe-combined immunodeficiency mice. *Virol J* **4**, 108.

Warfield, K. L., Bradfute, S. B., Wells, J., Lofts, L., Cooper, M. T., Alves, D. A., Reed, D. K., VanTongeren, S. A., Mech, C. A. & Bavari, S. (2009). Development and characterization of a mouse model for Marburg hemorrhagic fever. *J Virol* **83**, 6404-6415.

Watanabe, K., Handa, H., Mizumoto, K. & Nagata, K. (1996). Mechanism for inhibition of influenza virus RNA polymerase activity by matrix protein. *J Virol* **70**, 241-247.

Watt, A., Moukambi, F., Banadyga, L., Groseth, A., Callison, J., Herwig, A., Ebihara, H., Feldmann, H. & Hoenen, T. (2014). A novel life cycle modeling system for Ebola virus shows a genome length-dependent role of VP24 in virus infectivity. *J Virol* **88**, 10511-10524.

Weik, M., Enterlein, S., Schlenz, K. & Mühlberger, E. (2005). The Ebola virus genomic replication promoter is bipartite and follows the rule of six. *J Virol* **79**, 10660-10671.

Welsch, S., Kolesnikova, L., Krähling, V., Riches, J. D., Becker, S. & Briggs, J. A. (2010). Electron tomography reveals the steps in filovirus budding. *PLoS Pathog* **6**, e1000875.

Wenigenrath, J., Kolesnikova, L., Hoenen, T., Mittler, E. & Becker, S. (2010). Establishment and application of an infectious virus-like particle system for Marburg virus. *J Gen Virol* **91**, 1325-1334.

Whelan, S. P., Barr, J. N. & Wertz, G. W. (2004). Transcription and replication of nonsegmented negative-strand RNA viruses. *Curr Top Microbiol Immunol* **283**, 61-119.

WHO (2012). Marburg haemorrhagic fever. http://www.who.int/mediacentre/factsheets/fs_marburg/en/: WHO.

WHO (2014). Guidance on temporary malaria control measures in Ebola-affected countries.

WHO (2016a). Ebola virus disease. http://www.who.int/mediacentre/factsheets/fs103/en/.

WHO (2016b). Situation Report Ebola virus disease. http://apps.who.int/iris/bitstream/10665/208883/1/ebolasitrep_10Jun2016_eng.pdf?ua=1.

Yamayoshi, S., Noda, T., Ebihara, H., Goto, H., Morikawa, Y., Lukashevich, I. S., Neumann, G., Feldmann, H. & Kawaoka, Y. (2008). Ebola virus matrix protein VP40 uses the COPII transport system for its intracellular transport. *Cell Host Microbe* **3**, 168-177.

7 Materials

7.1 Equipment

Incubator HERAcell150	Thermo Fisher, Hudson (USA)
Incubator Function line BB16	Thermo Fisher, Hudson (USA)
DNA- Gel chambers	bsb11, Schauenburg (GER)
Ice machine	Ziegra, Isernhagen (GER)
Eppendorf centrifuge 5415R	Eppendorf, Hamburg (GER)
Centrifuge Mikro 200R	Hettich, Tuttlingen (GER)
Eppendorf Research Plus® Pipetten	Eppendorf, Hamburg (GER)
Micro scale	Sartorius, Göttingen (GER)
Gel documentation system GelDoc 2000	Biorad, Hercules (USA)
Light microscope Axiovert200M	Zeiss, Jena (GER)
Light microscope Wilovert®	Will, Wetzlar (GER)
Luminometer Centro LB 960	Berthold, Bad Wildbad (GER)
Magnetic stirrer	Heidolph, Kelheim (GER)
Metal block Thermostat TCS	neoLab®, Heidelberg (GER)
Microwave	Bosch, Stuttgart (GER)
Table centrifuge Sprout	Heathrow scientific, Illinois (USA)
PCR Cycler Primus 25	Peqlab, Erlangen (GER)
pH-Meter Φ32	Beckmann Coulter, Palo Alto (USA)
Pipetting aid Pipetboy	Integra Bioscience, Chur (CH)
Power Supply PowerPacTM HC	Biorad, Hercules (USA)
Power Supply Standard Power Pack P25	Biometra, Göttingen (GER)
Vortex	neoLab®, Heidelberg (GER)
Rotor Ultracentrifuge SW32, SW41, SW60	Beckmann Coulter, Palo Alto (USA)
SDS-Gel chamber XCell Sure Lock	Thermo Fisher, Carlsbad (USA)
SDS-Gel chamber Mini-Protean	Biorad, Hercules (USA)
SemiDry Blot chamberTrans-Blot SD	Biorad, Hercules (USA)
NuAire Biological Safety Cabinets Class II	NuAire, Plymouth (USA)
Spectrophotometer NanoDrop Lite	Thermo Fisher, Waltham (USA)
StepOne™ ABI, RealTime PCR Cycler	Applied Biosystem, Carlsbad (USA)
Thermomixer compact	Eppendorf, Hamburg (GER)

Tabletop-ultracentrifuge Optima™ MAX-XP	Beckmann Coulter, Palo Alto (USA)
Ultracentrifuge Optima™ L-100K/ -80XP	Beckmann Coulter, Palo Alto (USA)
UV-Light table 302 nm	Bachofer, Reutlingen (GER)
Vacuumpump Mini-Vac E1	Axonlab, Reichenbach (GER)
Weight scale excellence	Sartorius, Göttingen (GER)
Water bath MT	Lauda, Lauda-Königshofen (GER)
Leica SP5 confocal microscope	Leica, Wetzlar (GER)

7.2 Chemicals

Agarose *PeqGold* universal	Peqlab, Erlangen (GER)
Ammonium persulfate (APS)	Biorad, Hercules (USA)
Ampicillin	Serva, Heidelberg (GER)
BactoTM-Agar	Becto, Dickinson & Company, Sparks (USA)
Bovine serum albumin (BSA)	Sigma-Aldrich, München (GER)
Bromphenol blue (BPB)	Roth, Karlsruhe (GER)
Calcium chloride ($CaCl_2$ x 2 H_2O)	Merck, Darmstadt (GER)
Casein hydrolysate	Merck, Darmstadt (GER)
Coomassie® Brilliant Blue R250	Serva, Heidelberg (GER)
Chloroform	Merck, Darmstadt (GER)
D(+)- Glucose	Merck, Darmstadt (GER)
Dextran blue	Sigma-Aldrich, München (GER)
4’,6-Diamidino-2-phenylindol (DAPI)	Sigma-Aldrich, München (GER)
1,4 Diazabicyclo-[2.2.2]-octan (DABCO)	Sigma-Aldrich, München (GER)
Dimethyl sulfoxide (DMSO)	Merck, Darmstadt (GER)
Sodium carbonate (Na_2CO_3)	Merck, Darmstadt (GER)
Sodium hydrogen phosphate (Na_2HPO_4)	Merck, Darmstadt (GER)
Ethylenediaminetetraacetic acid (EDTA)	Roth, Karlsruhe (GER)
Acetic acid (HAc)	Merck, Darmstadt (GER)
Ethanol abs. (EtOH)	Sigma-Aldrich, München (GER)
Ethanol vergällt (EtOH)	Fischar, Saarbrücken (GER)
Ethidium bromide	Promega, Mannheim (GER)
Filipin III	Sigma-Aldrich, München (GER)

Fluorescein Phalloidin	Thermo Fisher, Carlsbad (USA)
Fluoprep	BioMérieux, Nürtingen (GER)
Formvar	Sigma-Aldrich, München (GER)
6x Gel Loading Dye	New England Biolabs, Frankfurt (GER)
Glutamine 200 mM	Gibco® /InvitrogenTM, Karlsruhe (GER)
Glutaraldehyde	Sigma-Aldrich, München (GER)
Glycerol	Roth, Karlsruhe (GER)
Glycine	Roth, Karlsruhe (GER)
Yeast extract	Merck, Darmstadt (GER)
4-(2-hydroxyethyl)-1-piperazineethanesulfonic acid (HEPES)	Sigma-Aldrich, München (GER)
Isopropanol	Sigma-Aldrich, München (GER)
Potassium chloride (KCl)	Merck, Darmstadt (GER)
Monopotassium phosphate (KH_2PO4)	Roth, Karlsruhe (GER)
Milk powder	Saliter, Obergünzburg (GER)
Magnesium chloride ($MgCl_2$ x $6H_2O$)	Merck, Darmstadt (GER)
Magnesium sulfate ($MgSO_4$ x $7H_2O$)	Merck, Darmstadt (GER)
Manganese(II) chloride ($MnCl_2$ x $4H_2O$)	Merck, Darmstadt (GER)
β-mercaptoethanol	Sigma-Aldrich, München (GER)
Methanol (MeOH)	Sigma-Aldrich, München (GER)
Roswell Park Memorial Institute 1640 Media (RPMI)	Gibco®/Invitrogen™, Karlsruhe (GER)
Sodium azide (NaN3)	Merck, Darmstadt (GER)
Sodium chloride (NaCl)	Roth, Karlsruhe (GER)
Sodium dodecyl sulfate (SDS)	Merck, Darmstadt (GER)
Sodium hydroxide (NaOH)	Riedel-de-Haën, Seelze (GER)
SuperSignal™ West Femto	Thermo Fisher, Carlsbad (USA)
N(onidet)P40	Merck, Darmstadt (GER)
Nycodenz	Axis-Shield, Oslo (NOR)
Paraformaldehyde (PFA)	Roth, Karlsruhe (GER)
Penicillin/Streptomycin 5000 IU/ml	Gibco® /InvitrogenTM, Karlsruhe (GER)
Trypone	Merck, Darmstadt (GER)

Phosphotungstic acid	Serva, Heidelberg (GER)
Phenylmethylsulfonyl fluoride (PMSF)	Sigma-Aldrich, München (GER)
Polyacrylamide Rotiphorese Gel 30	Roth, Karlsruhe (GER)
Hydrochloric acid (HCl)	Merck, Darmstadt (GER)
Nitrogen (99,996 %)	Messer-Griesheim, Siegen (GER)
Sucrose	Serva, Heidelberg (GER)
Tetramethylethylenediamine (TEMED)	Biorad, Hercules (USA)
TransIT® LT1 Transfection Reagent	Mirus Bio, Madison (USA)
Tris(hydroxymethyl)aminomethane (Tris)	Acros Organics, Geel (B)
TritonX- 100	Sigma-Aldrich, München (GER)
Tween® 20	neoLab®, Heidelberg (GER)
T-PER Tissue protein extraction reagent	Thermo Fisher, Carlsbad (USA)
Xylene cyanol FF	Gibco®/Invitrogen™, Karlsruhe (GER)
Dulbecco's Modified Eagle Medium (DMEM)	Gibco®/Invitrogen™, Karlsruhe (GER)
Fetal calf serum (FCS)	Gibco®/Invitrogen™, Karlsruhe (GER)
OptiMEM®	Gibco®/Invitrogen™, Karlsruhe (GER)
Trypsin-EDTA (0,5 %)	Gibco®/Invitrogen™, Karlsruhe (GER)

7.3 Consumables

6, 24, 96 well cell culture dishes	Greiner bio-one, Frickenhausen (GER)
25 cm², 75 cm², 175 cm² Cell culture flasks	Greiner bio-one, Frickenhausen (GER)
96 well Plates *LumiNunc*™	Nunc, Roskilde (DK)
2 ml Cryotubes	Corning ®, Acton (USA)
Blotting paper *GB 002* (3 mm)	Whatman, Maidstone (UK)
Coverslips, Ø 12 mm	Menzel, Braunschweig (GER)
Indicator paper	Merck, Darmstadt (GER)
Reaction tubes (screw top)	Sarstedt, Nürnbrecht (GER)
Object slide 76 x 22 mm	Menzel, Braunschweig (GER)
Parafilm	Pechiney Plastic, Menasha (USA)
PCR-Tubes, 0.2 ml	Biozym, Hess. Oldendorf (GER)

Petri dishes	Sarstedt, Nürnbrecht (GER)
Pipettes 1, 2, 5, 10, 25 ml *Cellstar*®	Greiner bio-one, Frickenhausen (GER)
Pipette tips 0.1-1 µL, 10-100 µL, 100-1000 µL *TipOne*® (with and without filter)	Starlab, Ahrensburg (GER)
Polypropylene reaction tubes 15 ml/50 ml	Greiner bio-one, Frickenhausen (GER)
Immobilion®-P (PVDF-Membrane), Pore size 0,45 µm	Millipore, Billerica (USA)
Reaction tube 1,5 ml	Sarstedt, Nürnbrecht (GER)
Reaction tube 2 ml	Eppendorf, Hamburg (GER)
Scalpel no.22	Feather Feather, Osaka (J)
Sterile filter Ø 0,2 µm	Schleicher & Schuell, Maidstone (UK)
Cell scraper	Sarstedt, Nürnbrecht (GER)
Centrifuge tubes, Ultra-Clear™ for SW41, SW60, SW32, TLA55	Beckmann, Palo Alto (USA)
NuPAGE Tris-Acetate Gels	Thermo Fisher, Carlsbad (USA)

7.4 Kits

Gibson Assembly	NEB, Ipswich (USA)
E.Z.N.A. Plasmid DNA Mini I	OMEGA bio-tek, Norcross (USA)
E.Z.N.A. FastFilter Plasmid DNA Maxi	OMEGA bio-tek, Norcross (USA)
E.Z.N.A. DNA Probe Purification	OMEGA bio-tek, Norcross (USA)
E.Z.N.A. Gel Extraction	OMEGA bio-tek, Norcross (USA)
QuikChange Multi Site-Directed Mutagenesis	Agilent Technologies, Waldbronn (GER)
QuikChange Site-Directed Mutagenesis	Agilent Technologies, Waldbronn (GER)
QIAamp Viral RNA Mini	Qiagen, Hilden (GER)
Gel Extraction	OMEGA bio-tek, Norcross (USA)
Z-Competent™ *E.coli* Transformation Kit	Zymo Research, Orange (USA)
Renilla-Juice	PJK GMBH, Kleinblittersdorf (GER)
RNeasy Mini Kit	Qiagen, Hilden (GER)
Beetle-Juice	PJK GMBH, Kleinblittersdorf (GER)
peqGOLD Plasmid MiniprepI	Peqlab, Erlangen (GER)

Pierce Silver Stain	Thermo Fisher, Carlsbad (USA)
QuantiTect® Probe RT-PCR	Qiagen, Hilden (GER)
QuantiTect® SYBR® Green RT-PCR	Qiagen, Hilden (GER)

7.5 Buffers and solutions

Lysis buffer for flotation analysis	10 mM	Tris Hcl, pH 7,5
	20 mM	Sucrose
	mM	EDTA
	200 µM	Orthovanadat
	1 mM	PMSF
	1 x	Complete
		in dH_2O
PBS_{def}, pH 7.5	0,2 g	KCl
	0,2 g	KH_2PO_4
	1,15 g	Na_2HPO_4
	8 g	NaCl
	ad 1 l	dH_2O
Protein sample buffer (4x)	10 ml	Mercaptoethanol
	200 mg	Bromphenolblue
	20 ml	Glycerine
	10 ml	1 M Tris/HCl, pH 6,8
	4 g	SDS
	ad 50 ml	dH_2O
SDS running buffer (10X)	144 g	Glycine
for Tris-glycine gels	10 g	SDS
	30 g	Tris-Base
	ad 1 l	dH2O

SDS running buffer (20X)	89.5 g	Tricine
for Tris-acetate gels	10 g	SDS
	60 g	Tris-Base
	ad 0.5 l	dH2O
SDS transfer buffer (1X)	100 ml	Ethanol
	144 mg	Glycin
	300 mg	Tris
	ad 1 l	dH2O
Blocking buffer for western blot	10 %	Milk powder
		in PBS_{def}
Blocking buffer for IFA	2 %	Bovines Serum albumin
	5 %	Glycerin
	0,05 %	NaN_3
	0,2 %	Tween® 20
		in PBS_{def}
SDS-PAGE stacking gel buffer	0,4 %	SDS
	1,5 M	Tris/HCl, pH 8.8
		in dH2O
SDS-PAGE separation gel buffer	0,4 %	SDS
	1,5 M	Tris/HCl, pH 8.8
		in dH2O
TAE buffer, pH 8.0 (50x)	100 ml	0.5 M EDTA, pH 8.0
	1 M	Acetic acid
	242 g	Tris-Base
	ad 1 l	dH2O

TNE-Puffer (1x)	1 mM	EDTA, pH 8.0
	150 mM	NaCL
	10 mM	Tris/HCl, pH 7.4
	in dH2O	
Dilution buffer for antibodies	1 %	Milkpowder
	0,1 %	Tween® 20
		in PBS_{def}
Washing buffer WB	0,1 %	Tween® 20
		in PBS_{def}

7.6 Solutions

Ampicillin stock solution	100 mg	Ampicillin
	ad 1 ml	dH2O
Coomassie®-Staining solution	300 ml	Ethanol
	100 ml	Acetic acid
	0,05 %	Coomassie Brilliant Blue R250
	ad 1 l	dH2O
Nycodenz 60 % in TNE	60 g	Nycodenz
	ad 1 l	TNE-Buffer (1x)

7.7 Growth media

7.7.1 Growth media for bacteria

LB-Agar (1,5 %)	3.75 g	Bacto™ Agar
	ad 250 ml	LB-Media
LB-Media	10 g	NaCl
	5 g	Yeast extract
	10 g	Tryptone
	ad 1 l	dH2O
SOB-Media	20 g	Tryptone
	5 g	Yeast extract
	0.58 g	NaCl
	0.19 g	KCl
	10 ml	1 M MgCl2
	10 ml	1 M MgSO4
	ad 1 l	dH2O

7.7.2 Growth media for mammalian cells

DMEM 10 % FCS + Q + P/S	500 ml	DMEM
(DMEM+++)	50 ml	FCS (fetal calf serum)
	5 ml	L-Glutamine 200 mM (100x)
	5 ml	Penicillin/Streptomycin 5.000 IU/ml
DMEM5 % FCS + Q + P/S	500 ml	DMEM
	25 ml	FCS (fetal calf serum)
	5 ml	L-Glutamine 200 mM (100x)
	5 ml	Penicillin/Streptomycin 5.000 IU/ml

DMEM3 % FCS + Q + P/S	500 ml	DMEM
	15 ml	FCS (fetal calf serum)
	5 ml	L-Glutamine 200 mM (100x)
	5 ml	Penicillin/Streptomycin 5.000 IU/ml
DMEM+ Q + P/S	500 ml	DMEM
	5 ml	L-Glutamine 200 mM (100x)
	5 ml	Penicillin/Streptomycin 5.000 IU/ml
RPMI 10 % FCS + Q + P/S (RPMI+++)	500 ml	DMEM
	50 ml	FCS (fetal calf serum)
	5 ml	L-Glutamine 200 mM (100x)
	5 ml	Penicillin/Streptomycin 5.000 IU/ml
RPMI 5 % FCS + Q + P/S	500 ml	DMEM
	25 ml	FCS (fetal calf serum)
	5 ml	L-Glutamine 200 mM (100x)
	5 ml	Penicillin/Streptomycin 5.000 IU/ml
RPMI 3 % FCS + Q + P/S	500 ml	DMEM
	15 ml	FCS (fetal calf serum)
	5 ml	L-Glutamine 200 mM (100x)
	5 ml	Penicillin/Streptomycin 5.000 IU/ml
RPMI+ Q + P/S	500 ml	DMEM
	5 ml	L-Glutamine 200 mM (100x)
	5 ml	Penicillin/Streptomycin 5.000 IU/ml

7.8 Nucleic acids and nucleotides

O'Gene Ruler™ 1 kb Plus DNA Ladder	75 bp-20 kb	Fermentas, St. Leon-Rot (GER)
dNTP-Mix	2'Desoxyadenosine 5'triphosphate 2'Desoxyzytosine 5'triphosphate 2'Desoxyguanosine 5'triphosphate 2'Desoxythymidine 5'triphosphate each 10 mM	Thermo Scientific, Waltham (USA)

7.9 DNA-Oligonucleotides

Primer #	Name	Sequence (5'-3')
16	MBV GP 1112 F	GAACATAAGTGATCCTCTCACT
28	Klon 1-258 F	GAG CTG TTT GGA ATA GCA GA
184	L 12846 F	TAT CAG CAT CTT TGG GAG TG
201	L 15144 F	AGAAGATAAGATCGGTTATC
202	L 15530 F	AGATATTGCATTGTCTCTTG
280	Lv - 17601	GAC GCA GAG ACC ACC AAG GAT GAA ACA AGG
1233	pCAGGS-forw	CCTTCTTCTTTTTCCTACAG
1234	pCAGGS-rev	CCTTTATTAGCCAGAAGTCAG
2124	11.MB AgeI 16274V	GTCATCGCTACCGGTTTGG
2283	MB16713SalIV	CTAGTCGAAAATTGTCGACCATCAGAGGG C
2620	Luc (-) NB	AGA ACC ATT ACC AGA TTT GCC TGA
2621	Luc (+) NB	GGC CTC TTC TTA TTT ATG GCG A
2863	mCherry-fwd	CGAATTCGTCTCTTCCAATGGTGAGCAAGG GCGAGG
2864	mCherry-rev	GGAATTCGTCTCACTTGCTTGTACAGCTCG TCCATGCC
3125	MARV VP40 D184N	GGCGCCCATCCAAGAATAAATTAATTGGG

3158	Sequenzierprimer MARV L	GTCCAGCGTCATGGGTG
3511	mcherry Bstb1S	gggTTCGAAAATGGTGAGCAAGGGCGAGGAGGA
3512	mcherry Bstb1AS	tacTTCGAATGCTTGTACAGCTCGTCCATGCCGCCG
3519	Sequenzierprimer Ende GFP	GTATGCGAATCC
3533	GA-mCherry-L_for	TTCAGTCTCCTCTAATCAACAAGTGACCAATTCGAAAATGGTGAGCAAGGGCGAGGAGGA
3534	GA-mCherry-L_rev	GTGATATTTTCTGGATAAACAATATACTTCGAATGCTTGTACAGCTCGTCCATGCCGCCG
3547	L-Mut_S741C-for	AATTAAAATTGAAGTCCTG**TGT**CATGGGTGATAATCAATGTATAA
3548	L-Mut_D758A-for	ACTCTAAGTCTTTTTCCAATT**GCG**GCTCCCAACGATTATCAAGAG
3549	L-Mut_A759D-for	ACTCTAAGTCTTTTTCCAATTGAT**GAC**CCCAACGATTATCAAGAG
3550	L-Mut_D758A, A759D-for	ACTCTAAGTCTTTTTCCAATT**GCGGAC**CCCAACGATTATCAAGAG
3553	pC_beL_for	CAGCCATTGCCTTTTATGGT
3554	pC_wiL1_for	TGATGAACTCCATGATCTCAATTT
3555	pC_wiL2_for	ATGGACTGGCAAAAGCATTC
3556	pC_wiL3mC_for	CAGAGATTATCAGACTTGTTATCACC
3557	pC_wimCh_for	GGAGCGCGTGATGAACTT
3558	pC_wiL3_for	ACCCAGGTTTTCGGAGTATGT
3595	MARV L PartFrag_For	GGGATCGATGTTATGGTGTGAAG
3596	MARV L PartFrag_Rev	GGGTCGCGAACTGTTTGTCTAAGGAACG
3653	MARV_L_rev_Nt3677	TCATATCGGAAGGCGAGGTT
3654	MARV_L_rev_Nt3249	CAACACTCCTGGTTCACAGC
3655	MARV_L_rev_Nt2904	ACGGGATGACCCCAATGCTT
3656	MARV_L_rev_Nt2146	CACACTGTGACCTTGCAGAA

3750	MARV-L Nt 5142	AAGGCTAATTGGTGCCACAC
3751	MARV-L Nt 8909	TCACGCCAAAGACAAGCAAT

The primer numbers reflect the unique identification within the research group. Thick letters indicate mutational site.

7.10 Plasmids

7.10.1 Vectors

Vector	Origin
pCAGGS	Institute for Virology, Marburg (GER)
pTM1	NIH, Bethesda, (USA)
pGL4	Promega, Mannheim (GER)
pGL4.73	Institute for Virology, Freiburg (GER)
pGL3	Institute for Virology, Freiburg (GER)

7.10.2 Plasmids encoding recombinant proteins

Vector	Encoded protein	Name	Origin
pCAGGS	T7-polymerase	pCAGGS-T7	Y. Kawaoka, Wisconsin (USA)
pAndy	3M-5M Luciferase	pAndy-3M-5M	Institute for Virology, Marburg (GER)
pCAGGS	GP	pCAGGS-GP	Institute for Virology, Marburg (GER)
pCAGGS	VP24	pCAGGS-VP24	Institute for Virology, Marburg (GER)
pCAGGS	VP30	pCAGGS-VP30	Institute for Virology, Marburg (GER)
pCAGGS	VP35	pCAGGS-VP35	Institute for Virology, Marburg (GER)
pCAGGS	L	pCAGGS-L	Institute for Virology, Marburg (GER)
pCAGGS	NP	pCAGGS-NP	Institute for Virology, Marburg (GER)

pCAGGS	VP40	pCAGGS-VP40	Institute for Virology, Marburg (GER)
pCAGGS	$VP40_{D184N}$	$pCAGGS\text{-}VP40_{D184N}$	Institute for Virology, Marburg (GER)
pCAGGS	VPS41mCherry	pCAGGS-VP41mCh	Institute for Virology, Marburg (GER)
pGL 4.73	*Renilla*	pGL.4.73	Institute for Virology, Marburg (GER)
pGL3	Mx1	pGL3 Mx1 reporter	Institute for Virology, Marburg (GER)
pCAGGS	L_{S741C}	$pCAGGS\text{-}L_1$	Institute for Virology, Marburg (GER)
pCAGGS	L_{D758A}	$pCAGGS\text{-}L_2$	Institute for Virology, Marburg (GER)
pCAGGS	L_{A759D}	$pCAGGS\text{-}L_3$	Institute for Virology, Marburg (GER)
pCAGGS	$L_{S741C, D758A}$	$pCAGGS\text{-}L_{1,2}$	Institute for Virology, Marburg (GER)
pCAGGS	$L_{S741C, A759D}$	$pCAGGS\text{-}L_{1,3}$	Institute for Virology, Marburg (GER)
pCAGGS	$L_{D758A, A759D}$	$pCAGGS\text{-}L_{2,3}$	Institute for Virology, Marburg (GER)
pCAGGS	$L_{S741C, D758A, A759D}$	$pCAGGS\text{-}L_{1,2,3}$	Institute for Virology, Marburg (GER)
pCAGGS	$mCherry\text{-}L_{S741C}$	$*pCAGGS\text{-}mChL_1$	Institute for Virology, Marburg (GER)
pCAGGS	$mCherry\text{-}L_{D758A}$	$*pCAGGS\text{-}mChL_2$	Institute for Virology, Marburg (GER)
pCAGGS	$mCherry\text{-}L_{A759D}$	$*pCAGGS\text{-}mChL_3$	Institute for Virology, Marburg (GER)
pCAGGS	$mCherry\text{-}L_{S741C, D758A}$	$*pCAGGS\text{-}mChL_{1,2}$	Institute for Virology, Marburg (GER)
pCAGGS	$mCherry\text{-}L_{S741C, A759D}$	$*pCAGGS\text{-}mChL_{1,3}$	Institute for Virology, Marburg (GER)
pCAGGS	$mCherry\text{-}L_{D758A, A759D}$	$*pCAGGS\text{-}mChL_{2,3}$	Institute for Virology, Marburg (GER)
pCAGGS	$mCherry\text{-}L_{S741C, D758A, A759D}$	$*pCAGGS\text{-}mChL_{1,2,3}$	Institute for Virology, Marburg (GER)

* The names of the mCherry-L encoding plasmids and the according mutants are shown without the mCh prefix, however it is indicated when MARV L encoding plasmids were used not containing a mCherry-tag (chapter 3.3.3)

Cloned plasmid		Template	Primer/Klonierung
pCAGGS	L_1	pCAGGS- mCherry-L_1	SC with RD with BstBI
pCAGGS	L_2	pCAGGS- mCherry-L_2	SC with RD with BstBI
pCAGGS	L_3	pCAGGS- mCherry-L_3	SC with RD with BstBI
pCAGGS	$L_{1,2}$	pCAGGS- mCherry-$L_{1,2}$	SC with RD with BstBI
pCAGGS	$L_{1,3}$	pCAGGS- mCherry-$L_{1,3}$	SC with RD with BstBI
pCAGGS	$L_{2,3}$	pCAGGS- mCherry-$L_{2,3}$	SC with RD with BstBI
pCAGGS	$L_{1,2,3}$	pCAGGS- mCherry-$L_{1,2,3}$	SC with RD with BstBI
pCAGGS	mCherry-L	pCAGGS-L + pCAGGS-VPS41mCherry	PCR of mCherry with 3533, 3544. BstBI digested pCAGGS-L + mCherry for Gibson assembly with 3533, 3544
pCAGGS	mCherry-L_1	pTM1-L_1	SC via RD with ClaI and NruI
pCAGGS	mCherry-L_2	pTM1-L_2	SC via RD with ClaI and NruI
pCAGGS	mCherry-L_3	pTM1-L_3	SC via RD with ClaI and NruI
pCAGGS	mCherry-$L_{1,2}$	pTM1-$L_{1,2}$	SC via RD with ClaI and NruI
pCAGGS	mCherry-$L_{1,3}$	pTM1-$L_{1,3}$	SC via RD with ClaI and NruI
pCAGGS	mCherry-$L_{2,3}$	pTM1-$L_{2,3}$	SC via RD with ClaI and NruI
pCAGGS	mCherry-$L_{1,2,3}$	pTM1-$L_{1,2,3}$	SC via RD with ClaI and NruI
pTM1	Frag-L	pCAGGS-L	SC via RD with ClaI
pTM1	Frag-L_1	pTM-L	MG with 3547
pTM1	Frag-L_2	pTM-L	MG with 3548
pTM1	Frag-L_3	pTM-L	MG with 3549
pTM1	Frag-$L_{1,2}$	pTM-L	MG with 3547, 3548
pTM1	Frag-$L_{1,3}$	pTM-L	MG with 3547, 3549
pTM1	Frag-$L_{2,3}$	pTM-L	MG with 3550
pTM1	Frag-$L_{1,2,3}$	pTM-L	MG with 3547, 3550

SC: Subcloning
RD: Restriction digest

The table contains only the unique assigned laboratory number, for more details see chapter 7.9

7.11 Proteins

7.11.1 Recombinant purified proteins

Recombinant interferon-α/β hybrid kindly provided by Dr. Stéphanie Devignot, Institute for virology, Justus-Liebig Universität Gießen

7.11.2 Enzymes

Calf intestine phosphatase (CIP)	Roche Diagnostics, Mannheim (GER)
Complete Protease Inhibitor Cocktail Tablets	Roche Diagnostics, Mannheim (GER)
T4 DNA ligase	NEB, Ipswich (USA)
Pwo polymerase	Peqlab, Erlangen (GER)

7.11.3 Restriction enzymes

All restriction enzymes and the associated Buffers (10x concentrated) were purchased at New England Biolabs (Frankfurt,GER) and Fermentas (St.Leon-Rot, GER)

7.11.4 Primary antibodies

Name	Species	Company	Dilution	
			IFA	WB
α-MARV VP40 (40-2-2)	Mouse	Institute for virology, Marburg (GER)	1:200	1:1000
α-MARV NP (59-9-10)	Mouse	Institute for virology, Marburg (GER)	-----	1:500
α-MARV NP (2)	Guinea pig	Institute for virology, Marburg (GER)	1:200	-----
α-MARV GP (50-6-10)	Mouse	Institute for virology, Marburg (GER)	-----	1:100

α-MARV VP35	Guinea pig	Institute for virology, Marburg (GER)	1:500	-----
α-mCherry	Mouse	Abcam, Cambridge (UK)	-----	1:1000
α-Vinculin	Mouse	Sigma-Aldrich, München (GER)	-----	1:2000
α-Tubulin	Mouse	Sigma-Aldrich, München (GER)	-----	1:5000

7.11.5 Secondary antibodies for IFA

Name	Species	Company	Dilution
α-mouse Alexa 488	Goat	Invitrogen, Karlsruhe (GER)	1:300
α-guinea pig Alexa 488	Goat	Invitrogen, Karlsruhe (GER)	1:300
α-mouse Alexa 488	Goat	Invitrogen, Karlsruhe (GER)	1:300
α-mouse Marina blue	Goat	Invitrogen, Karlsruhe (GER)	1:300

7.11.6 Secondary antibodies for WB

Name	Species	Company	Dilution
α-mouse HRP	Goat	Dako, Hamburg (D)	1:30.000

7.11.7 DNA marker

O'GeneRuler 1 kb Plus DNA Ladder, Thermo Scientific, Waltham (USA)

7.11.8 Proteinmarker

PageRuler™ Plus Prestained Protein Ladder 10-250 kDa, Fermentas, St. Leon-Rot (GER)

7.12 Cells and viruses

7.12.1 Prokaryotic cells

Bacteria	Origin
E. coli XL1 blue	Stratagene, Heidelberg (GER)
E.Coli XL10-Gold	Agilent technologies, Ratingen (GER)

7.12.2 Eukaryotic cells

Cell line	Origin
Huh-7 cells	Institute for virology, Marburg (GER)
HEK293 cells	Institute for virology, Marburg (GER)
104C1 cells	Robert Koch Institute, Berlin (GER)
GPC16 cells	ATCC, Wesel (GER)
VeroE6 cells	Institute for virology, Marburg (GER)

7.12.3 Viruses

Virus
Recombinant Marburg Virus Musoke, Wildtype $rMARV_{WT}$
Recombinant Marburg Virus Musoke, D184N mutation in VP40 $rMARV_{VP40(D184N)}$

7.12.4 Software

Software	Used for
BioEdit 7.0.5.3.	Sequence analysis
Clone Manager 9	Planning of cloning projects
DoubleDigest finder	Planning of restriction digests
EndNote Web	Reference Management
ImageJ 1.47v	Immunofluorescence analysis
Image Lab 5.2	Detection and quantification of Western blot membranes
Leica Application Suite X software	Inclusion body size measurements
Microsoft Excel 2013	Statistical analysis, Figure preparation
Microsoft Power Point 2013	Graphics and scheme preparation
Microsoft Word 2013	Protocol-/ Thesis writing
QuikChange Primer Design tool	Design of mutagenesis primers

8 List of tables

9 List of figures

10 List of abbreviations

104C1	Fibroblast cells, Guinea pig
APS	Ammonium persulfate
Ax1	Defensin-like protein
BDBV	Bundibugyo virus
bp	Base pairs
BSA	Bovine serum albumin
BSL-2	Biosafety level 2
BSL-3	Biosafety level 3
BSL-4	Biosafety level 4
CDC	Center for disease control
CIP	Calf intestine phosphatase
CPE	Cytopathic effect
CR	Constant region
C-terminus	Carboxyterminus
d	Day
d (in dH2O)	deionized
DC-SIGN	Dendritic Cell-Specific Intercellular adhesion molecule-3-Grabbing Non-integrin
DMEM	Dulbecco's Modified Eagle Medium
DNA	Desoxyribonucleic acid
dNTP	Deoxynucleoside triphosphate
E.coli	*Escherichia coli*
e.g.	exempli gratia, (engl.) for example
EBOV	Ebola virus
EM	Electron microscopy
ER	Endoplasmatic reticulum
ESCRT	Endosomal sorting complexes required for transport
FCS	Fetal calf serum
FITC	Fluorescein isothiocyanate
for	Forward
GP	Glycoprotein

GPC16	Adenocarcinoma cells, Guinea pig
h	Hour
HEK293	Kidney cells, Human
HRP	Horseradish peroxidase
Huh-7	Hepatoma cells, Human
IFA	Immunofluorescence analysis
IFN	Interferon
iVLP	Infectious virus-like particle
Jak1	Janus kinase 1
kb	Kilo bases
kDa	Kilo Dalton
L	Large Protein
LB media	Lysogeny broth
LLOV	Lloviu virus
LSECtin	Liver and lymph node sinusoidal endothelial cell C-type lectin
MA-MARV	Mouse adapted Marburg virus
MA-RAVV	Mouse adapted Marburg virus RAVV strain
MARV	Marburg virus
MeV	Measles virus
min	Minute
MOI	Multiplicity of infection
mRNA	Messenger RNA
NHP	Non human primate
NNS	Nonsegmented negative strand
NP	Nucleoprotein
NPC1	Niemann Pick 1
N-terminus	Amino-terminus
OD	Optical density
ORF	Open reading frame
p.i.	Post infection
p.t.	Post transfection
P/S	Penicillin/Streptomycin

PAGE	Polyacrylamide gel electrophoresis
PBS	Phosphate-buffered saline
PBS_{def}	Phosphate-buffered saline deficient in magnesium and calcium
PCR	Polymerase chain reaction
PFA	Paraformaldehyde
pH	potentia hydrogenii
pmol	Pico mol
RAVV	Marburg virus Ravn
RdRp	RNA-dependent RNA polymerase
REBOV	Reston ebolavirus
rev	Reverse
RIG-I	Retinoic acid inducible gene I
RL-MARV	Rodent-lethal Marburg virus
rMARV	Recombinant Marburg virus
RNA	Ribonucleic acid
rpm	Revolutions per minute
RPMI	Roswell Park Memorial Institute
RT	Reverse transcription
RT-PCR	Reverse transcription polymerase chain reaction
RT-qPCR	Quantitative reverse transcription polymerase chain reaction
SDS	Sodium dodecyl sulfate
sec	Second
siRNA	Short interference ribonucleic acid
SIV	Simian immunodeficiency virus
SUDV	Sudan virus
T7-pol	T7 DNA-dependent RNA polymerase
TAFV	Taï Forest virus
TCID50	Tissue culture infectious dose 50
TIM-1	T-cell immunoglobulin and mucin domain 1
tr	Transcription
TRITC	Tetramethylrhodamine

List of abbreviations

UV	Ultraviolet light
VeroE6	Kidney cells, African green monkey
VLP	Virus-like particles
VP24	Viral protein 24
VP30	Viral protein 30
VP35	Viral protein 35
VP40	Viral protein 40
VSV	Vesicular stomatitis virus
WHO	World health organization
ZEBOV	Zaire ebolavirus
α	Anti
λ	Lambda, Wavenlength

11 Amino acid one letter code

Amino acid	One letter code
Alanine	A
Arginine	R
Asparagine	N
Aspartic acid	D
Cysteine	C
Glutamic acid	E
Glutamine	Q
Glycine	G
Histidine	H
Isoleucine	I
Leucine	L
Lysine	K
Methionine	M
Phenylalanine	F
Proline	P
Serine	S
Threonine	T
Tryptophan	W
Tyrosine	Y
Valine	V

12 Curriculum vitae

Alexander Köhler

Anschrift	Ketzerbach 15 35094 Lahntal Deutschland
Kontaktdaten	+49 178 2555373 alexander_koehler@yahoo.de
Geburtsdatum und -ort	17.01.1987 in Paderborn
Nationalität	deutsch
Familienstand	Ledig

Beruf

Oktober 2013 – laufend	Wissenschaftlicher Mitarbeiter zum Abschluss einer Promotion **Institut für Virologie, Philipps Universität, Marburg**, **Prof. Dr. Becker** Thema der Doktorarbeit: “Pathogenesis of Marburg Virus”

Ausbildung

Okt. 2011 – Sep. 2013	Masterstudium: Molekulare Biologie **Westfälische Hochschule** Masterarbeit **Duke University, North Carolina, USA** **Institut für Molekulargenetik und Mikrobiologie** **Prof. Dr. Dr. Garcia-Blanco**
Sep. 2008 – Sep. 2011	Bachelorstudium: Molekulare Biologie **Fachochschule Gelsenkirchen** Bachelorarbeit: **Universitätsklinikum Essen** **Institut für Virologie** **Dr. Jia-Liu**
Sep. 2006 – Jul. 2008	Berufsausbildung zum biologisch-technischen Assistenten (BTA) **DIE SCHULE für Berufe mit Zukunft, Osnabrück**

Publikationen und Kongressbeiträge

Publikationen: 2015	Koehler et al. J Virol, A Single Amino Acid Change in the Marburg Virus Matrix Protein VP40 Provides a Replicative Advantage in a Species-Specific Manner

	2016	Koehler et al. J. Gen. Virol., An active site mutation increases the polymerase activity of the guinea pig-lethal Marburg virus
Kongressbeiträge:	2014	24. Frühjahrstagung der Gesellschaft für Virologie, Alpbach, Österreich Koehler A., Welzel U., Schudt G., Becker S. and Kolesnikova L. Role of a single amino acid mutation in VP40 for the enhanced virulence of guinea pig-adapted Marburg Virus. (Poster).
	2015	25. Frühjahrstagung der Gesellschaft für Virologie, Bochum, Deutschland Koehler A., Welzel U., Schudt G., Herwig A., Becker S. and Kolesnikova L. A single amino acid change in the matrix protein VP40 of Marburg virus improves viral fitness (Vortrag). Negative strand virus Meeting, Siena, Italien Koehler A., Welzel U., Schudt G., Becker S. and Kolesnikova L. A single amino acid change in the Marburg virus matrix protein VP40 improves viral fitness in a species-specific manner (Poster).
	2016	26. Frühjahrstagung der Gesellschaft für Virologie, Münster, Deutschland Koehler A., Welzel U., Schudt G., Kolesnikova L. and Becker S. A Single Amino Acid Change in the Marburg Virus Matrix Protein VP40 Provides a Replicative Advantage in a Species-Specific Manner (Poster).

Zusätzliche Qualifikationen	
Fortbildungen	GMP Kurs Scientific Writing Kurs Scientific Figures Kurs
Freiwillige Projektarbeit:	
Seit 2014	Organisation und Durchführung der Marphili Simulation
2014-2015	Betreuung der Mediziner im Praktikum der Parasitologie
Besondere Laborfähigkeiten:	
Seit Dezember 2014	Training und Arbeiten im BSL-4 (*biosafety level* 4) Hochsicherheitslabor Institut für Virologie, Philipps-Universität Marburg
2012-2013	BSL-3 Training am Human Vaccine Institute der Duke University, Durham, North Carolina

	Kenntnisse
Sprachen	Deutsch (Muttersprache), Englisch (fließend in Wort und Schrift)
IT-Kenntnisse	Microsoft Office, Grundkenntnisse im Umgang mit Photoshop
Sonstiges	PKW-Führerschein

13 Verzeichnis der akademischen Lehrer

Meine akademischen Lehrer an der Westfälischen Hochschule waren die Damen und Herren Professoren bzw. Privat Dozenten:

Beyer, Brinck, Eiden, Grammann, Loidl-Stahlhofen, Meyer, Perrey, Roll, Schubert, Schwenk, Stahlhofen, Sternemann, Strotmann Veith, Zielesny

Meine akademischen Lehrer an der Philipps Universität Marburg waren die Damen und Herren Professoren bzw. Privat Dozenten:

Becker, Kolesnikova

14 Ehrenwörtliche Erklärung

Ich erkläre ehrenwörtlich, dass ich die dem Fachbereich Medizin Marburg zur Promotionsprüfung eingereichte Arbeit mit dem Titel

„ The species-specific effects of guinea pig-adaptive mutations in Marburg virus VP40 and L on the protein's functions and viral fitness "

im Institut für Virologie unter Leitung von Prof. Dr. Stephan Becker ohne sonstige Hilfe selbst durchgeführt und bei der Abfassung der Arbeit keine anderen als die in der Dissertation aufgeführten Hilfsmittel benutzt habe.

Ich habe bisher an keinem in- oder ausländischen medizinischen Fachbereich ein Gesuch um Zulassung zur Promotion eingereicht, noch die vorliegende oder eine andere Arbeit als Dissertation vorgelegt.

Marburg, den 02. März 2017

Alexander Köhler

15 Acknowledgements

Life is the great indulgence - death the great abstinence. Therefore, make the most of life here and now!

- Anton Szandor LaVey

Ohne das wirken anderer Personen hätte ich diese Arbeit niemals schreiben können. Stephan, vielen Dank für dein Vertrauen und das spannende Projekt. Durch dich konnte ich mir mit der Arbeit im Hochsicherheitslabor einen wenn auch ungewöhnlichen, lang ersehnten Wunsch erfüllen.
Larissa thank you for your patience and the incredible amount of knowledge and experience that you shared with me. I could always rely on you and your truthful upfront opinions.
Vielen Dank AG Becker, für die stete Verfügbarkeit von Kaffee, Snacks und guter Laune. Besonderer Dank an Dirk, Katharina und Astrid die immer ausgeholfen haben als Not am Mann war. Vielen Dank auch an das BSL-4 Team, das die Arbeit im Klotz so angenehm gemacht hat.

Liebe Freunde, ne Doktorarbeit, wer hätte das vor 15 Jahren Gedacht? Ich ganz sicher nicht. Vielen Dank für all die tollen Dinge die ich mit euch erleben konnte und noch erleben werde. Sergej vielen Dank für die ganze Zeit die du wirklich jederzeit für mich genommen hast. Andreas und Daniel, ihr beiden habt mir durch eure ehrliche und direkte Art definitiv geholfen mir selbst treu zu bleiben.

Liebe Familie, was soll ich bloß sagen. Vielen Dank euch, ihr habt mich so sehr geprägt und dazu beigetragen der zu werden der ich nun bin. Julia, auch du bist Familie, vielen Dank für die grenzenlose Unterstützung während der Promotion. Du bist der Gegenpol den ich immer gebraucht habe. Was freue ich mich auf unsere Zukunft, und all die Dinge die wir noch mit unserem Bollerkopf erleben werden.

Zu guter Letzt, vielen Dank ans Eisen. An manchen Tagen ging es nicht um Gesundheit oder Muskeln sondern war Therapie und Ventil.

You can’t climb the ladder of success and happiness with your hands in your pockets.

- modified from Arnold Schwarzenegger